

REPUBLIC OF TURKEY
DİCLE UNIVERSITY
GRADUATE SCHOOL OF NATURAL AND APPLIED SCIENCES

**DEVELOPMENT OF SENSITIVE ANALYTICAL METHODS FOR
BISMUTH DETERMINATION BY ATOMIC SPECTROMETRIC
TECHNIQUES**

Ersin KILINÇ

**IN PARTIAL FULFILLMENT OF THE REQUIREMENTS
FOR
THE DEGREE OF DOCTOR OF PHILOSOPHY
IN
CHEMISTRY**

**DIYARBAKIR
JUNE 2012**

REPUBLIC OF TURKEY
DİCLE UNIVERSITY
GRADUATE SCHOOL OF NATURAL AND APPLIED SCIENCES
DİYARBAKIR

**DEVELOPMENT OF SENSITIVE ANALYTICAL METHODS FOR
BISMUTH DETERMINATION BY ATOMIC
SPECTROMETRIC TECHNIQUES**

submitted by **Ersin KILINÇ** in a partial fulfillment of the requirements for the degree of **Doctor of Philosophy in Chemistry Department, Dicle University** by examining committee.

Examining Committee Members

Prof. Dr. Recep ZİYADANOĞULLARI (Chairman)

Prof. Dr. Alaaddin ÇUKUROVALI

Prof. Dr. Berrin ZİYADANOĞULLARI

Assoc. Prof. Dr. Fırat AYDIN (Supervisor)

Assoc. Prof. Dr. Ali SATAR

Approval of the Graduate School of Natural and Applied Sciences

25/06/2012

Prof. Dr. Hamdi TEMEL
Director of Institute

I hereby declare that all information in this document has been obtained and presented in accordance with academic rules and ethical conduct. I also declare that, as required by these rules and conduct, I have fully cited and referenced all materials and results that are not original to this work.

.....
Ersin KILINÇ

DATE: 25.06.2012

ACKNOWLEDGEMENT

I am deeply grateful to Prof. Dr. O Yavuz ATAMAN and Assoc. Prof. Dr. Fırat AYDIN for their excellent supervision, help, guidance and encouragement they provided throughout my thesis. They always supported me by giving valuable suggestions throughout all stages of this thesis.

I owe my most sincere gratitude to Prof. Dr. Berrin ZİYADANOĞULLARI, Head of the Department of Chemistry, who gave me important guidance and helping during my thesis. Her kind support has been of great value in this thesis.

I warmly thank to Prof. Dr. Recep ZİYADANOĞULLARI, Rector of Siirt University, for his important support. In many ways he has always encouraged me. I am deeply grateful for his invaluable guidance throughout all stages of this thesis.

I wish to special thanks to Assoc. Prof. Dr. Sezgin BAKIRDERE for his expert advice and constructive comments in all possible ways and contribution in each part of this study.

My sincere thanks are due to the supervisory committee members, Prof. Dr. Recep ZİYADANOĞULLARI, Prof. Dr. Alaaddin ÇUKUROVALI, Prof. Dr. Berrin ZİYADANOĞULLARI, Assoc. Prof. Dr. Fırat AYDIN, Assoc. Prof. Dr. Ali SATAR, Assoc. Prof. Dr. Işıl AYDIN and Assoc. Prof. Dr. Sezgin BAKIRDERE for their detailed review, constructive and excellent advice during the preparation of thesis.

I am deeply grateful to AtaMAN Research group members, Assist. Prof. Dr. Yasin ARSLAN, Emrah YILDIRIM, Pınar AKAY, Selin BORA, Şefika EROĞLU and Feriye ŞENOL for their help, support and friendship.

I also would like to thank to Assist. Prof. Dr. M. Zahir DÜZ and Assoc. Prof. Dr. Osman AKBA for their support during the thesis, and researchers at Laboratory of Chemical Analysis in Chemistry Department-Dicle University.

Special thanks to my friend and roommate Dr. Murat YAVUZ from Dicle University, Department of Chemistry both his support and motivation to me during thesis and his friendship from we met.

The financially supports of the Dicle University Research Fund through grant DÜBAP 10-FF-31 and Technological Research Council of Turkey (TUBITAK-BİDEP) through scholarship during thesis are gratefully acknowledgement.

Last but not the least; I would like to thank my wife, Mutlu, for her unwavering support during the many long days which went into this endeavor. She provided continuous understanding, patience and love.

to my flower,

CONTENTS

	<u>Page</u>
ACKNOWLEDGEMENT	I
CONTENTS	V
ABSTRACT	XI
ÖZET	XV
LIST of TABLES	XIX
LIST of FIGURES	XXIII
LIST of ABBREVIATIONS	XXXIII
1. INTRODUCTION	1
1.1. Bismuth	2
1.1.1. Bismuth and Health	3
1.2. Atomic Absorption Spectrometry	3
1.2.1. Long Path Absorption Tube (LPAT)	5
1.2.2. Delves's Microsampling Cup	6
1.2.3. Slotted Quartz Tube	6
1.2.4. In situ Atom Trapping	9
1.2.5. Chemical Vapour Generation	14
1.2.6. Atom Trapping Hyphenated with Hydride Generation	16
1.3. Inductively Coupled Plasma - Optical Emission Spectrometry	18
1.3.1. Hydride Generation Hyphenated with Inductively Coupled Plasma Optical Emission Spectrometry	20
2. LITERATURE SURVEY	23
2.1. Bismuth Determination	23
3. MATERIAL and METHODS	31
3.1. Instrumentation	31
3.2. Chemical and Regents	32
3.3. Sampling	33
3.4. Coating Procedure for SQT	33
4. RESULTS and DISCUSSIONS	35
4.1. Optimization of FAAS Conditions for Determination of Bi	36
4.1.1. Investigation of Fuel Flow Rate for FAAS Determination of Bi	36
4.1.2. Investigation of Suction Rate of Sample Solution for FAAS Determination of Bi	36
4.1.3. Calibration Plot for Bi in FAAS Method	37

4.2.	Optimization of SQT-FAAS Conditions for Determination of Bi	38
4.2.1.	Investigation of Fuel Flow Rate for SQT-FAAS Determination of Bi	38
4.2.2.	Investigation of Suction Rate of Sample Solution for SQT-FAAS Determination of Bi	39
4.2.3.	Investigation of Height of SQT from Burner Head for SQT-FAAS Determination of Bi	39
4.2.4.	Calibration Plot for Bi in SQT-FAAS Method	40
4.3.	Optimization of SQT-AT-FAAS Conditions for Determination of Bi	42
4.3.1.	Effect of Organic Solvent for SQT-AT-FAAS Determination of Bi	42
4.3.2.	Investigation of Volume of Organic Solvent for SQT-AT-FAAS Determination of Bi	43
4.3.3.	Investigation of Sample Suction Rate for SQT-AT-FAAS Determination of Bi	44
4.3.4.	Investigation of Fuel Flow Rate for SQT-AT-FAAS Determination of Bi	45
4.3.5.	Optimization of Height of SQT from Burner Head for SQT-AT-FAAS Determination of Bi	46
4.3.6.	Investigation of Trapping Period for SQT-AT-FAAS Determination of Bi	47
4.3.7.	Calibration Plot for Bi in SQT-AT-FAAS Method	47
4.3.8.	Accuracy Check for SQT-AT-AAS Method and Application to Real Samples	50
4.3.9.	Interference Studies for SQT-AT-AAS Method	51
4.4.	Optimization of Metal Coated SQT-FAAS Conditions for Determination of Bi	54
4.4.1.	Investigation of Coating Metal for Metal Coated SQT-AAS Determination of Bi	54
4.4.2.	Investigation of Fuel Flow Rate for W Coated SQT-FAAS Determination of Bi	55
4.4.3.	Investigation of Sample Suction Rate for W Coated SQT-FAAS Determination of Bi	56
4.4.4.	Investigation of Height of SQT from Burner Head for W Coated SQT-FAAS Determination of Bi	56
4.4.5.	Calibration Plot for Bi by W Coated SQT-FAAS Method	57
4.5.	Optimization of Metal Coated SQT-AT-FAAS Conditions for Determination of Bi	59
4.5.1.	Investigation of Coating Material on Metal Coated SQT-AT-FAAS	59
4.5.2.	Effect of Organic Solvent for W Coated SQT-AT-FAAS Determination of Bi	59

4.5.3.	Investigation of Volume of Organic Solvent for W coated SQT-AT-FAAS Determination of Bi	60
4.5.4.	Investigation of Sample Suction Rate for W coated SQT-AT-FAAS Determination of Bi	60
4.5.5.	Investigation of Fuel Flow Rate for W coated SQT-AT-FAAS Determination of Bi	61
4.5.6.	Investigation of Height of SQT from Burner Head for W coated SQT-AT-FAAS Determination of Bi	62
4.5.7.	Investigation of Trapping Period for W coated SQT-AT-FAAS Determination of Bi	63
4.5.8.	Calibration Plot for W Coated SQT-AT-AAS Method	63
4.5.9.	Accuracy Check for W Coated SQT-AT-AAS Method and Application to Real Samples	66
4.6.	Interference Studies for W Coated SQT-AT-AAS Method	66
4.7.	Evaluation of System Performance	70
4.8.	Size Optimization for SQT	72
4.9.	Optimization of Continuous Flow Hydride Generation Inductively Coupled Plasma - Optical Emission Spectrometry for Determination of Bi	74
4.9.1.	Effect of Variables in Hydride Generation Efficiency	74
4.9.2.	Optimization of Instrumental Parameters	75
4.9.3.	Interference Studies on CF-HG-ICP-OES	78
4.9.4.	Analytical Figures of Merit	80
4.9.5.	Application of CF-HG-ICP-OES for Determination of Bi in Milk	82
5.	CONCLUSION	83
6.	REFERENCES	87
	CV	99

ABSTRACT

DEVELOPMENT OF SENSITIVE ANALYTICAL METHODS FOR BISMUTH DETERMINATION BY ATOMIC SPECTROMETRIC TECHNIQUES

Ersin Kılınç

Ph.D. Thesis

DİCLE UNIVERSITY
GRADUATE SCHOOL OF NATURAL AND APPLIED SCIENCES
DEPARTMENT OF CHEMISTRY

2012

Development of sensitive and economical analytical methods for determination of bismuth (Bi) by using flame atomic absorption spectrometry (FAAS) and improvement the sensitivity of inductively coupled plasma optical emission spectrometry (ICP-OES) for Bi were the main purposes of the thesis.

An uncoated slotted quartz tube (SQT) device with two slots with an angle of 180° with respect to each other was used for sensitivity improvement in the initial stages of research. Uncoated SQT was also used for atom trapping (SQT-AT) studies. Then, several coating materials were used to modify the surface of SQT. These coatings materials were selected among the metals or metal oxides with relatively high melting and boiling points to assure their persistence on the surface of SQT during analytical procedures. Experimental variables such as acetylene flow rate, sample suction rate, height of SQT from burner, type and volume of organic solvent for revolatilization of Bi from SQT and trapping time of Bi solution in were optimized. By using double slotted SQT, sensitivity of FAAS was improved as 2.9 times.

Further improvement in sensitivity was achieved using SQT as atom trapping device. It was decided to use of 50.0 μL of methyl ethyl ketone for the revolatilization of Bi from SQT surface. Using the optimum parameters, linear calibration range was determined as 7.5-100.0 ng mL^{-1} for Bi. Enhancement, E, with respect to FAAS was found as 256 by SQT-AT-FAAS. By considering the 6.0 min collection of Bi solution at 6.0 mL min^{-1} sample flow rate E_t and E_v values were calculated as 43 min^{-1} and 7.1 mL^{-1} , respectively.

Non-volatile elements, Mo, Zr, W and Ta were tried as coating metal for SQT. It was observed that W coated SQT gave the highest absorption signal for Bi. LOD and LOQ were calculated as 0.14 and 0.46 $\mu\text{g mL}^{-1}$, respectively. Enhancement factor was calculated as 4.0 with respect to FAAS.

W coated SQT was also used as trapping device for Bi in FAAS. Trapping of Bi for 5.0 min at sample flow rate of 5.5 mL min^{-1} , LOD and LOQ were calculated as 0.51 ng mL^{-1} and 1.7 ng mL^{-1} , respectively. Characteristic concentration was calculated as 1.4 ng mL^{-1} . Enhancement, E, with respect to FAAS was 613.

The possible interference effects of the various cations and anions were investigated for SQT-AT-FAAS and W coated SQT-AT-FAAS. The accuracy of the techniques was checked by analyzing a standard reference material of simulated fresh water (NIST 1643e).

In addition, SQT devices with different inner and outer diameters were tested in order to investigate the possible effect on Bi signal depending on the wall thickness of the tube. Variation in Bi signal depending on length of upper slit was also investigated.

Experimental and instrumental variables in CF-HG-ICP-OES were optimized for Bi determination. LOD and LOQ were found as 0.16 ng mL^{-1} and 0.53 ng mL^{-1} , respectively. 12 times improvement with respect to conventional ICP-OES from slope ratio of linear calibration plots was achieved by optimizing of CF-HG-ICP-OES. Possible interferences effects of Cd, Co, Cu Fe, Ni, As, Hg, Sn and Sb ions in the determination of Bi by CF-HG-ICP-OES were investigated.

Keywords: Flame Atomic Absorption Spectrometry, Bi, Slotted Quartz Tube, Atom Trapping, Sensitivity Improvement, Continuous Flow Hydride Generation, Inductively Coupled Plasma Optical Emission Spectrometry

ÖZET

ATOMİK SPEKTROMETRİK TEKNİKLER İLE BİZMUT TAYİNİ İÇİN DUYARLI ANALİTİK YÖNTEMLERİN GELİŞTİRİLMESİ

Ersin Kılınç

Ph.D. Thesis

DİCLE ÜNİVERSİTESİ
FEN BİLİMLERİ ENSTİTÜSÜ
KİMYA ANABİLİM DALI

2012

Alevli atomik absorpsiyon spektrometri (AAAS) ile Bizmut (Bi) tayini için duyarlı analitik ve ekonomik metodların geliştirilmesi ve (indüktif eşleşmiş plazma optik emisyon spektrometresi) İEP-OES'de Bi'un duyarlılığını artırmak tezin asıl amacını oluşturmaktadır.

Çalışmanın ilk aşamalarında, üzerinde karşılıklı olarak 180° lik bir açı ile iki ayrı yarık bulunan ve yüzeyi kaplanmamış yarıklı kuvars tüp (YKT) duyarlılığı artırmak amacıyla denenmiştir. Kaplı olmayan bu YKT'ler atom tuzak (AT-YKT) çalışmalarında da kullanılmıştır. Daha sonra, YKT'ün yüzeyini modifiye etmek için farklı kaplama materyalleri kullanılmıştır. Bu kaplama materyalleri analitik prosedürler esnasında YKT yüzeyinde Bi'un tuzaklanmasıının sağlanması için ergime ve kaynama noktaları yüksek olan metal veya metal oksitler arasından seçilmiştir. Asetilen akış hızı, örnek çıkış hızı, YKT'ün alev başlığından uzaklığı, YKT yüzeyinden Bi'un yeniden uçucu hale getirilmesi için kullanılacak organik çözücüün tipi ve hacmi ve Bi çözeltisinin tuzaklama süresi gibi deneysel değişkenler optimize edilmiştir. Çift yarıklı YKT kullanılarak AAAS'nın duyarlılığında 2.9 kat iyileştirme sağlanmıştır.

YKT atom tuzaklayıcı bir aparat olarak kullanıldığından ise duyarlılıkta daha fazla artışlar sağlanmıştır. $50.0 \mu\text{L}$ metil etil ketonun YKT yüzeyinden Bi'un tekrar uçucu hale getirilmesi için kullanılmıştır. Optimum parametreleri kullanarak, Bi için lineer kalibrasyon aralığı $7.5\text{--}100.0 \text{ ng mL}^{-1}$ olarak belirlenmiştir. YKT-AT-AAAS kullanarak AAAS'ye göre 256 kat duyarlılık artışı elde edilmiştir. 6.0 mL min^{-1} örnek akış hızında Bi'un 6.0 min boyunca toplanması ile E_t ve E_v değerleri sırasıyla 43 min^{-1} ve 7.1 mL^{-1} olarak hesaplanmıştır.

Uçucu olmayan Mo, Zr, W ve Ta gibi elementler YKT için kaplama materyali olarak denenmiştir. W kaplı YKT'ün Bi için en yüksek absorpsiyon sinyali verdiği belirlenmiştir. Gözlenebilme ve tayin limitleri sırasıyla 0.14 ve $0.46 \mu\text{g mL}^{-1}$ olarak hesaplanmıştır. AAAS'ye göre duyarlılık artışı 4.0 olarak hesaplanmıştır.

W kaplı YKT, AAAS'de Bi için atom tuzaklayıcı aparat olarak da kullanılmıştır. 5.5 mL dak^{-1} akış hızında 5.0 min süre ile Bi'un tuzaklanması ile gözlenebilme sınırı ve tayin sınırı

sırasıyla 0.51 ng mL^{-1} ve 1.7 ng mL^{-1} olarak hesaplanmıştır. Karakteristik konsantrasyon değeri 1.4 ng mL^{-1} olarak bulunmuştur. AAAS' ye göre 613 katlık bir duyarlılık artışı sağlanmıştır.

Değişik katyon ve anyonların olası girişim etkileri YKT-AT-AAAS ve W kaplı YKT-AT-AAAS için incelenmiştir. Tekniklerin doğruluğu standart referans su örneğine (NIST 1643e) uygulanması ile kontrol edilmiştir.

YKT tüp duvarının kalınlığına bağlı olarak Bi sinyalindeki olası farklılıklar araştırmak için farklı iç ve dış çaplara sahip YKT'ler denenmiştir. Üst yarık uzunluğuna bağlı olarak Bi sinyalindeki değişiklikler de araştırılmıştır.

Bi tayini için sürekli akış-hidrür oluşturmalı induktif eşleşmiş plazma optik emisyon spektrometrisinde (SA-HO-İEP-OES) deneysel ve instrumental değişkenler optimize edilmiştir. Gözlenebilme ve tayin sınırları sırası ile 0.16 ng mL^{-1} and 0.53 ng mL^{-1} olarak bulunmuştur. SA-HO-İEP-OES ile ilgili parametreleri optimize ederek lineer kalibrasyon eşitliklerindeki eğim oranları üzerinden duyarlılıkta İEP-OES'e karşı 12 kat artış sağlanmıştır. SA-HO-İEP-OES ile Bi tayininde Cd, Co, Cu, Fe, Ni, As, Hg, Sn and Sb iyonlarının olası girişim etkileri araştırılmıştır.

Anahtar Kelimeler: Alevli Atomik Absorpsiyon Spektrometri, Bi, Yarıklı Kuvars Tüp, Atom Tuzaklama, Duyarlılık Artışı, Sürekli Akışlı Hidrür Oluşturma, İndüktif Eşleşmiş Plazma Optik Emisyon Spektrometri

LIST of TABLES

<u>Table No</u>		<u>Page</u>
Table 1.1.	Physical and chemical properties of Bi (NAS-NS 1977, Sun 2011)	2
Table 3.1.	Operating parameters of Bi hollow cathode lamp for FAAS	31
Table 3.2.	Operating conditions of ICP-OES and CF-HG-ICP-OES for Bi determination	32
Table 4.1.	Analytical characteristics of FAAS for Bi	38
Table 4.2.	Conditions of SQT-FAAS method for Bi	40
Table 4.3.	Analytical performance of SQT-FAAS for Bi	41
Table 4.4.	Effect of organic solvents on 100.0 ng mL ⁻¹ Bi signal for SQT-AT-FAAS method	42
Table 4.5.	Conditions for SQT-AT-FAAS method for Bi	47
Table 4.6.	Analytical performance of SQT-AT-FAAS for Bi (36.00 mL trapping, 6.0 min collection)	49
Table 4.7.	Results of the accuracy test for SQT-AT-FAAS method	50
Table 4.8.	Concentration of Bi in water samples by SQT-AT-FAAS	50
Table 4.9.	Effect of interfering ions on 75.0 ng mL ⁻¹ of Bi by SQT-AT-FAAS	54
Table 4.10.	Effect of coating material on 10.0 µg mL ⁻¹ Bi signal for metal coated SQT-FAAS method.	55
Table 4.11.	Conditions for W coated SQT-FAAS method for Bi	57
Table 4.12.	Analytical performance of W coated SQT-FAAS for Bi	59
Table 4.13.	Effect of organic solvents on 20.0 ng mL ⁻¹ Bi signal for W coated SQT-AT-FAAS method	59
Table 4.14.	Conditions for W coated SQT-AT-FAAS method for Bi	63
Table 4.15.	Analytical performance of W coated SQT-AT-FAAS for Bi	65
Table 4.16.	Results of the accuracy test for Bi by W coated SQT-AT-FAAS method (n=3)	66
Table 4.17.	Effect of interfering ions on 20.0 ng mL ⁻¹ of Bi in W coated SQT-AT-FAAS method	70
Table 4.18.	Analytical features of optimized methods	72
Table 4.19.	Effect of size of SQT on 10.0 µg mL ⁻¹ of Bi signal (length of SQT was 14.0 cm in all cases)	73
Table 4.20.	Effect of interferent concentrations on 10.0 ng mL ⁻¹ of Bi by CF-HG-ICP-OES	79
Table 4.21.	Optimized parameters of CF-HG-ICP-OES for Bi	80

Table 4.22.	Analytical characteristics of ICP-OES and CF-HG-ICP-OES methods for Bi determination.	80
Table 4.23.	Comparison of analytical features of optimized method versus literature	81
Table 4.24.	Determination of Bi in milk samples by CF-HG-ICP-OES	82

LIST of FIGURES

<u>Figure No</u>		<u>Page</u>
Figure 1.1.	Long-tube absorption cell a) open ended, b) T-shaped (Matusiewicz 1997)	5
Figure 1.2.	Delves' microsampling cup system (Lajunen 1992)	6
Figure 1.3.	Schematic representation of SQT (Watling 1977)	7
Figure 1.4.	Schematic representation of flame AAS-gas screen-slotted quartz tube (Gholami et al. 2011)	8
Figure 1.5.	Schematic presentation of water-cooled atom trap system (Ataman 2008)	9
Figure 1.6.	Design of water cooled atom traps (a) single tube, (b) double tube and (c) end view of triple tube (Brown et al 1987)	10
Figure 1.7.	Schematic presentation of slotted-tube water-cooled atom-trap (STWCAT) system (Matusiewicz and Kopras 1997)	11
Figure 1.8.	Optimization of SQT slot positions with respect to each other for In (Arslan et al. 2011)	13
Figure 1.9.	Hydride generation with <i>in situ</i> preconcentration in a palladium coated graphite atomizer for Cd determination, DDAB:didodecyldimethylammonium bromide (Infante et al. 2006)	16
Figure 1.10.	Schematic presentation of slotted quartz tube-atom trap-hydride generation atomic absorption spectrometric determination of lead (Ertaş et al. 2008)	17
Figure 1.11.	Schematic presentation of quartz T-tube and W-coil trap (Kula et al. 2008)	18
Figure 1.12.	Emission process of individual metal in plasma (Boss and Fredeen 2004)	18
Figure 1.13.	Schematic presentation of ICP-OES instrument (Boss and Fredeen 2004)	19
Figure 2.1.	Schematic presentation of hydride generation-integrated atom trap-atomic absorption spectrometric determination of Bi (Matusiewicz and Krawczyk 2007b)	25
Figure 2.2.	Schematic presentation of W coil HG-AAS (a) general configuration (b) W-trap placed in silica T-tube (Cankur et al. 2002)	26
Figure 2.3.	Schematic diagrams of gas-liquid separators for bismuth hydride (Chen et al. 2002).	28
Figure 3.1.	Schematic presentation of hydride generation manifold	32
Figure 4.1.	Investigation of acetylene flow rate for FAAS determination of Bi; 20.0 $\mu\text{g mL}^{-1}$ Bi; flow rate of air: 4.0 L min^{-1} , sample suction rate: 5.5 mL min^{-1}	36

Figure 4.2.	Investigation of suction flow rate for FAAS determination of Bi; 20.0 $\mu\text{g mL}^{-1}$ Bi, flow rate of air: 4.0 L min^{-1} , flow rate of acetylene: 1.5 L min^{-1}	37
Figure 4.3.	Linear calibration plot for Bi in FAAS; flow rate of air: 4.0 L min^{-1} , flow rate of acetylene: 1.5 L min^{-1} , sample suction rate: 8.5 mL min^{-1}	37
Figure 4.4.	Investigation of acetylene flow rate for SQT-FAAS determination of Bi; 15.0 $\mu\text{g mL}^{-1}$ Bi; flow rate of air: 4.0 L min^{-1} , sample suction rate: 5.5 mL min^{-1} , 2.0 mm height of SQT from burner	38
Figure 4.5.	Investigation of suction rate of sample for SQT-FAAS determination of Bi; 15.0 $\mu\text{g mL}^{-1}$ Bi, flow rate of air: 4.0 L min^{-1} , flow rate of acetylene: 1.5 L min^{-1} , 2.0 mm height of SQT from burner	39
Figure 4.6.	Investigation of height of SQT from burner for SQT-FAAS determination of Bi; 15.0 $\mu\text{g mL}^{-1}$ Bi; flow rate of air: 4.0 L min^{-1} , flow rate of acetylene: 1.5 L min^{-1} , sample suction rate: 8.5 mL min^{-1}	40
Figure 4.7.	Linear calibration plot for Bi in SQT-FAAS; flow rate of air: 4.0 L min^{-1} , flow rate of acetylene: 1.5 L min^{-1} , sample suction rate: 8.5 mL min^{-1} , 2.0 mm height of SQT from burner	41
Figure 4.8.	Investigation of volume of organic solvent for SQT-AT-FAAS determination of Bi; 100.0 ng mL^{-1} Bi; 2.0 mm height of SQT from burner, flow rate of air: 4.0 L min^{-1} , flow rate of acetylene: 0.6 L min^{-1} , sample suction rate: 5.5 mL min^{-1} , 2.0 min of trapping time	43
Figure 4.9.	Investigation of sample suction rate for SQT-AT-FAAS determination of Bi; 100.0 ng mL^{-1} Bi; 2.0 mm height of SQT from burner, flow rate of air: 4.0 L min^{-1} , flow rate of acetylene: 0.6 L min^{-1} , 2.0 min of trapping time, 50.0 μL of MEK	44
Figure 4.10.	Investigation of acetylene suction rate for SQT-AT-FAAS determination of Bi; 100.0 ng mL^{-1} Bi; 2.0 mm height of SQT from burner, flow rate of air: 4.0 L min^{-1} , sample suction rate: 6.0 mL min^{-1} , 2.0 min of trapping time, 50.0 μL of MEK	45
Figure 4.11.	Investigation of height of SQT from burner for SQT-AT-FAAS determination of Bi; 100.0 ng mL^{-1} Bi; flow rate of air: 4.0 L min^{-1} , flow rate of acetylene: 0.5 L min^{-1} , sample suction rate: 6.0 mL min^{-1} , 2.0 min of trapping time, 50.0 μL of MEK	46
Figure 4.12.	Investigation of trapping time for SQT-AT-FAAS determination of Bi; 100.0 ng mL^{-1} Bi; 2.0 mm height of SQT from burner, flow rate of air: 4.0 L min^{-1} , flow rate of acetylene: 0.5 L min^{-1} , sample suction rate: 6.0 mL min^{-1} , 50.0 μL of MEK.	47
Figure 4.13.	Analytical signals for 75.0 ng mL^{-1} Bi, total signal (a), corrected signal (b), D2 background signal (c) by SQT-AT-FAAS using the conditions in Table 4.5.	48
Figure 4.14.	Calibration plot for Bi in SQT-AT-FAAS using the parameters in Table 4.5.	48
Figure 4.15.	Linear calibration plot for Bi in SQT-AT-FAAS using the parameters in Table 4.5.	49

Figure 4.16.	Interference effects of Na, Ca and Mg on 75.0 ng mL ⁻¹ of Bi signal in SQT-AT-FAAS	51
Figure 4.17.	Interference effects of Mn, Cr, Fe, Zn and Al on 75.0 ng mL ⁻¹ of Bi signal in SQT-AT-FAAS	52
Figure 4.18.	Interference effects of Co, Cu, Ni and Mo on 75.0 ng mL ⁻¹ of Bi signal in SQT-AT-FAAS	52
Figure 4.19.	Interference effects of Sn, Sb and Se on 75.0 ng mL ⁻¹ of Bi signal in SQT-AT-FAAS	53
Figure 4.20.	Interference effects of SO ₄ ²⁻ , NO ₂ ⁻ and Cl ⁻ on 75.0 ng mL ⁻¹ of Bi signal in SQT-AT-FAAS	53
Figure 4.21.	Investigation of acetylene flow rate for W coated SQT-FAAS determination of Bi; 10.0 µg mL ⁻¹ Bi; flow rate of air: 4.0 L min ⁻¹ , sample suction rate: 4.5 mL min ⁻¹ , 2.0 mm height of SQT from burner	55
Figure 4.22.	Investigation of suction rate of sample for W coated SQT-FAAS determination of Bi; 10.0 µg mL ⁻¹ Bi; flow rate of air: 4.0 L min ⁻¹ , flow rate of acetylene: 0.6 L min ⁻¹ , 2.0 mm height of SQT from burner	56
Figure 4.23.	Investigation of height of SQT from burner for W coated SQT-FAAS determination of Bi, 10.0 µg mL ⁻¹ Bi; flow rate of air: 4.0 L min ⁻¹ , flow rate of acetylene: 0.6 L min ⁻¹ , sample suction rate: 5.6 mL min ⁻¹	57
Figure 4.24.	Calibration plot for Bi by W coated SQT-FAAS method, 2.0 mm height of SQT from burner, flow rate of air: 4.0 L min ⁻¹ , flow rate of acetylene: 0.6 L min ⁻¹ , sample suction rate: 5.6 mL min ⁻¹	58
Figure 4.25.	Linear calibration plot for Bi in W coated SQT-FAAS method, 2.0 mm height of SQT from burner, flow rate of air: 4.0 L min ⁻¹ , flow rate of acetylene: 0.6 L min ⁻¹ , sample suction rate: 5.6 mL min ⁻¹	58
Figure 4.26.	Investigation of volume of MIBK for W coated SQT-AT-FAAS determination of Bi; 20.0 ng mL ⁻¹ Bi; 2.0 mm height of SQT from burner, flow rate of air: 4.0 L min ⁻¹ , flow rate of acetylene: 0.6 L min ⁻¹ , sample suction rate: 4.5 mL min ⁻¹ , 2.0 min of trapping time	60
Figure 4.27.	Investigation of suction rate of sample for W coated SQT-AT-FAAS determination of Bi; 20.0 ng mL ⁻¹ Bi; 2.0 mm height of SQT from burner, flow rate of air: 4.0 L min ⁻¹ , flow rate of acetylene: 0.6 L min ⁻¹ , 2.0 min of trapping time, 50.0 µL of MIBK	61
Figure 4.28.	Investigation of flow rate of acetylene for W coated SQT-AT-FAAS determination of Bi; 20.0 ng mL ⁻¹ Bi; 2.0 mm height of SQT from burner, flow rate of air: 4.0 L min ⁻¹ , sample suction rate: 5.5 mL min ⁻¹ , 2.0 min of trapping time, 50.0 µL of MIBK	62
Figure 4.29.	Investigation of height of W coated SQT for W coated SQT-AT-FAAS determination of Bi; 20.0 ng mL ⁻¹ Bi; flow rate of air: 4.0 L min ⁻¹ , flow rate of acetylene 0.6 L min ⁻¹ , sample suction rate: 5.5 mL min ⁻¹ , 2.0 min of trapping time, 50.0 µL of MIBK	62

Figure 4.30.	Investigation of trapping period for W coated SQT-AT-FAAS determination of Bi; 20.0 ng mL ⁻¹ Bi; flow rate of air: 4.0 L min ⁻¹ , flow rate of acetylene 0.6 L min ⁻¹ , 2.0 mm height of SQT from burner, sample suction rate: 5.5 mL min ⁻¹ , 50.0 µL of MIBK	63
Figure 4.31.	Analytical signals for 20.0 ng mL ⁻¹ Bi, corrected signal (a), total signal (b), D2 background signal (c) by W coated SQT-AT-FAAS using the conditions in Table 4.14.	64
Figure 4.32.	Calibration plot for Bi by W coated SQT-AT-FAAS using the conditions in Table 4.14.	64
Figure 4.33.	Linear calibration plot for Bi by W coated SQT-AT-FAAS using the conditions in Table 4.14.	65
Figure 4.34.	Interference effects of Na, Ca and Mg on 20.0 ng mL ⁻¹ of Bi signal in W coated SQT-AT-FAAS	67
Figure 4.35.	Interference effects of Mn, Cr, Fe, Zn and Al on 20.0 ng mL ⁻¹ of Bi signal in W coated SQT-AT-FAAS	67
Figure 4.36.	Interference effects of Co, Cu, Ni and Mo on 20.0 ng mL ⁻¹ of Bi signal in W coated SQT-AT-FAAS	68
Figure 4.37.	Interference effects of Sn, Sb and Se on 20.0 ng mL ⁻¹ of Bi signal in W coated SQT-AT-FAAS	69
Figure 4.38.	Interference effects of SO ₄ ²⁻ and NO ₂ ⁻ and Cl ⁻ on 20.0 ng mL ⁻¹ of Bi signal in W coated SQT-AT-FAAS	69
Figure 4.39.	Investigation of concentration of HCl; experimental conditions; 10.0 ng mL ⁻¹ of Bi, argon flow rate: 17.0 L min ⁻¹ , carrier argon flow rate 0.6 L min ⁻¹ , Rf power: 1450 Watt, flow rate of standard solution, NaBH ₄ and waste: 1.5 mL min ⁻¹ , 0.25% NaBH ₄ in 1.0% NaOH, reaction coil 11.0 cm, stripping coil 35.0 cm	74
Figure 4.40.	Investigation of concentration of NaBH ₄ in 1.0 % NaOH; experimental conditions; 10.0 ng mL ⁻¹ of Bi in 5.0 mol L ⁻¹ HCl, argon flow rate: 17.0 L min ⁻¹ , carrier argon flow 0.6 L min ⁻¹ , Rf power: 1450 Watt, flow rate of standard solution, NaBH ₄ and waste: 1.5 mL min ⁻¹ , reaction coil 11.0 cm, stripping coil 35.0 cm	75
Figure 4.41.	Investigation of flow rate of carrier argon; experimental conditions; 10.0 ng mL ⁻¹ of Bi in 5.0 mol L ⁻¹ HCl, reductant 1.0% NaBH ₄ in 0.25% NaOH, argon flow rate: 17.0 L min ⁻¹ , Rf power: 1450 Watt, flow rate of standard solution, NaBH ₄ and waste: 1.5 mL min ⁻¹ , reaction coil 11.0 cm, stripping coil 35.0 cm	76
Figure 4.42.	Investigation of RF power; experimental conditions; 10.0 ng mL ⁻¹ of Bi in 5.0 mol L ⁻¹ HCl, reductant 1.0% NaBH ₄ in 0.25% NaOH, argon flow rate: 17.0 L min ⁻¹ , 0.5 mL min ⁻¹ of flow rate of carrier, flow rate of standard solution, NaBH ₄ and waste: 1.5 mL min ⁻¹ , reaction coil 11.0 cm, stripping coil 35.0 cm	76

Figure 4.43. Investigation of flow rates of sample solution and reductant; 77
experimental conditions; 10.0 ng mL⁻¹ of Bi in 5.0 mol L⁻¹ HCl,

reductant 1.0% NaBH₄ in 0.25% NaOH, argon flow rate: 17.0 L min⁻¹,
Rf power: 1375 Watt, flow rate of waste 1.5 mL min⁻¹, reaction coil
11.0 cm, stripping coil 35.0 cm

Figure 4.44. Linear calibration graph for Bi by CF-HG-ICP-OES (experimental 81
conditions were given in Table 4.21.)

LIST of ABBREVIATIONS

AES	Atomic Emission Spectrometry
AFS	Atomic Fluorescence Spectrometry
CCD	Charge Coupled Device
CF-HG-ICP-OES	Continuous Flow – Hydride Generation – Inductively Coupled Plasma-Optical Emission Spectrometry
CRM	Certified Reference Material
CVG	Chemical Vapour Generation
CVAAS	Cold Vapour Atomic Absorption Spectrometry
DBD	Dielectric Barrier Discharge
DDAB	Didodecyldimethylammonium bromide
DLLME	Dispersive Liquid Liquid Micro Extraction
EcHG	Electrochemical Hydride Generation
Ec-HG-AFS	Electrochemical Hydride Generation Atomic Fluorescence Spectrometry
FAAS	Flame Atomic Absorption Spectrometry
FDA	Food and Drug Administration
FI-AAS	Flow Injection - Atomic Absorption Spectrometry
GC-ICP-MS	Gas Chromatography - Inductively Coupled Plasma - Mass Spectrometry
GF-AAS	Graphite Furnace - Atomic Absorption Spectrometry
HG	Hydride Generation
HG-AAS	Hydride Generation - Atomic Absorption Spectrometry
HG-AFS	Hydride Generation - Atomic Fluorescence Spectrometry
HG-DBD-AFS	Hydride Generation Dielectric Barrier Discharge Atomic Fluorescence Spectrometry
HG-ETV-MIP-OES	Hydride Generation - Electrothermal Vaporization - Microwave Induced Plasma - Optical Emission Spectrometry
HG-ICP-OES	Hydride Generation - Inductively Coupled Plasma - Optical Emission Spectrometry

HG-N ₂ -MIP-AES	Hydride Generation-Nitrogen-Microwave Induced Plasma - Optical Emission Spectrometry
IAT	Integrated Atom Trap
i.d	Inner Diameter
ICP-OES	Inductively Coupled Plasma - Optical Emission Spectrometry
ICP-MS	Inductively Coupled Plasma - Mass Spectrometry
LPAT	Long-Path Absorption Tube
LOD	Limit of Detection
LOQ	Limit of Quantification
MEK	Methyl Ethyl Ketone
MIBK	Methyl Isobutyl Ketone
NIST	National Institute of Standard and Technology
o.d.	Outer Diameter
RSD	Relative Standard Deviation
SEM	Scanning Electron Microscopy
SQT	Slotted Quartz Tube
SQT-FAAS	Slotted Quartz Tube – Flame Atomic Absorption Spectrometry
SQT-AT-FAAS	Slotted Quartz Tube – Atom Trapping - Flame Atomic Absorption Spectrometry
SRM	Standard Reference Material
TMB	Trimethyl Bismuth
TCM	Traditional Chinese Medicine
THF	Tetrahyrofuran
VGAAS	Vapour Generation - Atomic Absorption Spectrometry
WC-IAT	Water Cooled - Integrated Atom Trap
XPS	X-ray Photoelectron Spectroscopy

1. INTRODUCTION

It is well known that metals either essential or not have an important role in living organism. Some of them are dangerous to health or to the environment (e.g. mercury, cadmium, lead, chromium), some may cause corrosion (e.g. zinc, lead), some are harmful in other ways (e.g. arsenic may pollute catalysts). Classification of metals depends on their concentrations in related matrixes. Some of these are actually necessary for humans at trace levels (selenium, copper, chromium, manganese) while others are carcinogenic or toxic, affecting, the central nervous system (manganese, mercury, lead, arsenic), the kidneys or liver (mercury, lead, cadmium, copper) or skin, bones, or teeth (nickel, cadmium, copper, chromium). Nowadays, a growing trend by the researchers has been focused on the speciation of certain metals such as selenium (II and IV), chromium (III and VI) and arsenic (III and V). In particular, alkylated metals and metalloids are become a matter of primary. Furthermore, elemental composition has a critical importance for alloys in view of their physical and chemical properties such as melting point, conductivity, corrosion resistance, analysis of impurities in high-purity metals etc. Thus, the concentration of metals should be defined for different matrixes such as foods, waters, plants and also anthropogenic wastes. Consequently a chemical analysis for individual species is needed.

Flame atomic absorption spectrometry (FAAS), graphite furnace atomic absorption spectrometry (GF-AAS), inductively coupled plasma optical emission spectrometry (ICP-OES), inductively coupled plasma mass spectrometry (ICP-MS) and rarely atomic fluorescence spectrometry (AFS) have been employed for the determination of metals at trace, minor and major levels. The selection of the technique is dependent on their concentrations in final solution and availability of the instrument. While AAS and ICP-OES can be used for the determination at $\mu\text{g mL}^{-1}$ level, GF-AAS and ICP-MS can be applied for ultra trace determination of metals at the level of ng mL^{-1} . To decide the method, total cost per analysis should be also considered by users. As a general approach, the prices of instruments which should be considered can be listed from highest to lowest one as ICP-MS, ICP-OES, ET-AAS, AAS, respectively. The most important issue which is paid sufficient attention is the detection limits of the techniques. Nowadays, ICP-MS is employed as a powerful analytical technique at the concentration level of ng mL^{-1} level around 8 orders of magnitude of concentration units as dynamic range from lithium to uranium. This technique is also widely used the field of radiometric dating, in which it is used to analyze relative abundance of different isotopes over the others.

On the other hand, ICP-MS or GF-AAS instruments are not often available in any laboratory, especially in developing countries. To overcome these problems, many preconcentration methods are presented in literatures. Less of these are found ways to application area, because, these are based on the use of time consuming and expensive chemical procedures. The techniques based on *in situ* trapping such as the use of long path absorption tubes, slotted quartz tube and vapour generation have been attempted to overcome this problem by the analytical chemists. Among them, slotted quartz tube and vapour generation by hydride formation were commercialized by manufacturers.

1. INTRODUCTION

Up to now, there is no unique method to overcome these problems. Thus, many of the researchers have focused on solving this problem for individual elements. Among them, Bi has been received special attention by analytical chemists.

The reason of it is insufficient sensitivity of AAS for Bi. The aim of this study as a Ph.D is to development of sensitive analytical methods for Bi by flame AAS. For this purpose, an uncoated slotted quartz tube (SQT) device with two slots with an angle of 180° with respect to each other will be used for sensitivity improvement in the initial stages of research. Uncoated SQT was also used for atom trapping (SQT-AT) studies. Then, several coating materials will be used to modify the surface of SQT and sensitivity comparisons will be made. These coatings will mainly include the metals or metal oxides with relatively high melting and boiling points to assure their persistence on the surface of SQT during analytical procedures. In addition, SQT devices with different inner and outer diameters will be tested in order to investigate the possible differences in analytical behavior depending on the wall thickness of the tube. All the parameters for uncoated and coated SQT's will also be optimized for atom trapping studies. The possible interference effects of the cations and anions will be evaluated for above mentioned techniques. The accuracy of the techniques will be checked by analyzing the standard reference samples which contains Bi.

1.1 Bismuth

Bi (New Latin *bisemutum* from German *Wismuth*, perhaps from *weiße Masse*, "white mass") was confused in early times with tin and lead because of its resemblance to those elements. It has been known since ancient times, so no person is credited with its discovery (Wikipedia 2012). Bi, a white, crystalline, brittle metal with a pinkish tinge, is a member of periodic table in Group V with nitrogen, phosphorus, arsenic and antimony. Bismuth has two valencies of 3+ and 5+. In the Earth's crust, bismuth, 0.00002%, is about twice as abundant as gold. Bi naturally occurs in the ore as bismite (Bi_2O_3), bismuthinite (Bi_2S_3) and bismuthite ($(\text{BiO})_2\text{CO}_3$) (NAS-NS 1977, Sun 2011). Physical and chemical properties of Bi are summarized in Table 1.1.

Table 1.1. Physical and chemical properties of Bi (NAS-NS 1977, Sun 2011)

Parameter	Value
Atomic number	83
Atomic weight	208.980
Density	9.8 g mL ⁻¹
Melting point	271 °C
Boiling point	1560 °C
Electronegativity x^P (Pauling scale)	2.02
Atomic radius	1.55 Å
Ionization energies, kJ mol ⁻¹	
$\text{M} \rightarrow \text{M}^+$	703.2
$\text{M}^+ \rightarrow \text{M}^{2+}$	1610
$\text{M}^{2+} \rightarrow \text{M}^{3+}$	2466
$\text{M}^{3+} \rightarrow \text{M}^{4+}$	4372
$\text{M}^{4+} \rightarrow \text{M}^{5+}$	5400

Bi has attracted attention as semiconductors, medicine for treatment of syphilis, peptic ulcers and dermatological disorders, alloys, catalyst, metallurgical additives, fuel carrier, and coolant for nuclear reactor and as neutron windows in medical reactors (NAS-NS 1977, Das et al. 2006). Interestingly, Bi found an application area in cosmetic products such as pigments in eye shadow, lipsticks and hair dyes (Das et al. 2006). Bismuth salicylate is used to preserve the wine from bacteria and other harmful entities (Chinesepo 2012).

China is market leader as producer of Bi with 40% market share (Wikipedia 2012a). According to the data on 2009, mine production of bismuth was 7,300 tonnes, with the major contributions from China (4,500 tonnes), Mexico (1,200 tonnes) and Peru (960 tonnes) (USGS 2010). This price of Bi mine was \$28.97 per kg in 1Q 2009, \$27.33 per kg in 2Q 2009, \$23.77 per kg in 3Q 2009, and \$27.83 in 4Q 2009 (Basicmines 2010) over the world.

1.1.1. Bismuth and Health

Due to low absorption of Bi, it was considered as one of the least toxic heavy metals (Cadore et al. 1998; Das et al. 2006). Bismuth compounds have been used in medicine for more than 200 years in a variety of gastrointestinal disorders, because of their demulcent properties (Afkhami et al. 2006). Bi was used to treatment for syphilis, 70 years ago (Burguera et al. 1999). It has been used in medicines for the treatment of helicobacter pyloric-induced gastritis (Madrakian et al. 2003). Metabolism of Bi and its compounds in humans is as yet unknown. Some of the microorganism which methylates the Bi is known components of the human intestinal microflora (Boertz et al. 2009). Due to the rather low toxicity of Bi compounds, some bismuth thiol biocides have been tested for use as disinfectors in drinking water instead of other more toxic counterparts such as copper and silver species (Codony et al. 2003).

Recently, U.S. Food and Drug Administration (FDA) announced that bismacine/chromacine, contains high amounts of bismuth, used as a purported treatment for Lyme disease can cause serious health problem such as bismuth poisoning include cardio-vascular collapse and kidney failure (FDA 2006, Wikipedia 2012b). It is highlighted that bimacine is not approved in any form for use by injection, and recommended not use its because two deaths are recorded following the use of intravenous bismacine to treat Lyme disease (Wikipedia 2012b).

1.2. Atomic Absorption Spectrometry

‘Why couldn’t atomic absorption spectra be used for elemental analysis’ was the Walsh’s question. Last six decade showed that it was an ending point.

Flame atomic absorption spectrometry (FAAS) is a well known analytical technique using for elemental analysis over the world. It is used for a number of applications such as research-development, food quality, environmental analysis, pollution control process, etc. Independently, Walsh from Australia and Alkemade and Milatz from

1. INTRODUCTION

Netherlands published their papers about AAS in 1955 (Alkemade et al; 1955; Walsh 1955). It was accepted as a milestone for atomic spectroscopy in the further development in AAS.

An AAS instrument contains a radiation source such as hollow cathode lamp (HCL) or electrodeless discharge lamp (EDL), which emits the spectrum of the analyte element; an atomizer such as flame or graphite furnace, in which the analyte atoms in samples are atomized; a monochromator for the spectral dispersion of the radiation with an exit slit for an selection of the resonance line; a detector to measurement the intensity of radiation; an amplifier and display (Ewing 1960; Mester and Sturgeon 2003).

HCL is used for one element, but multi-element lamps are also commercially available. Main drawback of multi elements lamps is that often compromising operating conditions must be used, which may have an unfavorable effect on the signal-to-noise ratio and linear range for some of the analytes. EDL's are more expensive than HCL but give higher light intensity than HCL. Higher sensitivity and enhanced detection limit were obtained for As using EDL (Mester and Sturgeon 2003).

There are two major factors which limit the sensitivity of the AAS. The first one is about the low efficiency of the conventional nebulization process. Only a small portion of sample, 1-10%, can be transported to atomizer as aerosol. The remaining part of the sample which contains analyte atoms is sent to waste. When the sample aerosol enters the atom cell, it is desolvated by flame and then it dissociates the salts present into their constituent atoms. The individual atoms of the analyte will then absorb the light emitted from the light source and the amount of light absorbed can be related to the concentration of the analyte in the sample. A mixture of air and acetylene is the common flame type. Three type of flame are employed as following: fuel rich (here a yellow flame that has reducing properties is produced), fuel lean (a blue flame that is chemically oxidizing) or stoichiometric (an intermediate flame that is blue but also has yellow "feathers" at its base). It should be optimized for each of elements. According to the type of flame, temperature changes in the range of 1700 and 2200 K. However, some refracter elements require higher temperature. In this case nitrous oxide–acetylene (2500–2700 K) may be employed. Another optimization is the amounts of acetylene and nitrous oxide (Mester and Sturgeon 2003; Skoog et al. 1998).

Intensity of monochromatic radiation from light source decreases when it is absorbed by detected atom. Photomultiplier tube (PMT) or solid-state electronic devices (such as a charge coupled device -CCD- or charge injection device -CID- or diode array) are employed to detect the radiation. Decreasing in intensity is given as absorbance. The absorbance is defined as the logarithm of ratio of intensity of incident power to transmitted monochromathic radiation power. Since absorption is a ratio, it has no units (Mester and Sturgeon 2003; Skoog et al. 1998).

Therefore, only a small portion of analytes can reach to burner and absorb the monochromatic radiation from light source. As a result lower analytical signal is recorded during partial nebulization. The second drawback of AAS is about the short residence time of analyte in the measurement zone. It means that less interactions of atoms with monochromatic light and therefore loss in signal. Short residence time of

analytes on optical path is accepted as limitation (Yaman and Akdeniz 2006; Ataman 2007; Ataman 2008). Researches have been focused to solve this problem is the cause of birth of the sensitivity enhancement methods such as atom trapping, chemical vapour generation (CVG) and also electrothermal atomizer for AAS. L'vov mentioned about this that in his paper as 'I accidentally came across Walsh's paper at the end of 1955' (L'vov 2005). In 1957, graphite furnace contained a few crystals of sodium chloride used by L'vov in his first experiments (Welz 1999).

However, the sensitivity of FAAS does not meet the demands of trace and ultra-trace analysis for some samples. Attempts about sensitivity enhancement are summarized in following subsections.

1.2.1. Long-Path Absorption Tube (LPAT)

Long-path absorption tubes (LPAT) as long as a meter was suggested to enhance the sensitivity of AAS by increasing the popularity and life time of analyte atoms on optical path. LPAT are either open ended (Figure 1.1.a.) or T shaped (Figure 1.1.b.). Ten times sensitivity increasing was obtained for Pt by using T-shaped flame adaptor. Cu, Ag, Au and Cd were determined with 5.0-13.0 times sensitivity improvements by using similar one. It should be noted that the sensitivity is not proportional to the length of tube (Matusiewicz 1997; Ataman 2008). Different materials such as silica, vycor, alundum, ceramic and alumina, were used as material for LPAT. LPAT-FAAS was employed in a variety of analysis such as Cd determination in urine and blood serum, Sn in hydrogen peroxide solution, Zn in biological liquids and alloy, Se in aminoacid and protein etc (Matusiewicz 1997).

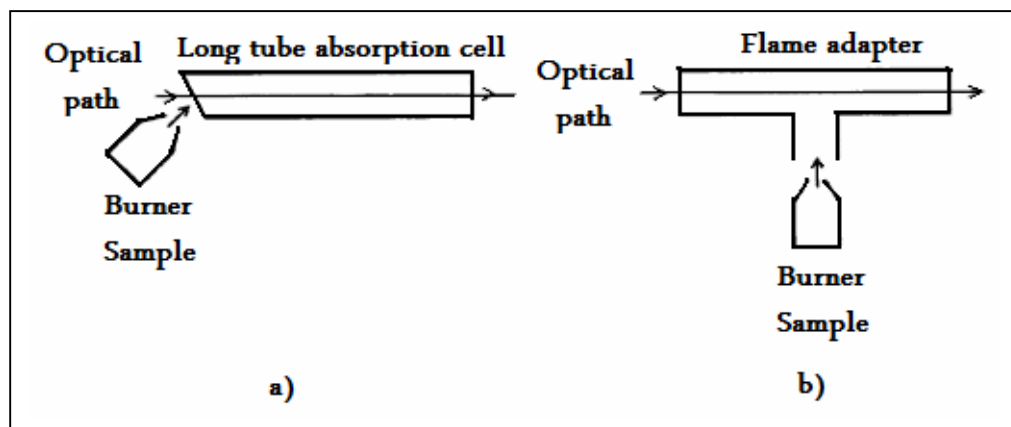


Figure 1.1. Long-tube absorption cell a) open ended, b) T-shaped (Matusiewicz 1997)

Main drawbacks of LPAT were physical limitations and strong background absorption by molecular species in the flame gases and scattering in tube. Although, favorable results were obtained and published by using LPAT, it was not commercialized (Matusiewicz 1997). In addition, memory effect was observed during the experiments (West 1988).

1. INTRODUCTION

1.2.2. Delves' Microsampling Cup

Delves' cup microsampling technique was shown schematically in Figure 1.2 was developed for determination lead in biological samples. The main idea was present an alternative sample introduction over the conventional nebulization via aspiration of solution and increase the residence time of free analyte atoms in the long cylindrical tube of multislot burner positioned about 2 cm below. It required a micro amount of sample added to nickel crucible. Micro amount of sample is placed in cup and dried by holding it in flame or heated plate. Then, it is transferred to hottest region of flame to vaporize the sample. Atomic vapour from flame enters a horizontal quartz tube. It provides longer residence time of analyte atoms in optical path (Ewing 1960). It was applied to determination of some Ag, As, Bi, Cd, Se, Te, Tl and Zn (Lajunen 1992). In case of acidic materials, nickel cups must be neutralized before use or different cup made of tantalum or other inert materials should be used (Ewing 1960).

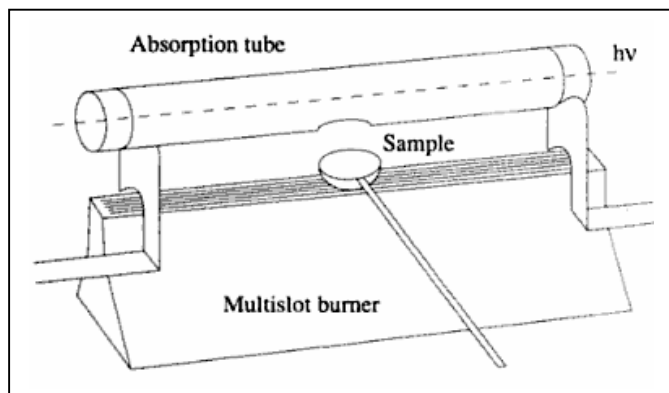


Figure 1.2. Delves' microsampling cup system (Lajunen 1992)

Better sensitivity and longer lifetime of tube were investigated by trying stainless-steel, carbon and ceramic instead of nickel as a cup material. The use of Ir cup was recommended especially for Ag, Cu and Mn. Applications of Delves' cup microsampling technique were extended by using nitrous oxide-acetylene flame instead of air-acetylene flame through the analysis of relatively non-volatile elements.

Although this technique was commercialized by Perkin-Elmer, it did not find a routine application in long term (Matusiewicz 1977).

1.2.3. Slotted Quartz Tube

Anyone could say that SQT technique developed by Watling had obvious advantages over the LPAT and Delves' techniques.

In 1977, Watling recommended the use of SQT for the analysis of trace metals in fresh water. Fourteen elements include Bi were investigated and sensitivity enhancements were obtained for all except for iron (Watling 1977). It was positioned above the 5 mm

to burner head and contained two slots (Figure 1.3.). The internal slot, near to burner, was longer from the external one which flame quit the tube from here. La solution of 1% (m/v) was used to prevent the SQT from devitrification and to increase the reusability of the tube. By using SQT, 2-5 times sensitivity enhancements were obtained (Watling 1977) for volatile elements. The increased residence time of analyte on optical path due to a slower flame speed and more interaction with together were causes the sensitivity enhancement. Although SQT studies were performed by using inexpensive quartz material, stainless steel, silicon nitride and graphite tubes were also tried for same purpose. An improvement up to 9 was obtained from these experiments.

SQT was also presented as an accessory of AAS by Philips, Carl Zeiss Jena, Varian, GBC, Unicam and Perkin Elmer.

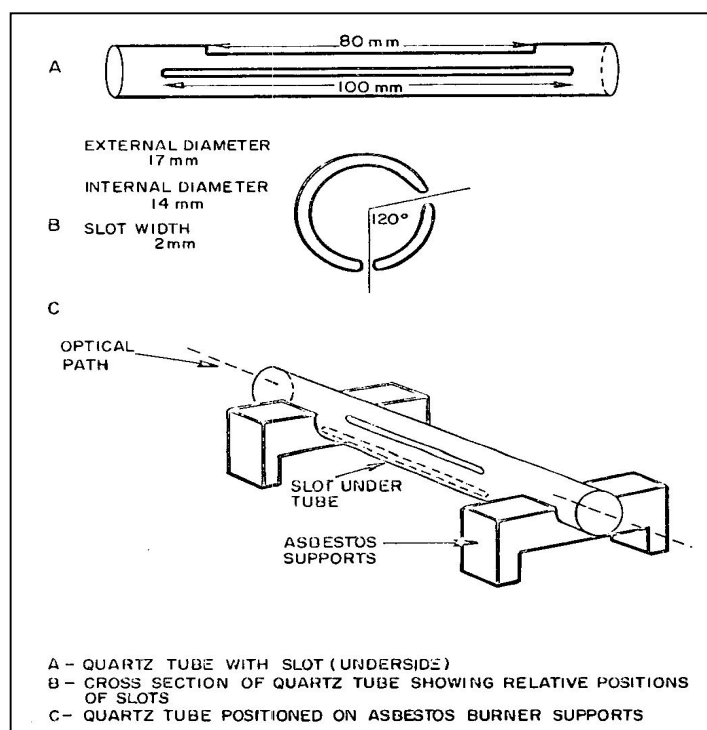


Figure 1.3. Schematic representation of SQT (Watling 1977)

Applications of SQT to enhance the sensitivity of AAS for the determination of Pb, Cd, and Cu in river and drinking water, whole blood and urine, Pb and Cd in paint, soil and leaves, Bi, Cd, Cu, Mn, Pb, Zn in soil, fertilizers, waste water, air, Ag, As, Bi, Cd, Hg, Pb, Se, Te, Tl, Zn in aqueous solutions were given in review by Matusiewicz (1997).

Improvement sensitivities were obtained for lead and cadmium by changing the diameters of tube and lengths of slits. LOQs were calculated as 35.0 and 4.0 ng mL⁻¹ respectively for Pb and Cd by Yaman (2005). In another work, Pb, Cd and Cu were determined in plant leaves sampled around industrial region by STAT-FAAS (Kaya and Yaman 2008). Cu concentrations in cancerous and non-cancerous human thyroid tissues were determined by using STAT-FAAS. Effect of inner and outer diameter and

1. INTRODUCTION

length of tube was also investigated. 3.5 times sensitivity improvement was achieved for Cu (Yaman and Akdeniz 2004).

SQT was also used combination with flow-injection flame atomic absorption spectrometry (FI-AAS) with advantages over the conventional use of SQT. Cu, Pb, Cd and Au were determined in urine with improved sensitivity. In addition, the life of tube was improved by a factor of 5.0-6.0 (Xu et al. 1992).

A gas screen (GS) was adapted to SQT to obtain additional increase in sensitivity. GS-SQT was used for Cd, Co, Cu, Mn, Ni, Pn, Se and Zn for sensitivity enhancement by Gholami et al. (2011). Schematic presentation of FAAS-GS-SQT was given in Figure 1.4.

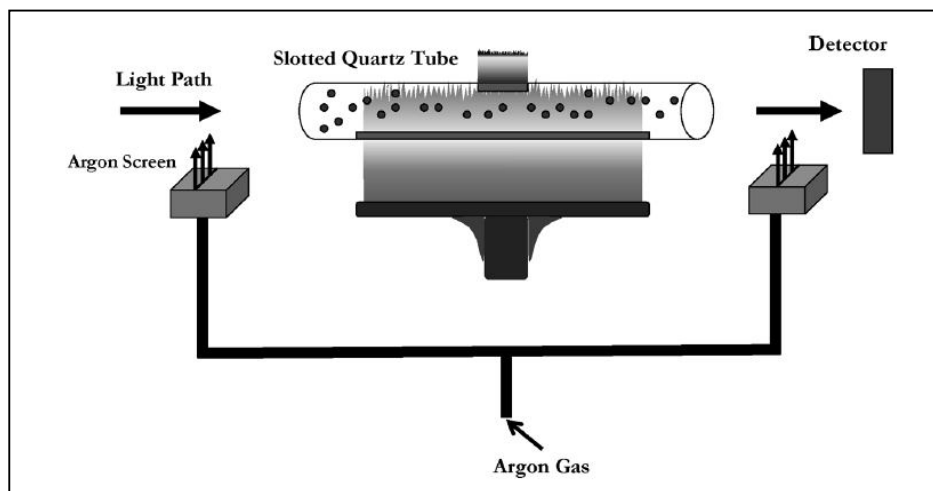


Figure 1.4. Schematic representation of flame AAS-gas screen-slotted quartz tube (Gholami et al. 2011)

Two aluminium blocks as gas screen were placed in both sides of SQT. Air, argon and nitrogen were tried to cut the flame from both sides of SQT and Ar was selected. Increasing in residence time of analyte atoms in optical path was the main advantage of method. Thus, sensitivities were improved. In addition, damage in quartz windows was avoided using GS-SQT in FAAS.

A two slot quartz tube was commercialized by Agilent Technology, Pye Unicam, Varian, Thermo, Perkin Elmer.

In SQT by Agilent, slots were positioned at 120° to each other. Sensitivity of FAAS for Ag, Au, Bi, Cd, Cu, Fe, Hg, Mn, Pb, Pt, Sb, Se, Te and Tl was improved by 2.7, 2.7, 2.9, 2.3, 2.4, 1.5, 2.8, 2.1, 2.9, 1.0, 3.1, 3.3, 2.7 and 2.6 times with respect to conventional FAAS (Moffett App. Note).

1.2.4. *In situ* Atom Trapping

Atom trapping can be considered as an effective method to increase AAS. It is based on the collection of analyte atoms on surfaces which cooled with water or nitrogen flow or resistively heated metal surface like iridium and tungsten, this step can be called as *collection*, and releasing the free atoms on surface by stopping the flow of cooler or increase the applied voltage, this step can be called as *revolatilization*. As a result of this process, a transient signal can be obtained (Matusiewicz 1977; West 1988; Ataman 2008). The concept of atom trapping was firstly applied to determination of lead by U-Tube atom trap by Lau *et al.*, sensitivity was improved by 38 times (Lau *et al.* 1976). U tube trap tube, Figure 1.5., is positioned above the burner (air-acetylene flame) so that the beam from light source passes above the tube. Due to high melting point and a low thermal expansion coefficient, quartz was selected for atom trap device. The analyte was condensed onto the cold silica surface via continuous nebulization into the spray chamber-burner system for a optimized time interval. Afterwards the blown out of water flow, quartz tube rapidly heated and vaporizing analyte atoms into the light path. Studies showed that Ag, Au, Cd, Co, Cu, Fe, Ni, Pb, Se, and Zn were trapped on the cooled surface in the free form whereas K, Li, Na, Cr, Mg and Mn were trapped on it as their oxides or silicates.

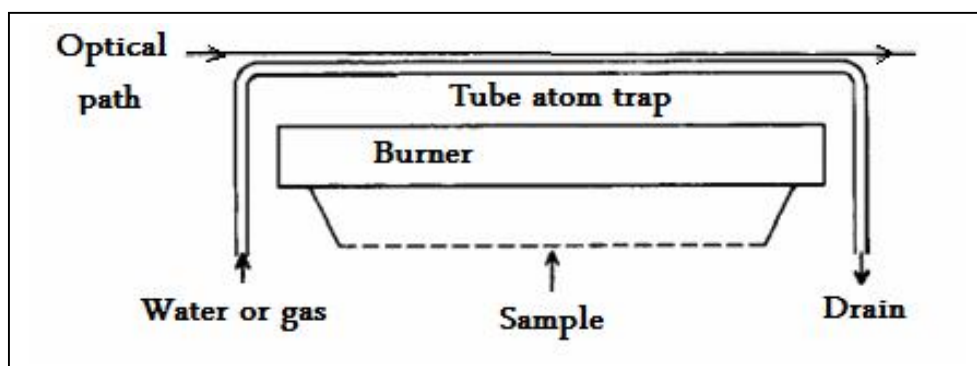


Figure 1.5. Schematic presentation of water-cooled atom trap system (Ataman 2008)

After preconcentration of the analyte atoms on the surface of the water-cooled U-shaped silica tube, the trapped species were released owing to the changing flame conditions using the flame alteration or organic solvent aspiration techniques, while the water circulated continuously (Ertaş *et al.* 2002).

Various configuration of the silica tube including single, double and triple tube were evaluated and the best results were obtained when dual silica tube was used (Figure 1.6.). In addition, precoating of the tube with Al, V and La provided notably enhancement for Cd and Pb. LODs were 0.8 and 0.1 ng mL⁻¹ for Pb and Cd, respectively, using 2.0 min collection time (Brown *et al* 1987).

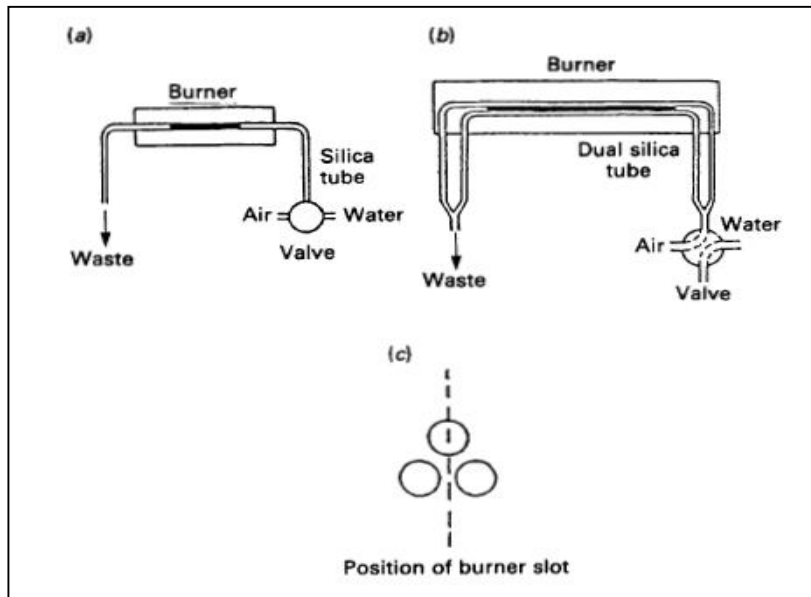


Figure 1.6. Design of water cooled atom traps (a) single tube, (b) double tube and (c) end view of triple tube (Brown et al 1987)

It was applied to determination of Cd in calcium chloride, frequently used as extractant in soil analysis. $0.0016 \mu\text{g mL}^{-1}$ of Cd as LOD was achieved. The accuracy of the method was checked by standard addition method (Fraser et al.1986).

Important parameters for the automated dual silica tube water cooled atom trap were determined by applying the Plackett-Burman and Birnbaum plots. The results showed that coating of the U-tube increased the sensitivity of Pb, Cd, As and Ag (Roberts and Kahokola 1989).

New design of water cooled dual tube was suggested and experimental details were investigated. The shape of the tubes was altered from the flat type to a bent tube. It was found that the use of new bent model through the analysis of Pb and Cd, higher sensitivities were obtained over the flat model. The characteristic concentrations were improved by 2.46 and 1.18 times, respectively for Cd and Pb (Turner et al. 1995). As, Sb, Cu and Mn were also determined by using this technique (Ellis and Roberts 1996). Fuel flow rate, percentage obscuration of the light beam, and the height of the tubes above the burner were optimized. It was found that high fuel flow, high percentage obscuration and low tube height were critical in obtaining high sensitivity. The sensitivities for As, Sb, Cu and Mn, using this technique were 8.6, 8.0, 0.93 and 0.38 $\mu\text{g mL}^{-1}$, respectively.

Instead of quartz as atom trapping material, stainless-steel was used for the direct determination of Pb in alcoholic drinks. The characteristic concentrations of Pb for the method were 0.044 and $0.0055 \mu\text{g mL}^{-1}$ when collection for 1.0 and 5.0 min, respectively. The interference effects of some elements were investigated and it was decided to use Na₂EDTA to eliminate the effect of Fe (III), Al (III) and Si (IV) (Hawwen et al 1996).

Another use of the water cooled system was a combination of U-shaped cooling system integrated with slotted quartz tube (Figure 1.7.). It was called as integrated atom trap (IAT) system by Matusiewicz and Kopras (Matusiewicz and Kopras 1997) and called as slotted tube water cooled atom trap (STWCAT) by Turner and Roberts (Turner and Roberts 1996). The primary advantages of this procedure lie in the inherent simplicity of the analytical technique and speed of analysis. The characteristic concentrations were obtained as 0.112 and 1.042 ng mL⁻¹ respectively for Cd and Pb (Turner and Roberts 1996). Condensation of water droplets on cold silica surface dropping off onto the STAT was a disadvantage of the method in view of high noise (Turner and Roberts 1996). It was found that there were not significantly differences between single silica tubes and double one (Turner and Roberts 1996, Matusiewicz and Kopras 1997). In addition, it was observed that the sensitivity of Cd, Cu, Pb, Tl and Zn was dependent on flame conditions, whereas Fe, In and Mn were not. The best sensitivity was obtained when a lean flame with 50 L h⁻¹ of acetylene was used for trapping these elements and a fuel-rich flame with 80 L h⁻¹ of acetylene was used for releasing (atomization). By applying the flame alteration technique, sharp signal was obtained rapidly (Turner and Roberts 1996).

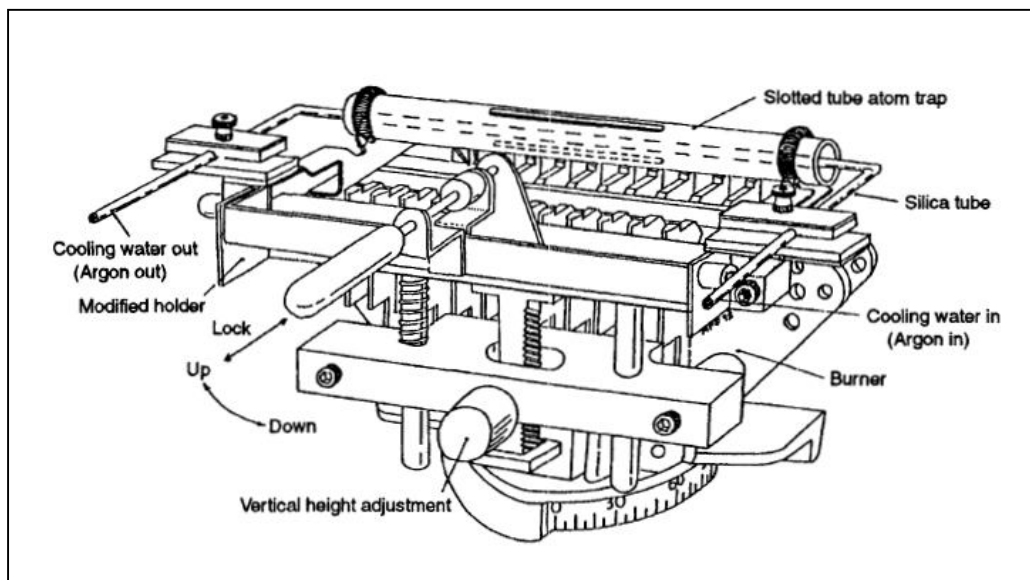


Figure 1.7. Schematic presentation of slotted-tube water-cooled atom-trap (STWCAT) system (Matusiewicz and Kopras 1997)

Ertaş et al. suggested the use of water cooled U-tube trap and combination of its with slotted quartz tube (Ertaş et al. 2002) with new approaches for the determination of Pb and Cd. Flame alteration and organic solvent aspiration techniques were applied by using water cooled U-shaped silica trap combined with slotted silica tube and slotted silica tube trap. In the condition of flame alteration, total acetylene flow was divided into two streams. Thus, one of the flow meter was allowed to flow during collection, and both of two were activated during atomization. Organic solvent aspiration is based on the collection of analyte on quartz surface in lean acetylene flame and atomization by adding organic solvent to increase to temperature of the flame (Ertaş et al. 2002).

1. INTRODUCTION

Several organic solvents include methyl isobutyl ketone (MIBK), methyl ethyl ketone (MEK), acetonitrile, iso-octane, acetone and hexane were tried during revolatilization step and it was decided to use IBMK at the volumes of 20.0 and 10.0 μL , respectively for Pb and Cd, that it was not only caused complete atomization but also provided the largest linear range in calibration plots. The results were good agreed with certified reference material. Characteristic concentrations were obtained as 2.2 and 0.35 ng mL^{-1} respectively for Pb and Cd in the case of flame alteration, 2.4 and 0.25 ng mL^{-1} respectively for Pb and Cd in the case of organic solvent aspiration (Ertaş et al. 2002). Korkmaz et al., investigated the nature of re-volatilization from atom trap surface (Korkmaz et al. 2002). According to their experiment results;

- the removal process is not a simple reduction
- direct contact with flame products is required
- heating is not necessarily associated with the removal of surface species
- a critical C/O value and thus an optimized flame

were required during revolatilization and atomization process (Korkmaz et al. 2002).

In another work, possible interference effects of KCl , $\text{NH}_4\text{H}_2\text{PO}_4$, $(\text{NH}_4)_2\text{CO}_3$, MgCl_2 , NH_4NO_3 , NaNO_3 , $(\text{NH}_4)_2\text{SO}_4$, $\text{MgSO}_4 \cdot 7\text{H}_2\text{O}$, CaCl_2 , $\text{Ca}(\text{NO}_3)_2$ and NaCl on Bi, Cd, In, Pb and Sb were investigated using the atom trapping technique with a double slotted silica tube. As a serious problem, devitrification which affect the lifetime of a slotted silica tube could occur at high content of alkali chlorides, especially NaCl (Korkmaz et al. 2003).

When analyte atoms were trapped on slotted quartz surface and revolatilized by addition of organic solvent, the method was called as slotted quartz tube – atom trap (SQT-AT). To improve the sensitivity in SQT-AT, flow rate of acetylene, suction flow rate of sample, collection time, type and volume of organic solvent and height of SQT from burner should be optimized. The advantages of SQT-AT to former trapping techniques were highlighted in a review by Ataman as increased sensitivity, decreasing the possible interferences, increased sample throughput, low cost and it is simple to use. Applicability of the SQT-AT was limited only volatile elements which were easily decomposed thermally in the primary reaction zone of air-acetylene flame (Ataman 2008).

Kumser studied the determination of Bi, Au and Mn by using uncoated SQT-AT-FAAS. Sensitivity improvements for Bi, Au and Mn as compared to FAAS were 94, 180 and 6.6 folds respectively (Arı 2009). Arı investigated Tl determination by Os coated SQT-AT and 3.5 fold enhancements in sensitivity was achieved as compared to uncoated SQT-AT (Arı 2009). Demirtaş developed a SQT-AT-FAAS method for the determination of Pb by using SQT which contained two slot positioned on 120° and 180°. Characteristic concentration was 0.11 ng mL^{-1} and characteristic mass is 4.50 ng and 1200 fold sensitivity enhancement was obtained with respect to FAAS at 8.1 mL min^{-1} suction flow rate of sample and 120° of SQT. Characteristic concentration was estimated as 0.1 ng mL^{-1} and characteristic mass is 3.70 ng and 1320 fold sensitivity enhancements was achieved with respect to FAAS at 7.4 mL min^{-1} suction flow rate of sample and 180° of SQT (Demirtaş 2009).

Effect of variations on inner (id) and outer diameters (od) of SQT was also studied by Demirtaş. Highest signal was obtained by using 10 mm of id, 13 mm of od in SQT. The effect of wall thickness of SQT on analytical signal was also investigated. It was found that highest signal to noise ratio was obtained by using a SQT with 0.5 mm of wall thickness (Demirtaş 2009).

Sensitivity of FAAS for indium (In) was improved using SQT. Enhancement factor (E) from slope ratio of calibration plot of FAAS to SQT-FAAS was found as 1.43. Further improvement was achieved using SQT for trapping of In in inner wall of SQT. E was found as 400 with respect to conventional FAAS and 279 with respect to SQT-FAAS. Characteristic concentration (c_0) and limit of detection values were found to be 3.63 ng mL^{-1} and 2.60 ng mL^{-1} , respectively, using a sample flow rate of 7.0 mL min^{-1} and a collection period of 5.0 min. In this study, positions of upper and lower slots were also examined. Three different SQT devices were produced where two slots were positioned at 90° , 120° and 180° with respect to each other (Figure 1.8.). It was found that higher In signal was obtained when two slots were positioned at 180° (Arslan et al. 2011).

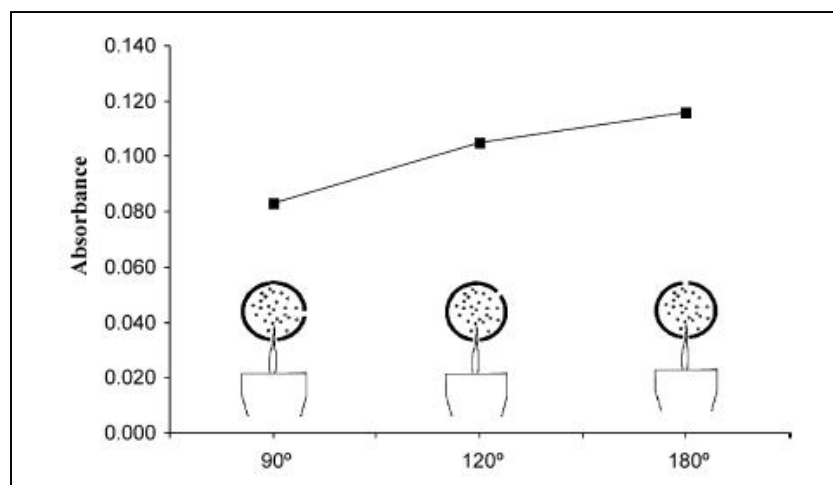


Figure 1.8. Optimization of SQT slot positions with respect to each other for In (Arslan et al. 2011)

SQT was coated with La solution to prevent the tube from devitrification by Watling (Watling 1977). This approach was investigated and developed to improve the sensitivity of FAAS. For this purpose, non-volatile elements were selected as coating material of SQT. W, Pd, Mo, Au, Ta, Zr, Ir, Ti, Os were selected in view of their higher melting and boiling points. It should be noted that melting point of the coating material must be higher than the analyte element (Ari 2009; Demirtaş 2009).

Ta coated SQT was used for Pb determination by SQT-AT-FAAS. LOD and LOQ were calculated as 0.15 ng mL^{-1} and 0.49 ng mL^{-1} respectively by using 19.5 mL of sample volume. 1653 fold sensitivity enhancement was obtained with respect to FAAS (Ari 2009).

1. INTRODUCTION

Os coated SQT was used for Tl determination by SQT-AT-FAAS. LOD and LOQ were calculated as 3.5 ng mL⁻¹ and 12 ng mL⁻¹ respectively by using 25.0 mL of sample volume. 319 fold sensitivity enhancements were obtained with respect to FAAS (Demirtaş 2009).

SQT was used as atom trap device for In by FAAS. Sensitivity was improved 400 fold using SQT-AT-FAAS system with respect to conventional FAAS. Characteristic concentration (c_0) and LOD values were found to be 3.63 ng mL⁻¹ and 2.60 ng mL⁻¹, respectively, using a sample flow rate of 7.0 mL min⁻¹ and a collection period of 5.0 min (Arslan et al. 2011).

1.2.5. Chemical Vapour Generation

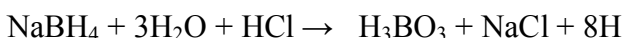
CVG which analyte is separated from the sample matrix by the generation of gaseous species as a result of a chemical reaction is a gas-phase sample introduction technique which increases the sensitivity of analyte in FAAS (IUPAC 2008).

There are several advantages of introducing analytes as a gas instead of a liquid. The first is that the analyte is separated from the bulk of the matrix. Together with higher sample uptake rates this means that spectroscopic interferences are minimal. Transport efficiency of gases is higher than liquids. Hence, improvement sensitivity by a factor of 30-50 could be reached by CVG (Mester and Sturgeon 2003).

This technique has received its widest application in AAS in the forms of cold vapour AAS (CV-AAS) for the determination of mercury and hydride generation AAS (HG-AAS) for elements forming gaseous covalent hydrides (As, Bi, Ge, In, Cd, Pb, Sb, Se, Sn and Te) (Campbell 1992; Brindle 2007). Among them, HG is the widely utilized one. Another application of CVG is carbonyl and halogen generation which is not mentioned more. Atom trapping technique has been successfully used with HGAAS (Tsalev 1999).

The pioneering work on HG was described by Marsh. However, Holak is known as the originator of the technique of vapour generation atomic absorption spectrometry (Holak 1969; Brindle 2007; Dedina 2007). A monography which includes theory, instrumentation, methodology and applications of HG was devoted to its importance by Dedina and Tsalev (Dedina and Tsalev 1995). Importantly, matrix effect can be eliminated by converting the volatile metals to their hydrides. Thus, interfering effects can be reduced and analyte atoms are preconcentrated. Inevitably, sensitivity of FAAS can be improved by using HG, especially for volatile elements.

HG reaction can be summarized as (Pohl 2004);



In batch experiment conditions, acidified sample is mixed with tetrahydroborate to produce volatile hydride. Metal hydride and the by-products of the reaction corresponding to the excess of H₂, CO₂ and H₂O are separated from the post reaction solution in a gas-liquid separator with inert gas flow and transferred to atomizer. Continuous flow and flow injections are the methods employed in HG. Liquid and gas phase interferences were discussed in a recent review with their solutions by Riyazuddin (Kumar and Riyazuddin 2010).

In other hand, disadvantages of the method should be considered. Oxidation state of hydride forming elements is an important issue for hydride formation process. As(III) forms a hydride far more efficiently and with a different sensitivity than does As(V). Similarly Se(IV) forms a hydride with relative ease whereas Se(VI) does not form a hydride at all. If element is in organic form such as arsenobetaine, selenomethionine volatile hydride is not formed. In this case, a reducing reagent such as L-cysteine to reduce As(V) and monomethylarsonic acid (MMAA) and dimethylarsinic acid (DMAA) to As(III), alkaline persulfate to oxidize arsenobetaine is required to form hydride (Mester and Sturgeon 2003).

Transition metals such as Zn, Cu and Fe and of precious group metals such as Au, Pd and Pt can interfere with the hydride formation process. Addition of a chelating agent, such as 1,10-phenanthroline (Doncker et al. 1985; Narasaki and Ikeda 1990), 8-hydroxyquinoline (Deng et al. 2001; Liao and Deng 2006) or picolinic acid (Campos et al. 2002) is required to prevent interferences (Mester and Sturgeon 2003).

Although it is not a new technique, electrochemical hydride generation (EC-HG) has attained much interest in last a decade (Bolea et al. 2001). The advantages of EC-HG were listed in a recent review as (Laborda et al. 2007);

- The using of NaBH₄ is alleviated by EC-HG. Thus, it is an expensive chemical and is a source of contamination
- Volatile hydrides can be formed as simultaneously
- Effect of different oxidation state of analyte is less effective on hydride yield

EC-HG was employed prior to instrumental detection by spectrophotometer (Arhab-Zavar and Hashemi 2000), FAAS (Menemenlioglu et al., 2007; Arhab-Zavar et al. 2009), AFS (Jiang et al. 2009; Jiang et al. 2010). An electrochemical hydride generation system with polyaniline-modified lead cathode was developed for tin determination by coupling with AFS. LOD was 1.5 ng mL⁻¹ (3 σ) and the relative standard deviation (RSD) was 3.3% for 11 consecutive measurements of 50 ng mL⁻¹ Sn(IV) standard solution (Jiang et al. 2010). An integrated electrochemical hydride generation cell, mainly composed of three components (a gas liquid separator, a graphite tube cathode and a reticulate Pt wire anode) was laboratory constructed and employed for the detection of arsenic by coupling to AFS. LOD of As (III) for the sample blank solution was 0.2 ng mL⁻¹ (3 σ) and the relative standard deviation was 3.1% for nine consecutive measurements of 5 ng mL⁻¹ As (III) standard solution (Jiang et al. 2009).

1.2.6. Atom Trapping Hyphenated with Hydride Generation

It can be clearly said that sensitivity of the FAAS has greatly increased by introducing the hydride generation instead of conventional liquid phase sample introduction.

A very sensitive analytical method with *in situ* trapping of trace level of cadmium hydride on palladium coated graphite atomizer for ET-AAS was developed by Infante (Infante et al. 1996). Schematic presentation of system was given in Figure 1.9. LOD was obtained as 60 ng L^{-1} of Cd for 1.4 mL of sample solution.

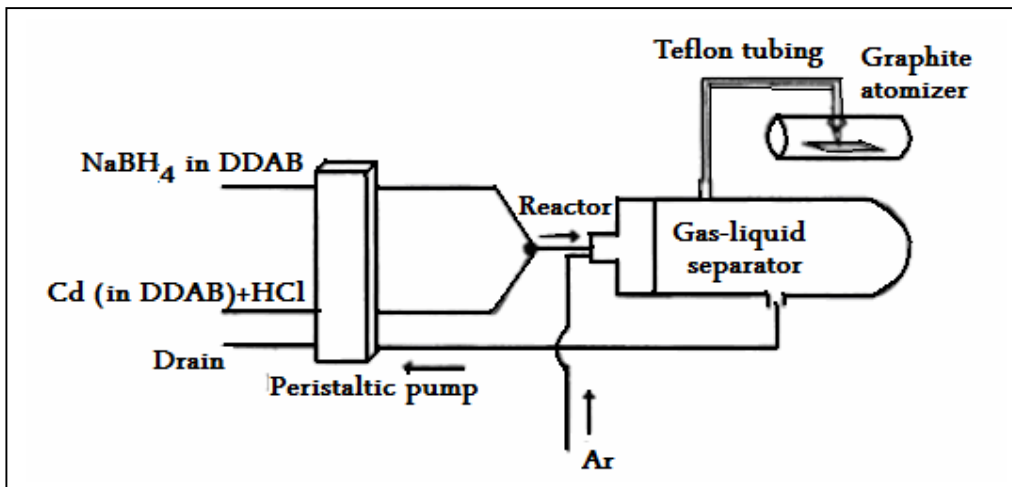


Figure 1.9. Hydride generation with *in situ* preconcentration in a palladium coated graphite atomizer for Cd determination, DDAB:didodecyldimethylammonium bromide (Infante et al. 2006)

Cd hydride was *in situ* trapped on inner wall of graphite tube furnace heated at 200°C and determined by AAS. Improved LOD, 10 ng L^{-1} , was obtained for Cd ET-AAS using KBH_4 as reductant. Trapping and releasing temperatures were optimized as 200 and 1800°C (Matusiewicz et al. 1997).

Concentrations of Pb in certified reference materials and tap water samples were determined by HGAAS with *in situ* concentration in a zirconium coated graphite tube. LOD was 0.44 ng mL^{-1} for Pb. Critical parameters were optimized. Detailed interference studies showed that Se and Te, hydride-forming elements, interfered the HG of Pb due to competitive reactions with NaBH_4 to form the corresponding hydrides. The transition metals Cd, Cr, Fe, Ni and Cu inhibit hydride generation, probably owing to coprecipitation of insoluble interfering compounds (Xiu-ping and Zhe-ming 1991).

Ultratrace level of Se converted to its hydride and following trapping on gold wire was determined in mineral water. LOD was found as 5 pg mL^{-1} for 5 min collection. Trapping and releasing temperatures were optimized as 200 and 900°C (Guo and Guo 2001).

Lead hydride (PbH_4), generated on-line by reacting lead in hydrochloric acid–potassium ferricyanide medium with sodium borohydride (NaBH_4), and was trapped on the interior walls of a slotted T-tube under highly oxidizing flame conditions (Figure 1.10.). Atomization was achieved by aspirating 50 μL of MIBK to the flame. LODs were 0.075, 0.047 and 0.028 ng mL^{-1} for 2.6, 5.2 and 7.8 mL of blank solution ($n = 13$), respectively. Calibration was linear up to 3.0 ng mL^{-1} for a 30 second trapping period (Ertaş et al. 2008).

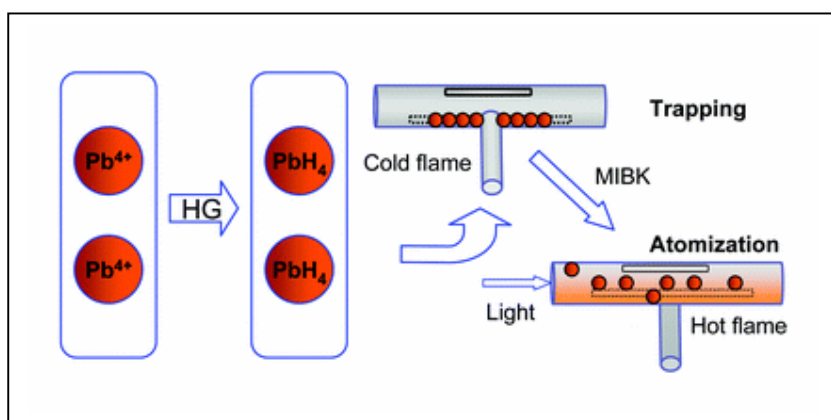


Figure 1.10. Schematic presentation of slotted quartz tube-atom trap-hydride generation atomic absorption spectrometric determination of lead (Ertaş et al. 2008)

Antimony hydride was in situ trapped on iridium-coated tungsten coil 0.028 ng mL^{-1} of Sb was calculated as LOD (Alp and Ertaş 2008).

Recently metal atom trap which resistively heated by passage of electricity through the device was used as alternative atomizers by Ataman research group. W coil is one of the most popular traps used first as an on-line preconcentration of Bi and for Se determination, and then it was used for Sb determination again in Ataman research group (Demirtaş 2009). Sb was converted to its volatile hydride and it was trapped on an electrically heated tungsten coil heated at 370 °C. Trapped antimony hydride was revolatilized and transported to flame heated quartz atom cell by increasing the trap temperature to 895 °C. Importance of concentrations of HCl and NaBH_4 solutions, H_2 and Ar gas flow rates, and collection and revolatilization temperatures of W-coil were highlighted by authors. LOD was found as 16 ng L^{-1} using a sample of 36 mL collected in 4.0 min. Enhancement factor in sensitivity was 17 (Titretir et al. 2008).

Se trapped on gold-coated W-coil after hydride formation (Figure 1.11) was determined by AAS. The LOD was 39 ng mL^{-1} in the conditions of 27.0 mL of sample solution and 4.0 min of collection (Kula et al. 2008). It was noted that Se signal could not be taken when bare W-coil was used as trapping surface, whereas gold coating provided convenient trapping and releasing for Se.

1. INTRODUCTION

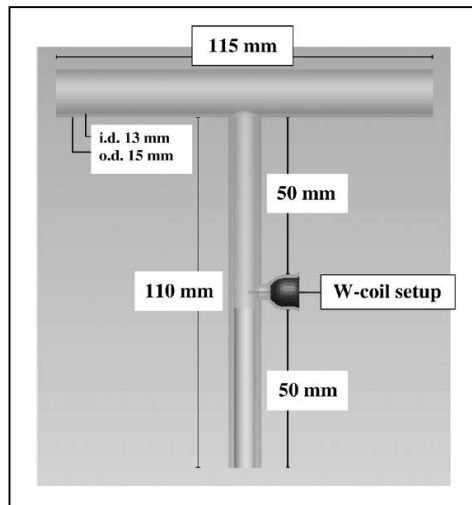


Figure 1.11. Schematic presentation of quartz T-tube and W-coil trap (Kula et al. 2008)

Atom trapping technique has been extensively studied about the trapping of analyte on raw or coated surface and determination by AAS and/or HG-AAS (Lau et al. 1988; Matusiewicz and Kopras 1997; Matusiewicz et al. 1997; Cankur et al. 2002; Docekal 2004; Docekal et al. 2004; Korkmaz et al. 2004; Korkmaz et al. 2005; Kratzer and Dedina 2005; Krejci et al. 2006; Matusiewicz and Krawczyk 2006; Cankur and Ataman 2007; Kratzer and Dedina 2007; Matusiewicz and Krawczyk 2007a; Matusiewicz and Krawczyk 2007b; Menemenlioglu et al. 2007; Kratzer and Dedina 2008; Kula et al. 2009; Kratzer et al. 2009). By applying this technique for AAS, satisfactory results were obtained which provided comparable sensitivity with GF-AAS and/or ICP-MS.

1.3. Inductively Coupled Plasma - Optical Emission Spectrometry

Inductively coupled argon plasma was found an important application in instrumental analytical chemistry as emission source. Liquid sample is usually transported to spray chamber by peristaltic pump. Inside the instrument, the liquid is converted into an aerosol through a process known as *nebulization*. The sample aerosol is then transported to the injector located in torch where it is desolvated, vaporized, atomized, and excited and/or ionized by the plasma. The process was summarized in Figure 1.12.

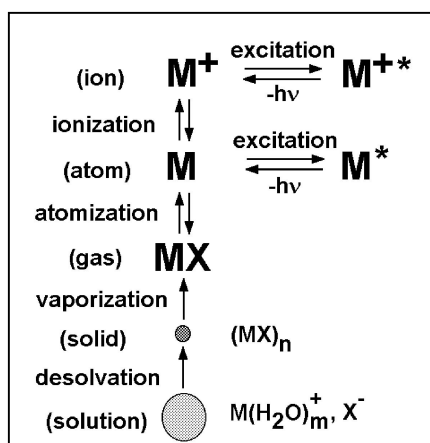


Figure 1.12. Emission process of individual metal in plasma (Boss and Fredeen 2004)

A torch consisting of three concentric tubes made of quartz or some other suitable material. A copper coil, called the load coil, surrounds the top end of the torch and is connected to a radio frequency (RF) generator. Typically, 700-1500 Watts are applied to generator. A spark from Tesla coil initiate the ionization of Ar. Electrons released from ionization of Ar were accelerated by magnetic field. Adding energy to the electrons by the use of a coil in this manner is known as *inductive coupling*. These high-energy electrons in turn collide with other Ar atoms, stripping off still more electrons. This collisional ionization of the argon gas continues in a chain reaction, breaking down the gas into plasma consisting of argon atoms, electrons, and argon ions, forming what is known as inductively coupled plasma (ICP) discharge. The ICP discharge is then sustained within the torch and load coil as RF energy is continually transferred to it through the inductive coupling process (Manning and Grow 1997; Skoog et al. 1998; Boss and Fredeen 2004)

The excited atoms and ions emit their characteristic radiation which is collected by a device that sorts the radiation by wavelength. The radiation is detected and turned into electronic signals that are converted into concentration information for the analyst. A representation of the layout of a typical ICP-OES instrument is shown in Figure 1.13.

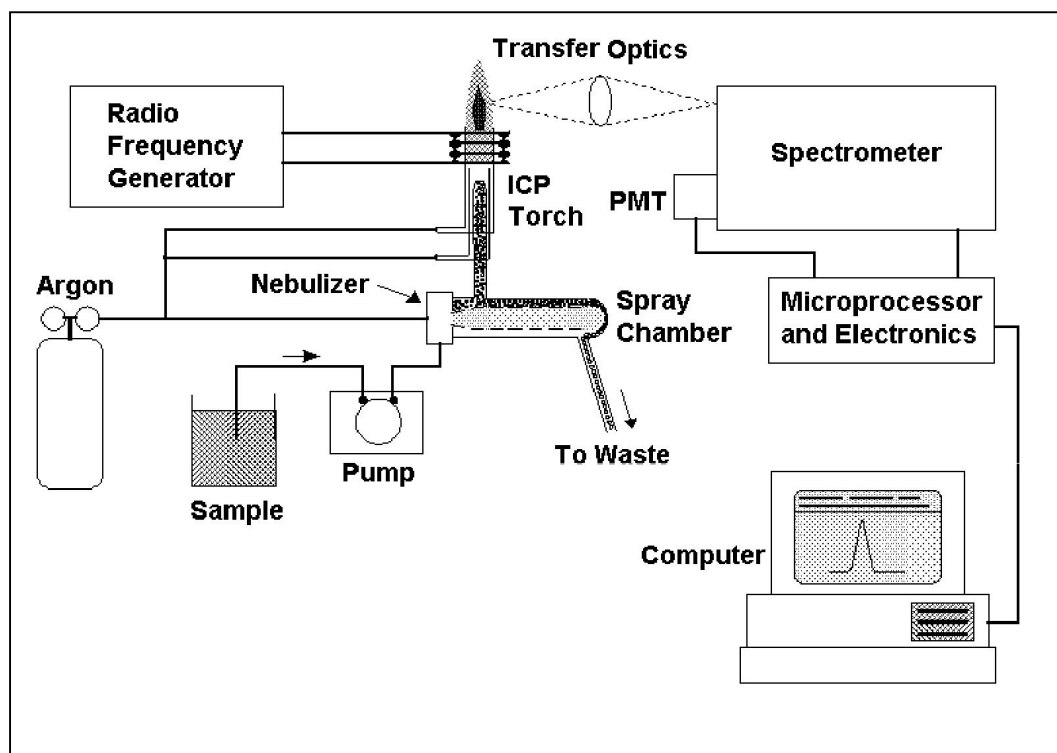


Figure 1.13. Schematic presentation of ICP-OES instrument (Boss and Fredeen 2004)

1.3.1. Hydride Generation Hyphenated with Inductively Coupled Plasma Optical Emission Spectrometry

Although atomic absorption spectrometry (AAS) and atomic absorption fluorescence spectrometry (AFS) are simple ways to measure analyte concentration from the metal hydride, these techniques are not capable of simultaneous determination of multiple analytes. That is why ICP and/or microwave induced plasma (MIP) sourced optical or mass spectrometers are increasingly used (Abranko et al. 2003).

HG is a popular technique in analytical chemistry for the determination of trace elements which generate volatile species in trace levels (Dedina and Tsalev 1995). It was also employed for speciation studies (Evans et al. 2009). As, Bi, Ge, Pb, Sb, Se, Sn, Cd and Te can be determined as their hydride (Campbell 1992). Main advantage of technique is separation of analyte from its matrix (Kumar and Riyazuddin 2010). Chemical hydride generation (CHG) by derivatization with tetrahydridoborate is common way to produce hydrides, while there are some others such as electrochemical, photochemical and sonochemical generation (D'Ulivo et al. 2011). In literature, recent advantages and limitations for this purpose were reviewed (Campbell 1992; Kumar and Riyazuddin 2010; D'Ulivo et al. 2011). HG can be done in different ways such as continuous-flow (CF) (Nakahara et al. 1987; Park 2004; Zhang et al. 2011), batch mode (Watanabe et al. 1999; Flores et al. 2002), and flow-injection (FI) (Aastroem 1982; Chan et al. 1990; Chen et al. 2002) systems. In CF, acidified sample/standard and blank are continuously pumped and mixed with a pumped stream of reductant, usually sodium borohydride to produce metal hydrides. At point of reaction, hydrogen gas is produced as a by-product resulting in a two phase mixture. A flow of argon is added to mixture and the hydrides are "stripped" into gas phase in stripping coil. A gas-liquid separator (GLS) is used to separate analyte hydride from liquid. By the effect of carrier gas, analyte hydride enters the ICP while remaining liquids are pumped to waste. It was reported that LOD could generally be improved by about two orders of magnitude over simple solution nebulization (Bonsak and Dovidowski; Dovidowski 1993; Bakirdere et al. 2011).

Although AAS and AFS are simple way to measure the metal hydride, these are not present simultaneous determination of analyte. That is why ICP and/or microwave induced plasma (MIP) sourced optical or mass spectrometer are increasingly used (Abranko et al. 2003). Main issue should be considered in ICP arise from excess of evolved hydrogen and carrier gas (Matusiewicz and Kopras 2003). In this case, plasma will be unstable and it can be extinguish in contrast to AAS and AFS. Because of HG apparatus was originally designed for AAS, it should be adapted for ICP by considering stability of the plasma (Matusiewicz and Ślachciński 2010). Another experimental problem in HG is back pressure in gas-liquid separator (Matusiewicz and Ślachciński 2010). Therefore, it is essentially required to optimize the variables which contribute the hydride forming process to reduce the excess of gases from hydride generation procedure.

In a continuous flow system, the acidified sample, blank, or standard, is continuously pumped and mixed with a pumped stream of reductant to produce the gaseous hydrides. At the point of reaction, hydrogen gas is produced as a by-product resulting in a two

phase mixture. A flow of argon is added to this mixture and the hydrides are "stripped" into the gas phase. A gas/liquid separator allows the gaseous, hydride containing phase, to enter the ICP for analysis, and allows the remaining liquids to be pumped to waste. Limits of detection can generally be improved by about two orders of magnitude over simple solution nebulization (Davidowski 1993).

Main issue should be considered in ICP arise from excess of evolved hydrogen and carrier gas (Matusiewicz and Kopras 2003). In this case, plasma will be unstable and it can extinguish in contrast to AAS and AFS. Because of HG apparatus was originally designed for AAS, it should be adapted for ICP by considering stability of the plasma (Matusiewicz and Ślachciński 2010). Another experimental problem in HG is back pressure in gas–liquid separator (Matusiewicz and Ślachciński 2010). Therefore, it is essentially required to optimize the variables which contribute to the hydride forming procedure to improve the sensitivity.

2. LITERATURE SURVEY

2.1. Bismuth Determination

Because Bi and its compounds are widely used in medicine, industry and cosmetics, it has spread in the environment and the chance of exposure of organisms to Bi has increased. Therefore, determination of Bi at ultra-trace levels in environmental and biological samples is an important environmental and analytical issue which analytical chemists have been focused. It was noted that the trace level of Bi as impurity in metallurgical materials changed the physical, mechanical, magnetic and electrical properties (Bedard and Kerbyson 1975; Das et al. 2006).

A recent review contain an extensive discussion about determination of Bi in solid environmental samples by using analytical techniques was published by Das (Das et al. 2006). There are many analytical techniques applied including spectrophotometric (Madrakian et al. 2003), electro analytical methods (Pouraghazi-Azar et al. 2001), solid phase extraction (Sahan et al. 2010) and cloud point extraction (Afkhami et al. 2006) methods. AAS is also widely used for determination of Bi (Das et al. 2006).

Bi was precipitated as its phosphate. It was noted that Cl^- and SO_4^{2-} ions were the major interferic ions. Co-precipitation of other salts as their phosphate was avoided by changing the acidity of solution (Blasdale and Parle 1936.). The phosphate method was improved by Silverman and Shideler (Silverman and Shideler 1954.). High recoveries were obtained for Bi at $\text{pH} < 1.5$. Cupferron was employed to separate the Bi from lead. Another gravimetric method for Bi was the precipitation of Bi with dimethylgloxime at $\text{pH}: 10.0$. From 50.0 to 500.0 mg of Bi was determined by this method. Ethylenedinitrilo tetra acetic acid and potassium cyanide were employed as masking agent (West and Coll 1955). Concentration of Bi in biological samples was determined by spectrophotometry at 490 nm as its bismuth dithizonate complex (Laug 1949).

Bi was determined as its diethyldithiocarbamate complex by spectrophotometry at 400 nm. Calibration plot was constructed in the range of 0.05-0.30 mg Bi in 25.0 mL of solution (Cheng et al. 1955). Complex of Bi with ethylenediaminetetraacetic acid was also determined by spectrophotometry. 263 nm was employed for measurement. Serious interferences were observed from Fe and Cu even if at low concentrations (West and Coll 1955). Heteropoly method was also used to form molybdo-bismuthophosphate complex. It was determined by spectrophotometry at 725 nm. Linear range of method was given as 5.0 to 100.0 ppb Bi (Guyon and Cline 1955).

Recently, Bi^{3+} was collected on activated carbon after complexation with thiourea and bromide ion in acidic media. The linear calibration ranges and limit of detection for the proposed method was $1.00 \cdot 10^{-9}$ - $1.50 \cdot 10^{-7}$ and $8.00 \cdot 10^{-10}$ mol L^{-1} , respectively. Method was applied to natural water samples to determine its Bi concentration (Madrakian et al. 2003).

Cloud point extraction (CPE) was also employed to separate Bi^{3+} from its bromopyrogallol red complex prior to spectrophotometric determination. Linearity was

2. LITERATURE SURVEY

obeyed in the range of 4.60–120.0 ng mL⁻¹ of Bi³⁺ ion. The detection limit of the method was 2.0 ng mL⁻¹ of Bi³⁺ ion. In order to evaluate the analytical applicability of the proposed method, it was applied to the determination of Bi³⁺ in urine samples (Afkhami et al. 2006).

Some of the researchers have been used different preconcentration method to improve the sensitivity of Bi. For example, Bi was on-line preconcentrated on quinolin-8-ol loaded Amberlite XAD-7 column and determined by FI-HG-ICP-OES. LOD was calculated as 0.03 ng mL⁻¹ for 100.0 ml of aqueous solution (Moyano et al. 1999).

An on-line preconcentration procedure based on solid phase extraction of Bi in minicolumn loaded with Lewatit TP-207 chelating resin including iminodiacetate group. The detection limit of the method was 2.75 µg L⁻¹ while RSD was 3.0% for 0.4 µg mL⁻¹. The accuracy of the developed method was tested by measuring the bismuth content in the two certified reference materials (TMDA-64 lake water and CWW-TM-D waste water) (Şahan et al. 2010).

Watling improved the Bi sensitivity of AAS as 4.0 fold in view of characteristic concentration by firstly using the SQT. It was 0.4 µg mL⁻¹ for AAS, while 0.1 µg mL⁻¹ for SQT-AAS [Walsh 1955]. Bi was trapped on iron oxide coated tube for 3.0 min and characteristic concentration was found as 0.004 µg mL⁻¹ of Bi (West 1988; Candolena 1994).

Lower level of Bi was determined in copper by employing hydride generation prior to AAS. The method provides a detection limit of 0.002 ppm for Bi in copper, a relative standard deviation of $\pm 8\%$. Characteristic mass was calculated as 30 ng. The working range of the method, in terms of Bi in copper samples was 0.002-1.0 ppm (Bedard and Kerbyson 1975).

Semi automated hydride generation of Bi was applied for AAS with 3.0 pg of sensitivity with equivalent for a 10.0 mL of sample volume (Lee et al. 1991).

Instead of AAS, GF-AAS was also employed for measurement of Bi. Plackett/Burman designs were employed for factor screening. Results showed that sodium tetrahydroborate concentration and trapping time were the most significant variables involve on the procedure. The best analytical performances, with characteristic mass of 35.0 pg and detection limit of 70.0 ng L⁻¹, were achieved by using U-treated graphite tube (Moscoso-Perez et al. 2003).

An on-line automated flow injection system with microwave-assisted sample digestion for the ET-AAS was applied to Bi determination in biological samples. In this paper, stannite ion was employed to precipitate Bi in basic medium. Precipitate was collected on the walls of a knotted coil, while the other matrix components flowed downstream to waste. The calibration graph was linear from the detection limit (8 pg) to 1.2 ng of Bi. Concentrations of Bi in urine and whole blood samples were in the range of 0.2 to 1.4 µg mL⁻¹ and from 0.5 to 1.9 µg mL⁻¹, respectively (Burguera et al. 1999).

The use of Mg-W cell in combination with ET-AAS was developed by Itoh et al. LOD was given as 7.8 pg mL^{-1} . Interference effects of Al, Ca, Cu, Fe, K, Na, Pb and Zn were eliminated by the Mg-W cell-electrodeposition method. The relative standard deviation (RSD) for 500 pg mL^{-1} was 5.1% (Itoh et al. 1999).

Rh-coated platforms (Rh), carbide plus rhodium coated platforms (W-Rh, Zr-Rh), carbidecoated platforms (W and Zr) with co-injection of RhCl_3 , solutions and uncoated platforms with injection of solutions of $\text{Pd}(\text{NO}_3)_2$, $\text{Mg}(\text{NO}_3)_2$, and RhCl_3 on the integrated platform of transversely heated graphite atomizer (THGA) were tested as modifiers for the simultaneous determination volatile elements include Bi. Integrated platform pretreated with W plus co-injection RhCl_3 was selected for Bi. LOD was given as 3.21 ng mL^{-1} for Bi (Freschi 2008).

Determinations of Bi, In and Pb in spiked synthetic and natural sea water by ET-AAS with Zeeman-effect background correction were investigated using tungsten containing chemical modifiers and tartaric acid TA as a reducing agent. The detection limit and characteristic mass were 8.5 ng mL^{-1} and 0.07 ng. A mixture of W+Pd+Tartaric acid was used as modifier.

Bi was determined in copper with a 30.0 ng of sensitivity without atom trapping (Bedard and Kerbyson 1975.). Hydride generation was employed as sample introduction technique with integrated atom trap for Bi determination in reference samples (Figure 2.1.). LOD was 0.4 ng mL^{-1} for 2.0 min collection of Bi in 2.0 mL of sample. Accuracy of the method was checked through the analysis of certified reference human hair sample (Matusiewicz and Krawczyk 2007b). Inconel 600 ® alloy was used as a metallic furnace atomizer in hydride generation atomic absorption spectrometry for the determination of Bi. LOD and LOQ were 0.7 and 2.3 ng mL^{-1} (Klassen et al. 2008).

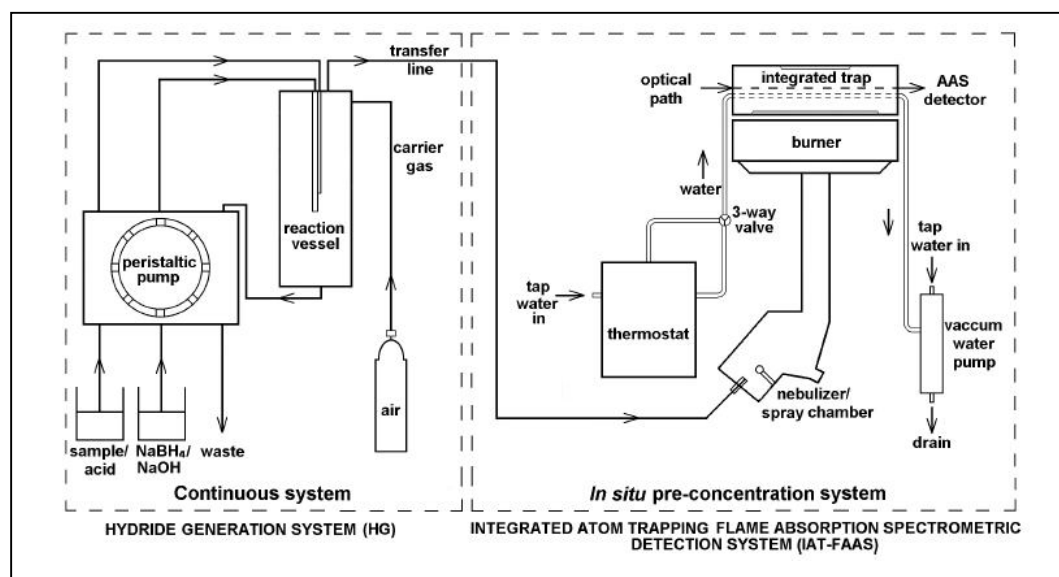


Figure 2.1. Schematic presentation of hydride generation-integrated atom trap-atomic absorption spectrometric determination of Bi (Matusiewicz and Krawczyk 2007b)

AFS was also employed for determination of Bi with LOD as 0.9 ng g^{-1} in garlic samples (Reyes et al. 2009). An atmospheric pressure dielectric barrier discharge (DBD) atomizer was also investigated for Bi determination with HG-AFS with 0.07 ng mL^{-1} of LOD (Xing et al. 2009).

Electrochemical hydride generation based on a screw-thread seal arrangement was used for determination of hydride forming elements by AFS with 0.15 ng mL^{-1} of LOD (Zhang et al. 2009).

The proposed method was successfully applied to the analysis of the certified reference materials (CRM) and traditional Chinese medicines (TCM) samples. Recently, multi-channel HG-AFS was used for determination of hydride forming elements includes Bi in tea leaves. Bi contents were in the range of $0.03\text{--}0.06 \mu\text{g g}^{-1}$. Method detection limit was $0.0080 \mu\text{g g}^{-1}$ (Zhang et al. 2011).

Resistively heated W coil was used as trapping surface for on-line preconcentration of Bi (Figure 2.2). A LOD of $0.0027 \text{ ng mL}^{-1}$ was obtained with 18 mL of sample volume. 270°C was chosen as collection temperature. It was noted that 350°C was enough for revolatilization without memory effect, 1200°C was selected due to rapid volatilization so that the use of peak height is justified. The characteristic mass was 41.0 pg (Cankur et al. 2002). The interference effects from chloride, sulfate and phosphate ions were significantly reduced as compared with the no-trap system, whereas the effects of Cd, Pb and Mg were in $\pm 10\%$. In contrast, Mn, Zn, Se, As, Na and Cu showed severe interference effect on Bi signal in without trap study (Kula et al. 2009).

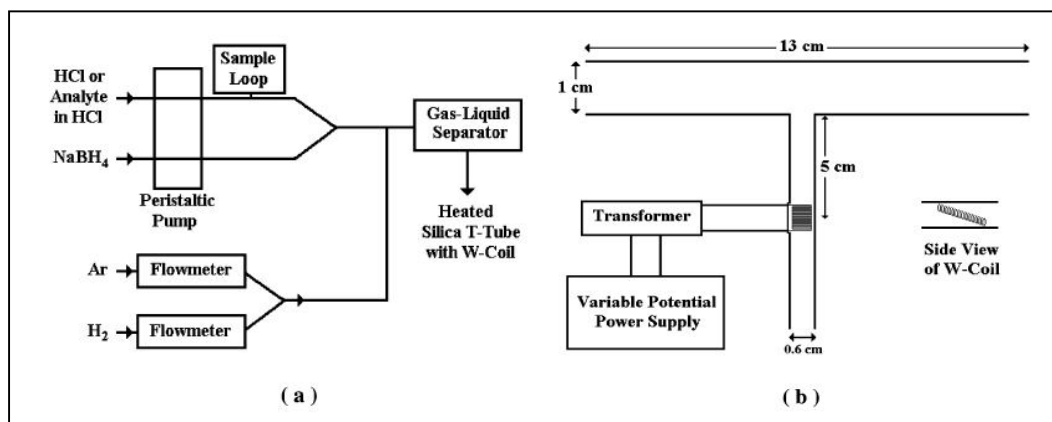


Figure 2.2. Schematic presentation of W coil HG-AAS (a) general configuration (b) W-trap placed in silica T-tube (Cankur et al. 2002)

Bi was on-line trapped on tungsten coil and subsequently electrothermally vaporized for the determination by AFS. With 120 s (12 mL sample volume) trapping time, LOD of 4.0 ng L^{-1} was obtained. Trapping efficiency was calculated as 73.0 ± 3.0 . It was highlighted that the tungsten coil hydride trap greatly improved the sensitivity in comparison with direct hydride generation. In addition interferent tolerance was also improved compared with conventional hydride generation. Improved sensitivity and

longer trapping time were attributed to great adsorption capacity of iridium-coated tungsten coil for bismuthine (Liu et al. 2008).

Sb, Se, Te, and Bi were determined in garlic samples by HG-AFS. LOD of the method was 0.9 ng g⁻¹ for Bi(III), in terms of sample dry weight (Reyes et al. 2009).

Method based on application of flow injection (FI) coupled with HG-AFS for ultratrace determination of Bi in environmental and biological samples was developed by Wu et al. Bi in solution was preconcentrated on a nylon fiber-packed microcolumn. The detection limit was calculated on the basis of three-times the standard deviation of the blank and was found to be 2.8 ng L⁻¹ with the liner range of the method between 0.01 and 2.5 µg mL⁻¹. The precision (RSD) of the 11 replicate measurements of 0.1 µg mL⁻¹ Bi was 4.4% (Wu et al. 2007).

Bi was determined in human hair by microwave digestion followed by continuous flow vapour generation atomic fluorescence spectrometry (Rahman et al. 2000). Instrumental and method detection limits for Bi were given as 10 ng L⁻¹ and 10 ng g⁻¹, respectively.

A new method was developed for determination of Bi in milk samples by HG-AFS after microwave-assisted sample digestion with HNO₃ and H₂O₂. LOD was calculated as 0.01 ng mL⁻¹. Bi concentrations in cow milk samples obtained from the Spanish market were in the range of 11.8-28.4 ng g⁻¹ (Cava-Montesinos et al. 2003).

Total concentration of Bi in Spanish vegetables was determined by using HG-AFS. LOD and LOQ were given as 1.4 and 4.7 ng g⁻¹. Bi contents in vegetables were found as 15 ng g⁻¹ in artichoke flour, 2.4 ng g⁻¹ in garlic, 48 ng g⁻¹ in zucchini, 6.9 ng g⁻¹ in tomato, 10 ng g⁻¹ in chard, 8.6 ng g⁻¹ in spinach, 15 ng g⁻¹ in string bean (Matos-Reyes et al. 2010).

In another study, bismuth hydride gas was collected on-line and determined via a new flow injection-hydride generation collection-flame atomic absorption spectrometry system. Four different type of gas-liquid separator (GLS) given in Figure 2.3. were tried for separate bismuthine from solution. GLS 3 is more sensitive in the determination of bismuth than the other three, because its longer argon inlet tube led to larger effective volume. LOD of method was given as 2.5 ng mL⁻¹. The linear range of this method was up to a Bi concentration of 100 ng mL⁻¹ (Chen et al. 2002).

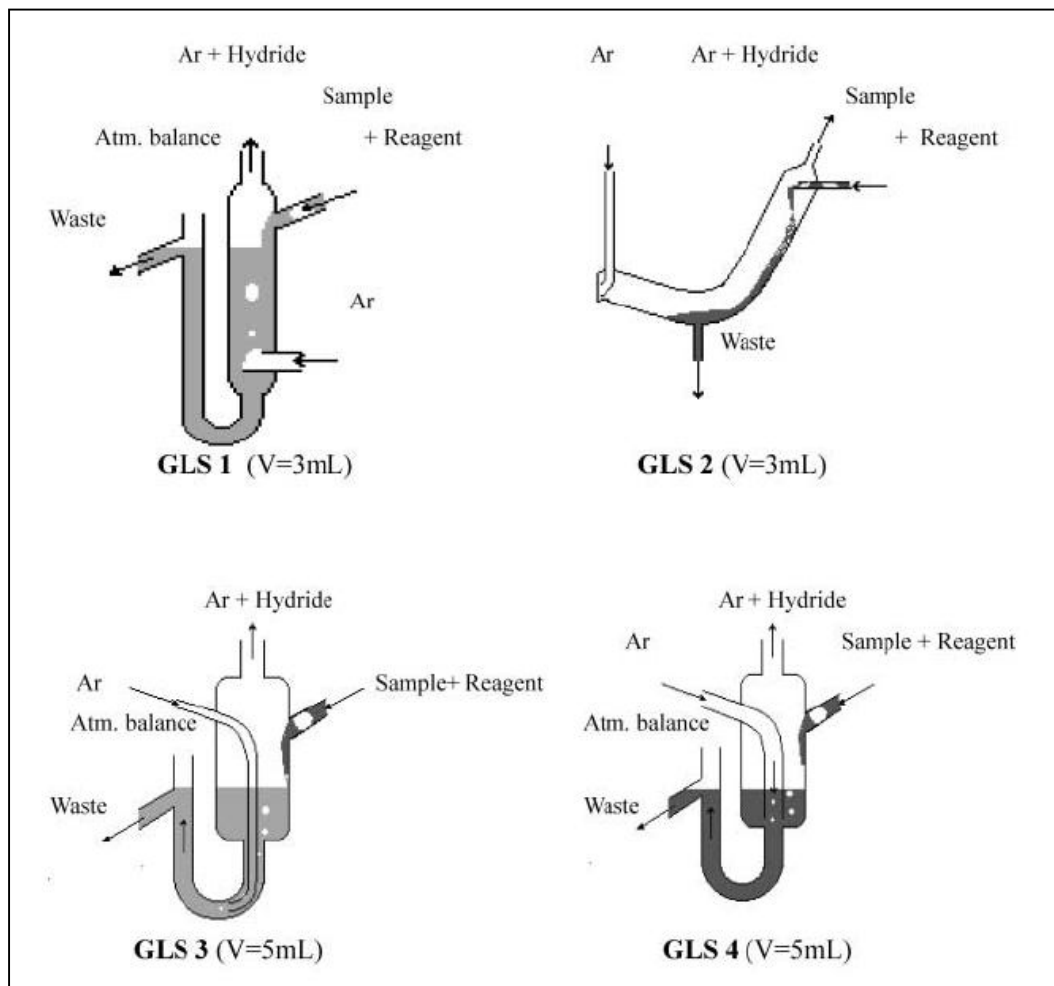


Figure 2.3. Schematic diagrams of gas-liquid separators for bismuth hydride (Chen et al. 2002).

Effect of hydrochloric, tartaric, citric, oxalic, acetic and sulfosalicylic acids on the hydride generation of Bi at trace levels in a continuous flow system in conjunction with ICP-OES detection was investigated. It was found that tartaric acid was the most suitable reaction medium, in terms of efficiency in the HG process and in the control of interferences. It was recommended that reduction of Bi to BiH_3 was more efficient in tartaric acid. Compared with conventional continuous nebulization, the HG as a gas phase sample introduction gives a sensitivity increase as two orders of magnitude. LOD was given as 0.5 ng mL^{-1} in tartaric acid medium (Marrero et al. 1999).

Complex of Bi (III) with 8-Hydroxyquinoline was extracted with Triton X-114 and concentration of Bi was determined flow injection inductively coupled plasma optical emission spectrometry. Due to lower cloud point temperature and higher density, Triton X-114 was used for phase separation. Under the optimal conditions, LOD was given as 0.12 ng mL^{-1} (Sun and Wu 2011).

Ultralow concentration of Bi was determined in snow samples by laser excited atomic fluorescence spectrometry. Calibration graph was constructed in the range of 0.05-50 pg g⁻¹, LOD was 2.5 fg of Bi (Candolena 1994).

Dispersive liquid-liquid microextraction (DLLME), miniaturized sample preparation method was employed to simultaneous determination of Cd, Pb and Bi in water samples combined with flow injection inductively coupled plasma mass spectrometry. The detection limit was 4.7 ng L⁻¹. The calibration graph was linear in the range of concentrations from <10 ng L⁻¹ to 1,000 ng L⁻¹. Concentrations of Bi in tap, rain and lake waters were found as 7.1, 36.4 and 32.6 ng L⁻¹, respectively (Jia et al. 2010).

Methylated species of Bi in the environmental samples was determined by using hydride generation followed gas chromatography-inductively coupled plasma optical mass spectrometry (GC/ICP-MS). Aqueous samples were acidified to pH: 2.0 with 1.0 mL HCl and reduced by using NaBH₄. The volatile hydrides of Bi as BiH₃, MeBiH₂, Me₂BiH, Me₃Bi were purged into a cooled trap (-196 °C). Among them, Me₃Bi (TMB) was found in analyzed samples; sewage gas, landfill gas, gas from the leachate pipeline in the concentration range of 0.0002-24.2 µg m⁻³ (Feldmann et al. 1999).

In literature, there are a few papers published where Bi has been determined by HG-ICP-OES. Bi in surfactant rich phase was determined by HG-ICP-OES after CPE. LOD was calculated as 0.12 ng mL⁻¹ (Sun and Wu 2011). In another work, it was found that volatile species of Co, Cr, Fe and Ni were formed during HG process (Pohl and Zyrnicki 2001). It was noted that acid concentration had an influence on plasma excitation conditions referred to the intensity of Ar atomic line spectrum only. Another issue which should be mentioned that type of acid have an important effect on volatile generation of interferic elements such as Cu. Volatile species of Cu in HNO₃ medium were about three times higher than this in HCl solution. It was highlighted that not only conditions, such as type of acid and its concentration but also presence of other elements in sample influences the transport efficiency of analyte into the plasma (Sturgeon et al. 1996; Moor et al. 2000; Pohl and Zyrnicki 2001; Kumar and Riyazuddin 2010).

Flow injection (FI) as an alternative sample introduction system was also used in HG but it was found that LOD values were slightly poorer than those observed with continuous flow sample introduction (Pyen and Browner 1988; Abrankó et al. 2003).

3. MATERIAL AND METHODS

3.1. Instrumentation

An ATI UNICAM 929 model AAS equipped with a Deuterium (D_2) background correction system was used for Bi determination. Air-acetylene type flame was used with a burner head of 100 mm (Varian). Cathodeon brand Bi hollow cathode lamp was used as a radiation source. Bi signals were recorded by using Solaar (929) software for this instrument. Instrumental conditions of Bi for AAS are given in Table 3.1.

Table 3.1. Operating parameters of Bi hollow cathode lamp for FAAS

Parameter	Bi
Wavelength, nm	223.1
Hollow cathode lamp current, mA	9.0
Slit width, nm	0.5

A Perkin Elmer Optima 2100 DV ICP-OES was used in hydride generation studies. Operating conditions of ICP-OES and CF-HG-ICP-OES are given in Table 3.2.

Table 3.2. Operating conditions of ICP-OES and CF-HG-ICP-OES for Bi determination

Parameter	ICP-OES	CF-HG-ICP-OES
RF power (W)	1450	1375
Plasma gas flow rate ($L\ min^{-1}$)	15.0	17.0
Auxiliary gas flow rate ($L\ min^{-1}$)	0.2	0.2
Nebulizer gas flow rate ($L\ min^{-1}$)	0.6	0.8
Sample flow rate ($L\ min^{-1}$)	1.5	2.45
View mode		Axial
Read		Peak area
Source equilibration time (s)	15.0	20.0
Read delay (s)	45.0	60.0
Replicates	3	3
Background correction		2-point (manual point correction)
Spray chamber	Scott type spray chamber	-
Detector		CCD
Purge gas		Nitrogen
Shear gas		Air
Gas		Argon
Analytical wavelength (nm)		Bi 223.061

Flow rate of sample solution and $NaBH_4$ were adjusted by using a peristaltic pump (Gilson Minipuls 3, Villiers-le-Bel, France) whereas flow rate of waste was controlled by pump of ICP-OES. Chemifold apparatus (Perkin Elmer) was used for hydride generation. Schematic presentation of its is given in Figure 3.1. Gaseous hydrides of bismuth were transported by the stripping argon flow directly into base of ICP torch.

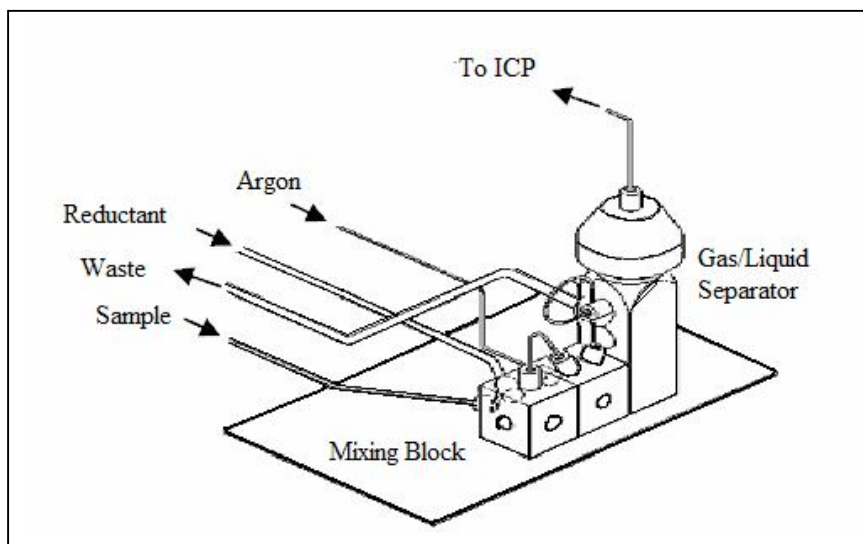


Figure 3.1. Schematic presentation of hydride generation manifold

3.2. Chemicals and Regents

Standard solutions were prepared by 100.0-1000.0 μL and 500.0-5000.0 μL micropipettes in polyethylene containers with a volume of 100.0 mL. Polyethylene containers with the capacity of 50.0 mL were used to store the solutions which kept in refrigerator. For the aspiration of organic solvent into flame, 1.0 mL plastic cups and adjustable micro pipettes were used.

Bi standard solution ($1000.0 \pm 3.0 \mu\text{g mL}^{-1}$) was supplied from High Purity Standards-Charleston; SC. Standards with lower concentrations were prepared by appropriate dilutions from stock solutions with distilled water. Sodium tetrahydroborate (NaBH_4) was granular product (>98%, Aldrich). PTFE tubings for hydride generation system were supplied from Perkin Elmer (Bridgeport Avenue, Shelton, CT). HCl, H_2O_2 , NaOH were also supplied from Sigma-Aldrich.

For the interference studies, the concentrations of interferents were 1.0, 10.0 and 100.0 folds in mass of the analyte concentration. Bi (High Purity Standards), Na, Mg, K, Fe, Co, Ni, Cu, Cd, Se, Sb, Zn, Sn, Al were prepared from $1000.0 \mu\text{g mL}^{-1}$ stock solution. SO_4^{2-} , Cl^- and NO_2^- standards were prepared from Na_2SO_4 , NaCl and NaNO_2 in water, respectively.

The accuracy of the method was checked by analyzing the standard reference water sample, trace elements in water-SRM 1643e, was supplied from NIST (Gaithersburg, MD).

3.3. Sampling

Tap water samples were collected and kept in 1.0 L glass bottles. Before the sample collection step, sample container was thoroughly cleaned. Samples were filtered through 0.45 μm membrane filter to remove particles and then acidified with 0.5 mL of HNO_3 to prevent precipitation. Two different brands of natural spring water were bought from local market of Diyarbakır. 1000 mL portion of each samples were transferred to a beaker. Dissolved gases in samples were removed by using ultrasonic bath for 10.0 min. For the river sample, 5.0 L sample water was collected in different locations of river and mixed. Sample was acidified by 2.5 mL of concentrated HNO_3 , transferred to laboratory and filtered through 0.45 μm membrane filter. All of the samples were analyzed at the same day of sample collection. External calibration method was applied in the measurements.

Milk samples were purchased from local market in Diyarbakır-Turkey and digested in microwave oven (Berghof MWS 3, Eningen-Germany). Generally, a 0.20-0.40 g portion of sample was used for microwave digestion according to recommendation of producer. If the mass was higher than these, samples could not be completely digested. By considering the organic matter content of milk samples, a pre-digestion procedure was applied before transfer the sample to microwave oven. Five bottles from each of milk samples from their 200.0 and/or 500.0 mL box were mixed and homogenized samples were used for analysis of its bismuth content. 2.0 mL mixture of HNO_3 and H_2O_2 (1:1, v/v) was added to 5.0 mL of milk samples. Vessel was heated until dryness on hot plate. This was repeated by two times. Then, 5.0 mL mixture of HNO_3 and H_2O_2 (2:3, v/v) was added to beaker and it was transported to microwave oven. Recommended procedure on handbook was applied to samples. The vessel was closed and it was placed inside the microwave oven and the following program was run: step 1; 2 min to reach 145 °C and 5 min held, step 2; 5 min to reach 170 °C 10 min held, step 3; 2 min at 190 °C 15 min held, step 4; cooling down-1 min to reach 100 °C 10 min held. After cooling, clear digests were transferred to beaker and acids were evaporated until dryness and then residue was dissolved in 5.0 mL of 5.0 mol L^{-1} HCl . After dissolving of 5.0 mL portion of each of samples, final volume was 5.0 mL. Therefore, there was no sample dilution. All of the procedures during dissolving process were applied to blank. Possible lost of analyte was checked from preliminary experiments and it was observed that there was not significantly lost of analyte from this procedure. For this purpose one of the samples was spiked with known amount of Bi (results were given in following sections).

3.4. Coating Procedure for SQT

A 140 mm long slotted quartz tube with two slots positioned at 180° with respect to each other was used; length of the lower and upper slots were 100.0 and 50.0 mm. Inner and outer diameter values were 10.0 and 12.0 mm. The slotted quartz tubes were obtained from Ataman Research Group – METU and Çalışkan Cam-Ostim-Ankara (Middle East Technical University-Ankara).

3. MATERIAL AND METHODS

For the coating of SQT, 100.0 mL of 100.0 $\mu\text{g mL}^{-1}$ solutions of Ta, Zr, W, and Mo were prepared from their solids, Ta_2O_5 , $\text{Zr}(\text{NO}_3)_4 \cdot 5\text{H}_2\text{O}$; Mo, W solution were prepared from their 1000.0 $\mu\text{g mL}^{-1}$ standard solutions (Ultra Scientific Standards). All coated tubes were prepared by aspirating of coating solution using a suction rate of 3.4 mL min^{-1} , in the presence of a lean flame.

Procedures for metal coating solutions are as follows:

- i. Ta_2O_5 was dissolved in 2.8 M HF solution.
- ii. $\text{Zr}(\text{NO}_3)_4 \cdot 5\text{H}_2\text{O}$ was dissolved in water.

All the solids were dissolved by using an ultrasonic bath.

4. RESULTS AND DISCUSSIONS

In this study, development of a sensitive method for Bi determination consists of six stages;

- i. The determination of Bi by simple FAAS.
- ii. Use of a SQT to improve sensitivity by increasing the residence time of analyte atoms in measurement zone (SQT-FAAS). SQT provides more stable chemical environment because of the elimination of air diffusion to flame.
- iii. The atom trap studies with uncoated SQT. (AT-SQT-FAAS)
- iv. Coating of SQT by using relatively high melting and boiling points of metals to assure their persistence on the surface of SQT during analytical procedures (metal coated SQT-FAAS).
- v. Atom trap studies on coated SQT (metal coated SQT- AT-FAAS).
- vi. In addition, inner and outer diameters of SQT on Bi signal were examined.

Improvement in sensitivity was evaluated in term of enhancement (E), unit time (E_t) and unit volume (E_v) (Ataman 2008). E was obtained from ratio of c_0 . Characteristic concentration, c_0 , concentration that corresponds to 0.00436 absorbance (1% absorption) was calculated as $c_0 = 0.00436 \times (\text{analyte concentration/absorbance})$.

Sensitivity enhancement also means ratio of calibration sensitivities (slopes). E_t is obtained by dividing E value by total time spent in terms of minutes, and E_v is obtained by dividing E value by total volume spent in terms of milliliters (Ataman 2008). Thus, it is possible to evaluate the contribution of trapping time and volume of trapping solution to enhancement. In order to evaluate the trapping efficiency, another term is used; characteristic mass, m_0 , is the mass of analyte which produces a defined peak that has an absorbance value of 0.00436 (or 1 % absorption). It is calculated as the (*volume of trapped analyte*) $\times (c_0)$. The limit of detection (LOD) and limit of quantitation (LOQ) were calculated from $3s/m$ and $10s/m$ (where s is standard deviation of lowest concentration of linear range, m is the slope of the linear calibration plot). RSDs were calculated from ten replicate measurements of the lowest concentration of linear range.

4. RESULTS AND DISCUSSION

4.1. Optimization of FAAS Conditions for Determination of Bi

4.1.1 Investigation of Fuel Flow Rate for FAAS Determination of Bi

Variations of the analytical signal of $20.0 \mu\text{g mL}^{-1}$ of Bi in 1.0 M HNO_3 as a function of acetylene flow rate were investigated $0.6\text{-}2.5 \text{ L min}^{-1}$ of acetylene flow while air flow rate was constant at 4.0 L min^{-1} (Figure 4.1.). The highest signal was obtained at 1.5 L min^{-1} acetylene flow rate; and this value was adapted for further studies.

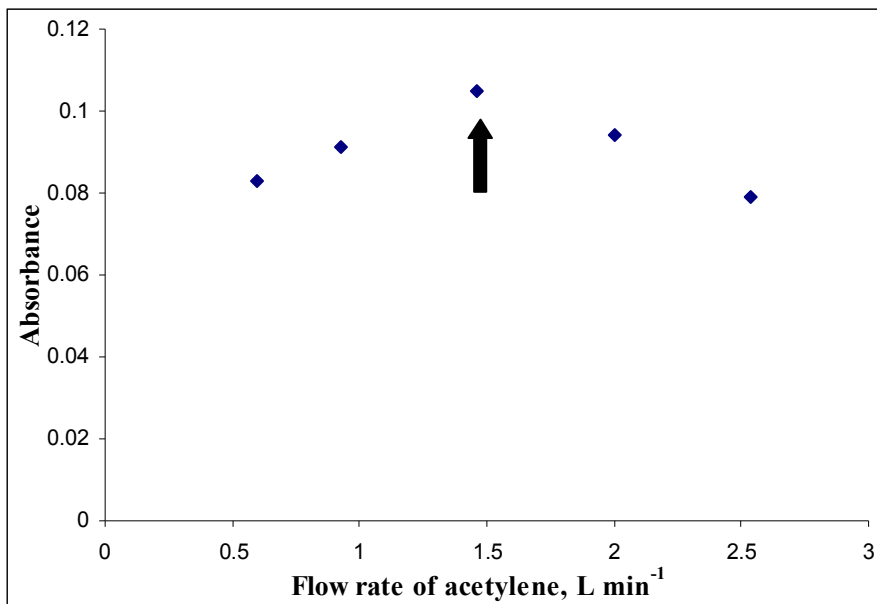


Figure 4.1. Investigation of acetylene flow rate for FAAS determination of Bi; $20.0 \mu\text{g mL}^{-1}$ Bi; flow rate of air: 4.0 L min^{-1} , sample suction rate: 5.5 mL min^{-1}

4.1.2. Investigation of Suction Rate of Sample Solution for FAAS Determination of Bi

It is well known that efficiency of nebulization system is dependent on the suction rate of sample/standard solution. At higher suction rate, many of analyte atoms reach to optical path and absorptions of the radiation by neutral atoms increase due to increasing the population of atoms. Effect of sample flow rate on analytical signal of $20.0 \mu\text{g mL}^{-1}$ of Bi was studied in the range of $2.4\text{-}8.5 \text{ mL min}^{-1}$ (Figure 4.2.). As expected, absorbance of Bi increased with increasing flow rate of sample. It was decided to continue the further experiments at sample flow rate of 8.5 mL min^{-1} .

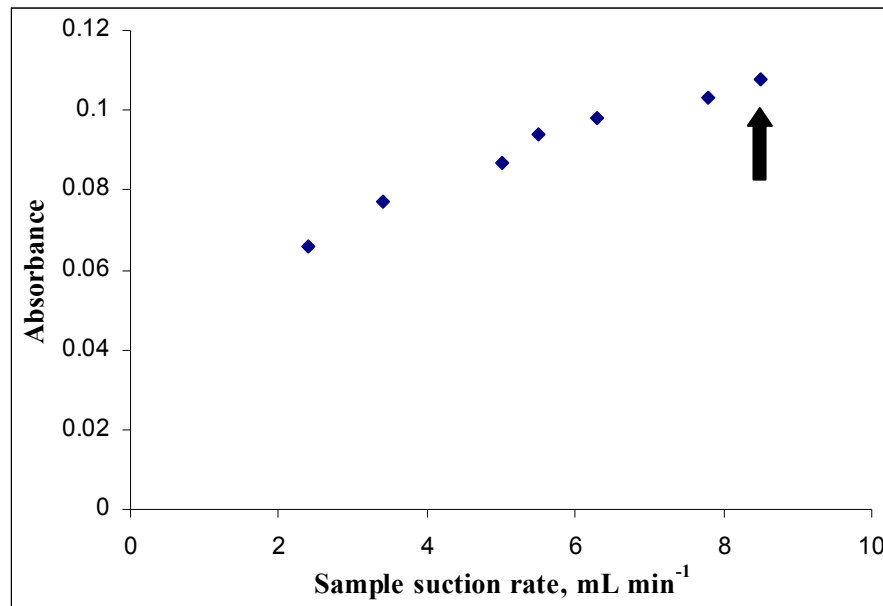


Figure 4.2. Investigation of suction flow rate for FAAS determination of Bi; $20.0 \text{ } \mu\text{g mL}^{-1}$ Bi, flow rate of air: 4.0 L min^{-1} , flow rate of acetylene: 1.5 L min^{-1}

4.1.3. Calibration Plot for Bi in FAAS Method

Linear calibration curve was obtained for Bi by using optimized values in FAAS (Figure 4.3.). The best line equation and correlation coefficient were $y = 0.0045x + 0.0128$ and 0.9986 respectively, in the concentration range of $2.0\text{--}50.0 \text{ } \mu\text{g mL}^{-1}$. RSD was calculated as 3.4% for ten replicate measurements of $2.0 \text{ } \mu\text{g mL}^{-1}$ of Bi solution.

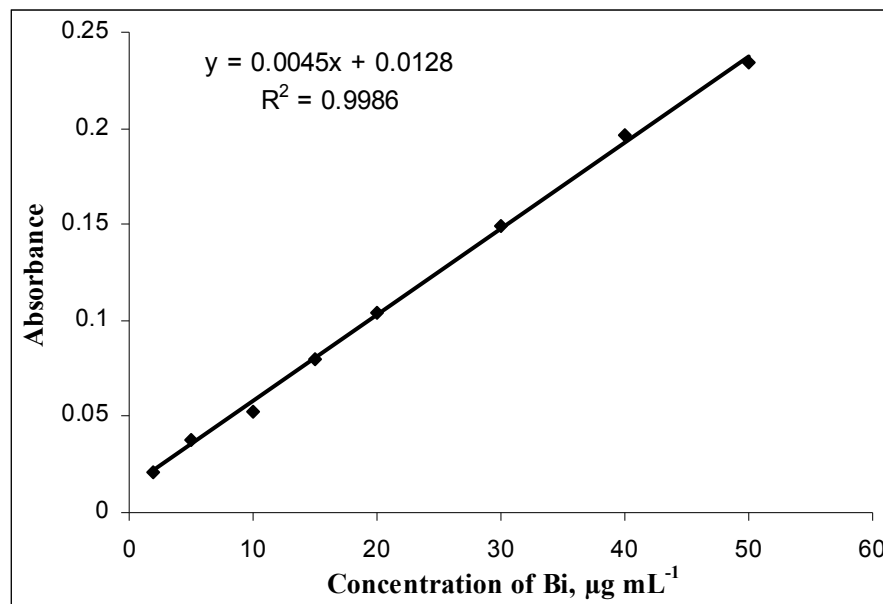


Figure 4.3. Linear calibration plot for Bi in FAAS; flow rate of air: 4.0 L min^{-1} , flow rate of acetylene: 1.5 L min^{-1} , sample suction rate: 8.5 mL min^{-1}

4. RESULTS AND DISCUSSION

As seen from the Table 4.1. LOD and LOQ were calculated as $0.47 \mu\text{g mL}^{-1}$ and $1.6 \mu\text{g mL}^{-1}$ respectively. Characteristic concentration was calculated as $0.87 \mu\text{g mL}^{-1}$. Ten measurements of $2.0 \mu\text{g mL}^{-1}$ Bi solution were used for LOD and LOQ determination,

Table 4.1. Analytical characteristics of FAAS for Bi

Parameter	FAAS
Limit of Detection (LOD), $\mu\text{g mL}^{-1}$	0.47
Limit of Quantitation (LOQ), $\mu\text{g mL}^{-1}$	1.6
Characteristic Concentration (c_0), $\mu\text{g mL}^{-1}$	0.87

4.2. Optimization of SQT-FAAS Conditions for Determination of Bi

4.2.1. Investigation of Fuel Flow Rate for SQT-FAAS Determination of Bi

In the SQT-FAAS system, sensitivity is improved by increasing the residence time of analyte in atomization zone in SQT. Only a momentary increase in signal is obtained, although the term trap is sometimes used for this mode, there is no collection and/or preconcentration. All of the system parameters were optimized in this system. First optimization parameter was acetylene flow rate. Effect of acetylene flow rate was studied in the range of $0.6\text{--}2.5 \text{ L min}^{-1}$ while air flow rate was kept constant at 4.0 L min^{-1} (Figure 4.4.). Optimum acetylene flow was selected as 1.5 L min^{-1} , as it was for FAAS.

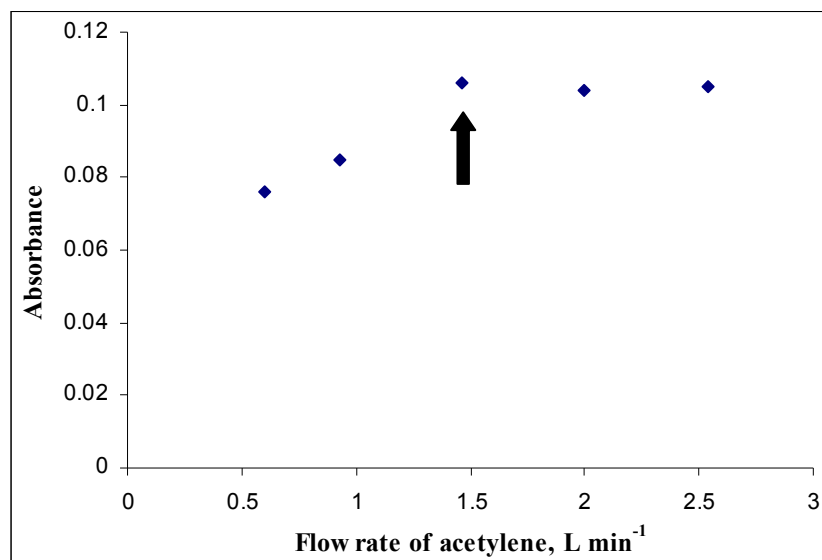


Figure 4.4. Investigation of acetylene flow rate for SQT-FAAS determination of Bi; $15.0 \mu\text{g mL}^{-1}$ Bi; flow rate of air: 4.0 L min^{-1} , sample suction rate: 5.5 mL min^{-1} , 2.0 mm height of SQT from burner

4.2.2. Investigation of Suction Rate of Sample Solution for SQT-FAAS Determination of Bi

Effect of sample flow rate on analytical signal of $15.0 \mu\text{g mL}^{-1}$ of Bi was studied in the range of $1.5\text{--}8.5 \text{ mL min}^{-1}$ (Figure 4.5). Flow rate of sample was adjusted by independent peristaltic pump. Increasing suction rate of sample caused an increase for Bi signal. The reason was same as FAAS study, increasing population of analyte atoms per unit time in flame. Thus, 8.5 mL min^{-1} was selected as suction rate for sample solution in SQT-FAAS method.

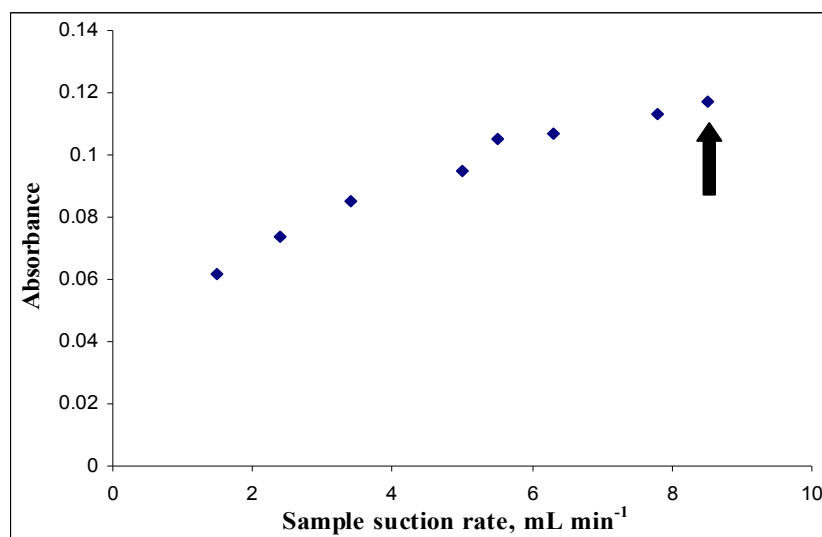


Figure 4.5. Investigation of suction rate of sample for SQT-FAAS determination of Bi; $15.0 \mu\text{g mL}^{-1}$ Bi, flow rate of air: 4.0 L min^{-1} , flow rate of acetylene: 1.5 L min^{-1} , 2.0 mm height of SQT from burner

4.2.3. Investigation of Height of SQT from Burner Head for SQT-FAAS Determination of Bi

Height of SQT from the burner head was also investigated in the range of 1.0–5.0 mm (Figure 4.6.). This parameter corresponds to the distance between the burner head and the lower end of SQT. As this value became smaller, a steady increase in signal was observed, corresponding to about 2-fold between 5.0 mm and 1.0 mm. At high values, sample transport into SQT is expected to be lower, causing a lower signal. However, in the case of 1.0 mm height, flame stability was adversely affected and it could be extinguished easily; therefore, height of SQT was selected as 2.0 mm for further studies.

4. RESULTS AND DISCUSSION

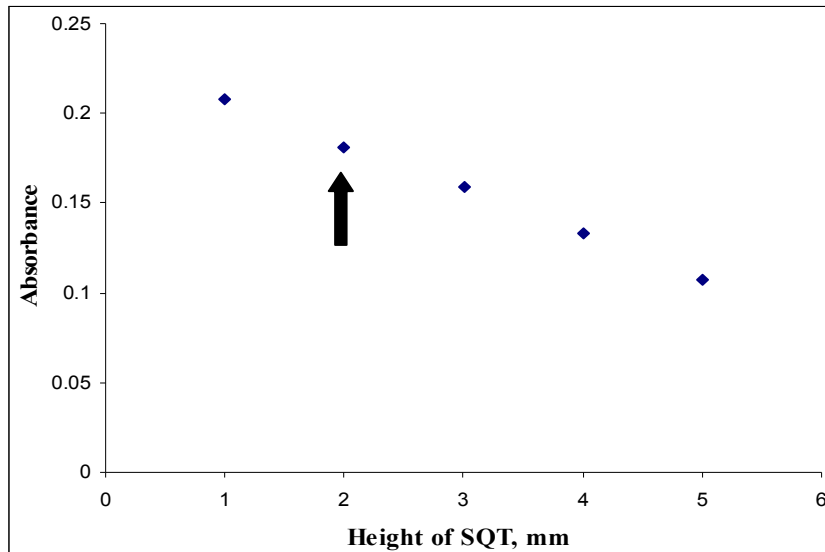


Figure 4.6. Investigation of height of SQT from burner for SQT-FAAS determination of Bi; $15.0 \mu\text{g mL}^{-1}$ Bi; flow rate of air: 4.0 L min^{-1} , flow rate of acetylene: 1.5 L min^{-1} , sample suction rate: 8.5 mL min^{-1}

4.2.4. Calibration Plot for Bi in SQT-FAAS Method

The optimized conditions of SQT-FAAS method were summarized in Table 4.2.

Table 4.2. Conditions of SQT-FAAS method for Bi

Parameter	SQT-FAAS
Flow rate of acetylene	1.5 L min^{-1}
Sample suction rate	8.5 mL min^{-1}
Height of SQT	2.0 mm

Linear calibration plot was obtained for Bi by using optimized values in SQT-FAAS. The best line equation and correlation coefficient were, $y = 0.0134x + 0.0106$ and 0.9981 respectively, in the concentration range of $0.5\text{-}20.0 \mu\text{g mL}^{-1}$ (Figure 4.7). RSD was calculated as 4.0% for nine replicate measurement of $0.5 \mu\text{g mL}^{-1}$ of Bi. Enhancement factor was calculated as 2.9 to with respect to conventional FAAS.

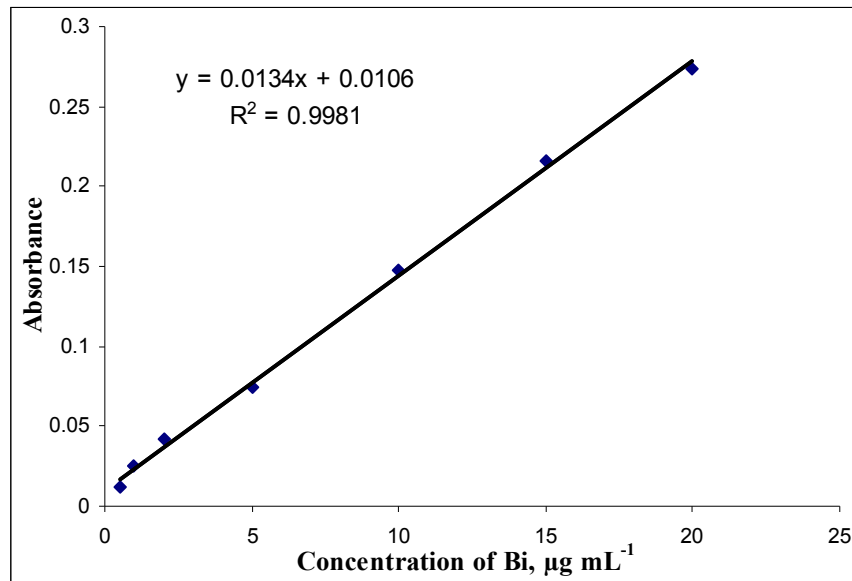


Figure 4.7. Linear calibration plot for Bi in SQT-FAAS; flow rate of air: 4.0 L min^{-1} , flow rate of acetylene: 1.5 L min^{-1} , sample suction rate: 8.5 mL min^{-1} , 2.0 mm height of SQT from burner

As seen from Table 4.3. LOD and LOQ were calculated as $0.11 \mu\text{g mL}^{-1}$ and $0.37 \mu\text{g mL}^{-1}$ respectively. Characteristic concentration was estimated as $0.30 \mu\text{g mL}^{-1}$. Enhancement factor obtained with respect to FAAS was 2.9. Ten measurements of $0.5 \mu\text{g mL}^{-1}$ solution were taken for LOD and LOQ determination

Table 4.3. Analytical performance of SQT-FAAS for Bi

Parameter	SQT-FAAS
Limit of Detection (LOD), $\mu\text{g mL}^{-1}$	0.11
Limit of Quantitation (LOQ), $\mu\text{g mL}^{-1}$	0.37
Characteristic Concentration (c_0), $\mu\text{g mL}^{-1}$	0.30
Enhancement (E) (with respect to FAAS)	2.9

Watling firstly used the SQT to improve sensitivity for fourteen elements include Bi (Watling 1977). A SQT with two slots positioned at 120° with respect to each other was used; length of the lower slot was 100.0 mm and the upper slot was 80.0 mm; inner diameter of the tube was 14.0 mm and the outer diameter was 17.0 mm. Characteristic concentrations were found by Watling as 0.4 and $0.1 \mu\text{g mL}^{-1}$, respectively for FAAS and SQT-FAAS. Enhancement as 2.9 was found by Brown (Brown et al. 1985).

4. RESULTS AND DISCUSSION

4.3. Optimization of SQT-AT-FAAS Conditions for Determination of Bi

In this part, SQT was used as an atom trap device; it was placed on the burner head. Bi solution was aspirated for a certain time into the flame by using a lean flame. Analyte atoms were collected on the inner surface of SQT. After collection, by aspiration of a low amount of organic solvent, atoms were released from the surface and a transient signal was obtained and recorded. Important optimization parameters such as flame conditions, suction rate of sample, height of the SQT from burner head, type and volume of organic solvent and trapping period were optimized.

4.3.1. Effect of Organic Solvent for SQT-AT-FAAS Determination of Bi

Various organic solvents such as ethyl alcohol, methyl alcohol, isopropyl alcohol, cyclopropanol, n-butanol, acetonitrile, methyl ethyl ketone (MEK) and methyl isobutyl ketone (MIBK) were used in revolatilization of Bi on SQT. The highest signal was obtained when MEK was used as organic solvent (Table 4.4).

Table 4.4. Effect of organic solvents on 100.0 ng mL⁻¹ Bi signal for SQT-AT-FAAS method

Type of organic solvent	Absorbance
Ethyl alcohol	0.033
Methyl alcohol	0.019
Isopropyl alcohol	0.036
Cyclopentanol	0.006
n-butanol	0.007
Acetonitrile	0.011
Methyl ethyl ketone	0.065
Methyl isobutyl ketone	0.037

4.3.2. Investigation of Volume of Organic Solvent for SQT-AT-FAAS Determination of Bi

Effect of volume of MEK on 100.0 ng mL^{-1} Bi signal was investigated in the range of 20.0-60.0 μL interval. It could be seen in Figure 4.8. that Bi signal reached to the highest value when 50.0 μL of MEK was used. Volumes different from this value gave the lower signals. The lower signals for volumes lower than 50.0 μL were attributed to insufficiency for revolatilization, whereas over flame in SQT was the reason of instability of flame and decreasing the Bi signal at volume higher than 50.0 μL .

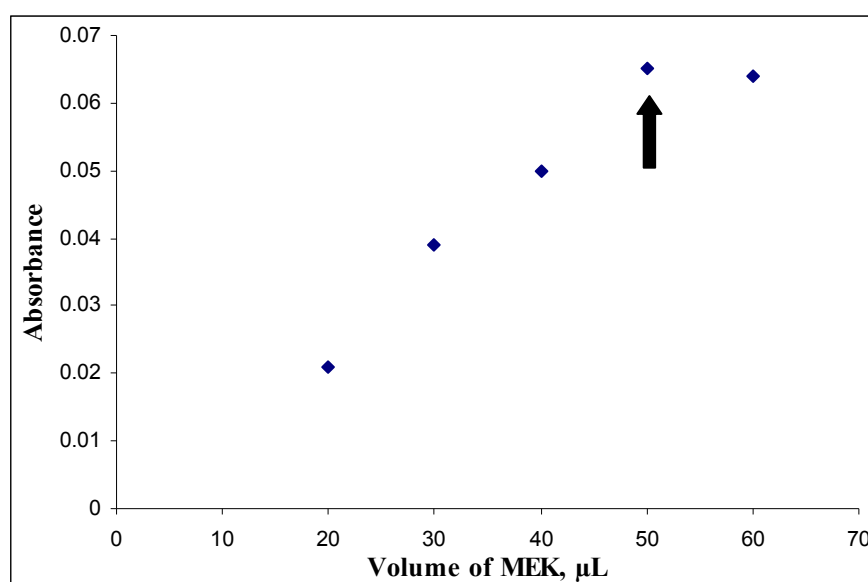


Figure 4.8. Investigation of volume of organic solvent for SQT-AT-FAAS determination of Bi; 100.0 ng mL^{-1} Bi; 2.0 mm height of SQT from burner, flow rate of air: 4.0 L min^{-1} , flow rate of acetylene: 0.6 L min^{-1} , sample suction rate: 5.5 mL min^{-1} , 2.0 min of trapping time

4. RESULTS AND DISCUSSION

4.3.3. Investigation of Sample Suction Rate for SQT-AT-FAAS Determination of Bi

Effect of sample suction rate on analytical signal of 100.0 ng mL^{-1} of Bi signal was investigated in the range of $4.0\text{-}6.0 \text{ mL min}^{-1}$. Results about suction rate on Bi signal were shown in Figure 4.9. Higher analytical signal was obtained for Bi at high suction rate. Therefore, 6.0 mL min^{-1} of sample suction rate was chosen as sample suction rate for Bi. Suction rate higher than this value was not employed by considering the sample consumption.

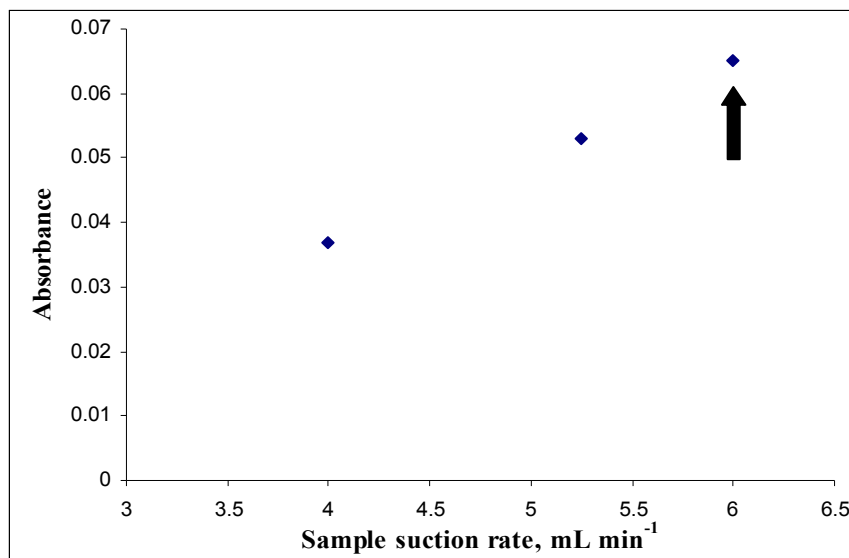


Figure 4.9. Investigation of sample suction rate for SQT-AT-FAAS determination of Bi; 100.0 ng mL^{-1} Bi; 2.0 mm height of SQT from burner, flow rate of air: 4.0 L min^{-1} , flow rate of acetylene: 0.6 L min^{-1} , 2.0 min of trapping time, $50.0 \mu\text{L}$ of MEK

4.3.4. Investigation of Fuel Flow Rate for SQT-AT-FAAS Determination of Bi

Effect of flow rate of acetylene was investigated in the range of 0.5-0.9 L min⁻¹ of acetylene. As seen from Figure 4.10., 0.5 L min⁻¹ of acetylene was selected as fuel flow. Decreasing in Bi signal was observed with increasing in flow rate of acetylene. Higher flow rate of acetylene could be a disadvantage during the trapping period. In addition, SQT was damaged at higher acetylene flow rates and it was cleaned by hold in 5.0 % HF for few minutes when needed.

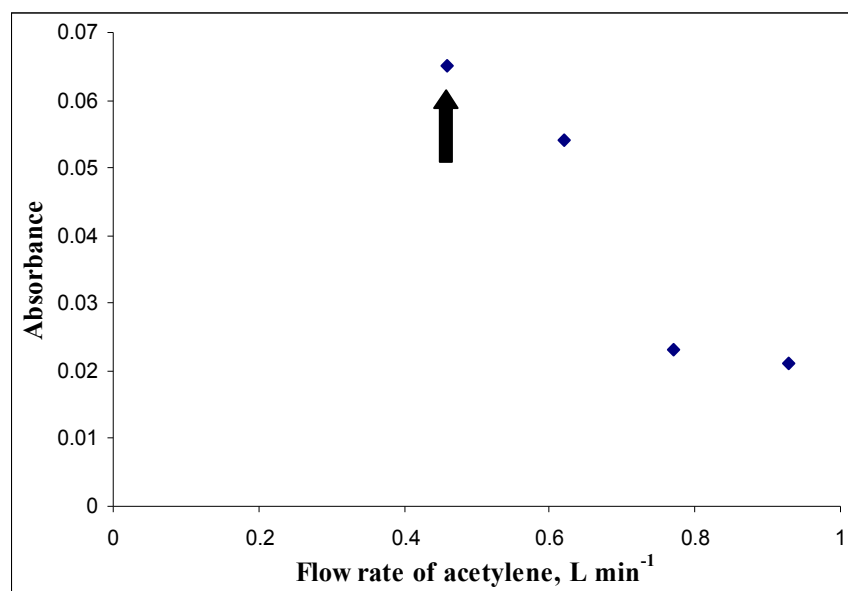


Figure 4.10. Investigation of acetylene suction rate for SQT-AT-FAAS determination of Bi; 100.0 ng mL⁻¹ Bi; 2.0 mm height of SQT from burner, flow rate of air: 4.0 L min⁻¹, sample suction rate: 6.0 mL min⁻¹, 2.0 min of trapping time, 50.0 µL of MEK

4. RESULTS AND DISCUSSION

4.3.5. Investigation of Height of SQT from Burner Head for SQT-AT-FAAS Determination of Bi

Effect of height of SQT from burner was investigated in the range of 2.0-5.0 mm (Figure 4.11.). The highest signal was obtained at the lowest height of SQT. It is likely that the aerosol from Bi solution could not enter the SQT at higher values of height. Insufficient trapping of analyte could be the reason for decreasing in signal. 2.0 mm of height was selected for further studies.

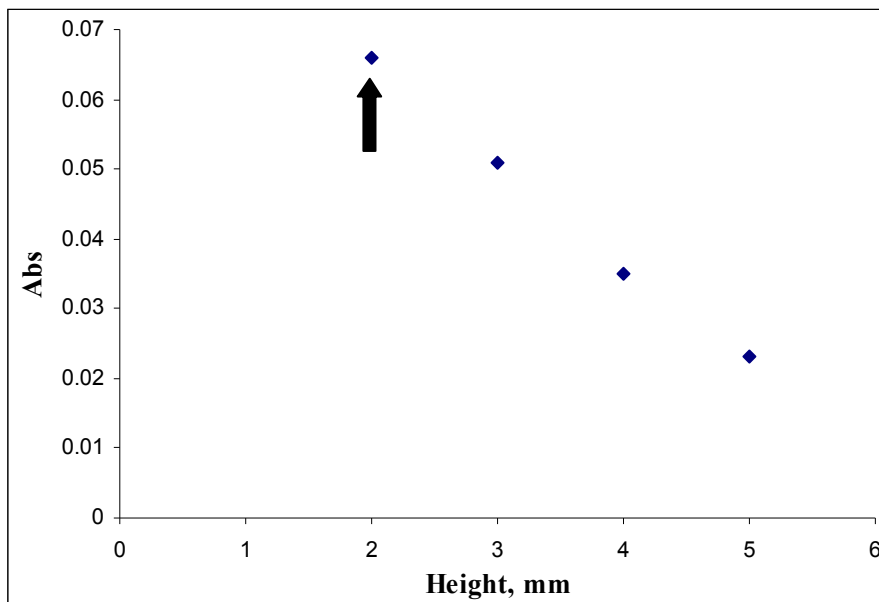


Figure 4.11. Investigation of height of SQT from burner for SQT-AT-FAAS determination of Bi; 100.0 ng mL^{-1} Bi; flow rate of air: 4.0 L min^{-1} ; flow rate of acetylene: 0.5 L min^{-1} ; sample suction rate: 6.0 mL min^{-1} , 2.0 min of trapping time, $50.0 \mu\text{L}$ of MEK

4.3.6. Investigation of Trapping Period for SQT-AT-FAAS Determination of Bi

Trapping of Bi on SQT was investigated for 1.0-6.0 min (Figure 4.12.). It was observed that Bi signal increased with increasing trapping time. By considering the time required for an analysis and decreasing in E_t , longer trapping periods were not examined. 6.0 min of trapping time was employed for further studies.

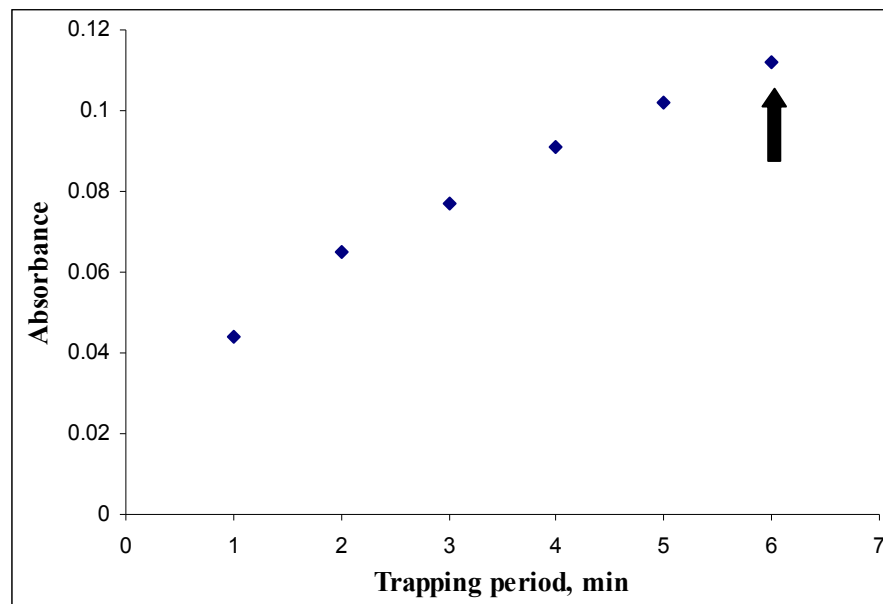


Figure 4.12. Investigation of trapping time for SQT-AT-FAAS determination of Bi; 100.0 ng mL^{-1} Bi; 2.0 mm height of SQT from burner, flow rate of air: 4.0 L min^{-1} , flow rate of acetylene: 0.5 L min^{-1} , sample suction rate: 6.0 mL min^{-1} , $50.0 \mu\text{L}$ of MEK.

4.3.7. Calibration Plot for Bi in SQT-AT-FAAS Method

The signal for 75.0 ng mL^{-1} Bi solution by SQT-AT-FAAS is given in Figure 4.13; the optimized conditions were summarized in Table 4.5. were used. The transient signal was sharp and has a half width of 0.33 s.

Table 4.5. Conditions for SQT-AT-FAAS method for Bi

Parameter	SQT-AT-FAAS
Type of organic solvent	MEK
Volume of organic solvent	$50.0 \mu\text{L}$
Flow rate of acetylene	0.5 L min^{-1}
Sample suction rate	6.0 mL min^{-1}
Height of SQT	2.0 mm
Trapping period	6.0 min

4. RESULTS AND DISCUSSION

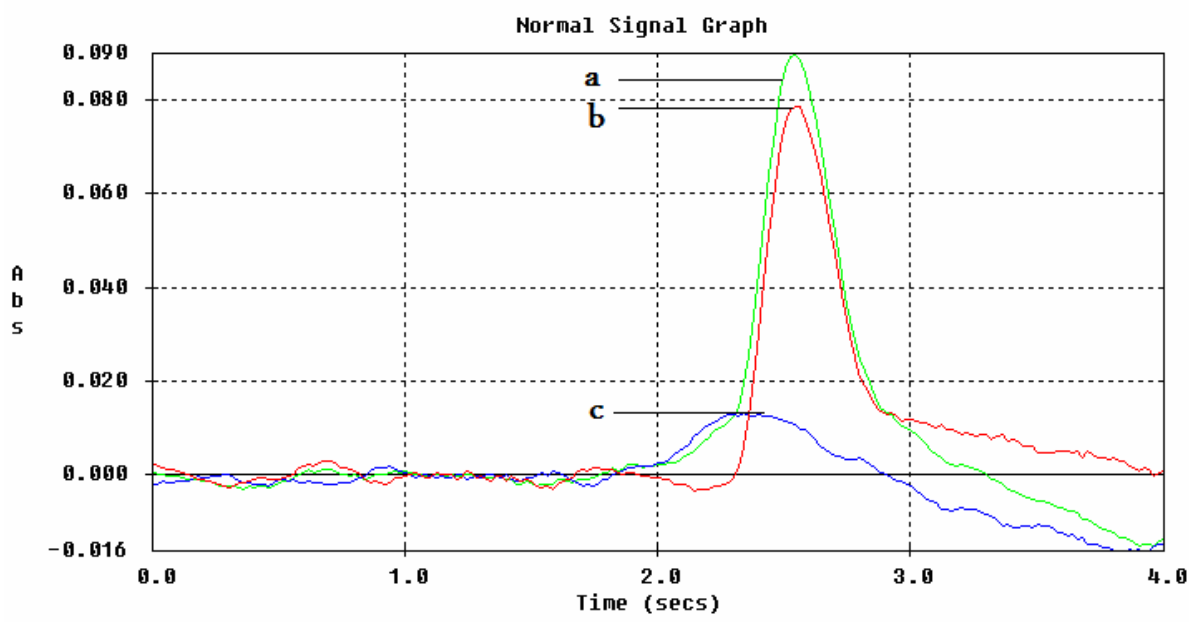


Figure 4.13. Analytical signals for 75.0 ng mL^{-1} of Bi, total signal (a), corrected signal (b), D2 background signal (c) by SQT-AT-FAAS using the conditions in Table 4.5.

Using the optimized parameters given in Table 4.5., absorbance values of Bi solutions in concentrations between $7.5\text{-}450.0 \text{ ng mL}^{-1}$ were measured (Figure 4.13). Calibration plot was linear between $7.5\text{-}100.0 \text{ ng mL}^{-1}$ (Figure 4.15). The best line equation and correlation coefficient were, $y = 1.0334x + 0.0063$ (concentration unit was $\mu\text{g mL}^{-1}$) and 0.9919 respectively.

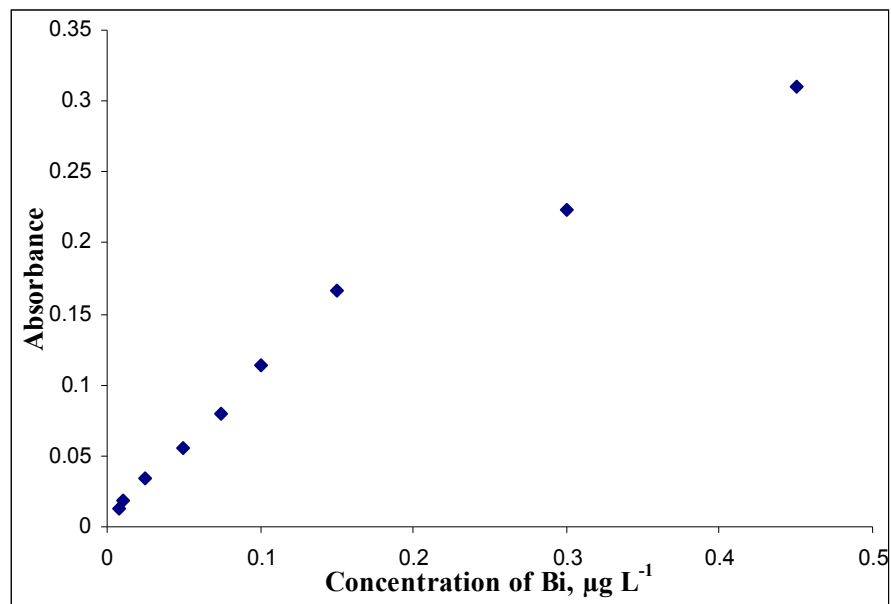


Figure 4.14. Calibration plot for Bi in SQT-AT-FAAS using the parameters in Table 4.5.

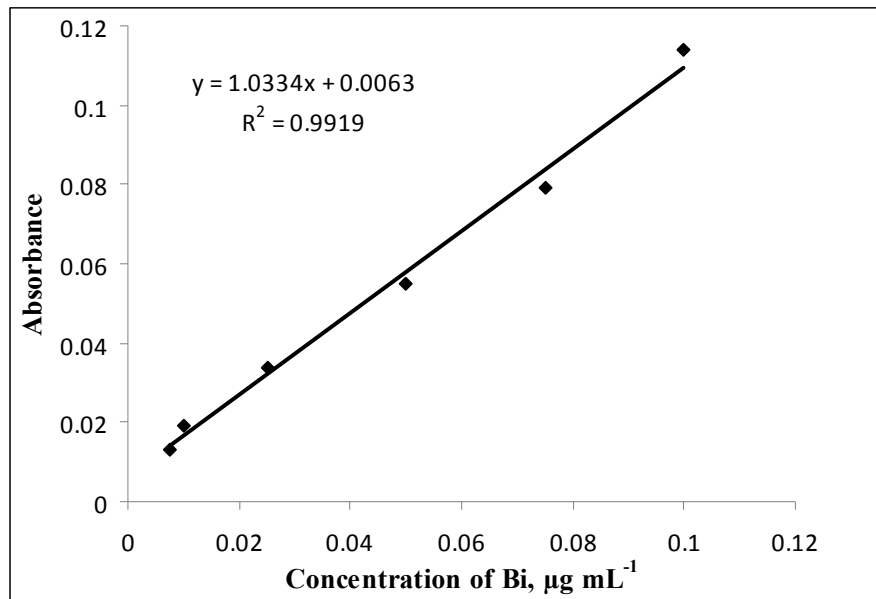


Figure 4.15. Linear calibration plot for Bi in SQT-AT-FAAS using the parameters in Table 4.5.

As seen from Table 4.6. LOD and LOQ were calculated as 1.6 ng mL^{-1} and 5.3 ng mL^{-1} respectively. Characteristic concentration was calculated as 3.4 ng mL^{-1} . By considering the 36.0 mL of trapping volume, characteristic mass was calculated as 122 ng. RSD was calculated as 4.0% for five replicate measurement of 7.5 ng mL^{-1} Bi by SQT-AT-FAAS. Enhancement factor obtained with respect to FAAS was 256. E_t and E_v values were calculated as 43 min^{-1} and 7.1 mL^{-1} , respectively.

Table 4.6. Analytical performance of SQT-AT-FAAS for Bi (36.00 mL trapping, 6.0 min collection)

Parameter	SQT-AT-FAAS
Limit of Detection (LOD), ng mL^{-1}	1.6
Limit of Quantitation (LOQ), ng mL^{-1}	5.3
Characteristic Concentration (c_0), $\mu\text{g mL}^{-1}$	3.4
Characteristic Mass (m_0), ng	122
Enhancement (E) (with respect to FAAS)	256
Enhancement (E_t)	43
Enhancement (E_v)	7.1

West found the c_0 as 4.0 ng mL^{-1} for 3.0 min trapping in silica tube. RSD for twelve measurements was 8%. Alumina and iron oxide were used to coat the inside walls of silica tube. For 2.0 min trapping time, c_0 was given as 10.0 ng mL^{-1} for alumina coated tube and 12.0 ng mL^{-1} for iron oxide coated tube, whereas it was 6 ng mL^{-1} for silica tube without coating (Lau et al. 1988; West 1988). Thus, it can be said that better results were obtained according to literature.

4. RESULTS AND DISCUSSION

4.3.8. Accuracy Check for SQT-AT-FAAS Method and Application to Real Samples

In order to demonstrate the reliability of the proposed method, it was applied to standard reference material, NIST 1643e to determine its Bi content. The analytical result ($13.58 \pm 1.11 \text{ ng mL}^{-1}$ (mean \pm s, $n=3$)) obtained for Bi compared well with the reference value ($14.09 \pm 0.15 \text{ ng mL}^{-1}$) from Table 4.7. Mean recovery ($n=3$) of Bi in SRM was as 96.4%, which indicated that the proposed method is reliable. RSD was found as 8.2%.

Table 4.7. Results of the accuracy test for SQT-AT-FAAS method

NIST 1643e Trace elements in water	Certified Bi ng mL ⁻¹	Founded ng mL ⁻¹
	14.09 ± 0.15	13.58 ± 1.11

^a Experimental conditions were given in Table 4.5.

The proposed method was applied to the determination of Bi in tap water samples from Elaziğ and Diyarbakır cities, natural spring waters and river water from Tigris River-Diyarbakır. Results were presented in Table 4.8.

Higher concentration of Bi was determined in river water versus literature whereas it was not found in tap water. Solid phase extraction method was developed for Bi determination by Taher et al. (Taher et al. 2004). Bi was not found in river water. In another study, Bi was found in waste water as 0.53 ng mL^{-1} whereas it was not detected in tap and river water (Niazi and Afshar 2011). Shemirani et al. determined the Bi in tap water as 0.16 ng mL^{-1} (Shemirani et al. 2005). 0.3 ng mL^{-1} of Bi was determined in river water using adsorptive stripping voltammetry couple with continuous wavelet transform (Khaloo et al. 2007). Bi was determined in Moskva River as lower than 4.1 ng mL^{-1} of sample (Gordeeva et al. 2003). Concentrations of Bi in human serum were in the range of $0.89\text{--}6.04 \text{ ng mL}^{-1}$ (Sun and Wu 2011).

Table 4.8. Concentration of Bi in water samples by SQT-AT-FAAS

Sample	Bi, ng mL ⁻¹	RSD, %
Tap water-1	<LOD	-
Tap water-2	<LOD	-
Natural spring water-1	<LOD	-
Natural spring water-2	<LOD	-
Tigris River water	11.96 ± 0.56	4.7

4.3.9. Interference Studies for SQT-AT-FAAS Method

Atom trapping technique does not only help achieve better sensitivity, but also may be advantageous from interference point of view. This advantage may be of two kinds; the first one is due to better sensitivity that allows dilution of the sample where interferent concentrations are also lowered. The second sort of advantage is due to the trapping technique itself where some of the interferents may not be trapped or released in the same manner as analyte. Therefore, any interference in solution phase may be lowered by the first advantage as the contents are diluted. The second sort of advantage will be helpful for only the interferences taking place in gas phase during atomization. Kula et al. studied effects of different interferents on bismuth determination by tungsten trap hydride generation atomic absorption spectrometry (Kula et al. 2009). They observed that interference effects of chloride, sulfate and phosphate ions were significantly reduced as compared with the no-trap system. Using trap, interferences due to Se, As, Mn, Cu and Zn were also lowered where the interferent to analyte concentration ratios were kept constant.

The potential interfering effect of various concomitant elements on the SQT-AT-FAAS technique for Bi determination was investigated. Effects of each element were evaluated by individually. Effects of ions on 75.0 ng mL^{-1} Bi were investigated in case of mass concentration of interferent were 1.0, 10.0 and 100.0 fold with respect to Bi concentration.

Figure 4.16. contains the effects of Na, Ca and Mg. It was found that Na, Ca and Mg showed serious interferences on Bi determination when their concentrations were 100 fold higher than Bi. In this case recoveries values were found lower than 90%. Decreasing was attributed to coating of surface with alkali metals. In this case, SQT was kept in 5% HF for a few minute.

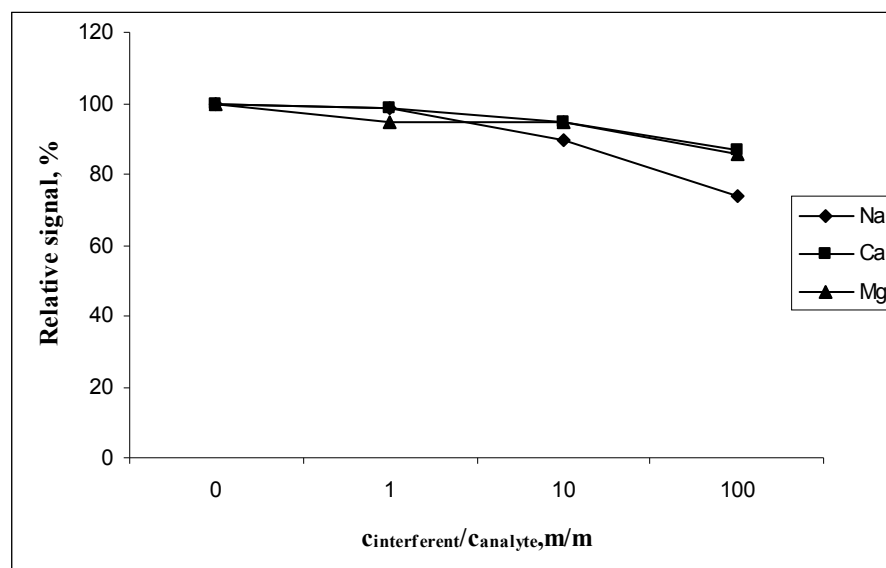


Figure 4.16. Interference effects of Na, Ca and Mg on 75.0 ng mL^{-1} of Bi signal in SQT-AT-FAAS

4. RESULTS AND DISCUSSION

Effect of Fe, Mn, Cr, Zn and Al is seen in Figure 4.17., 1.0, 10.0 and 100.0 folds of Fe, Mn, Cr and Zn did not change Bi signal significantly. Positive interferences were observed in case of mass concentration of Al were 1.0 and 100.0 fold higher than Bi.

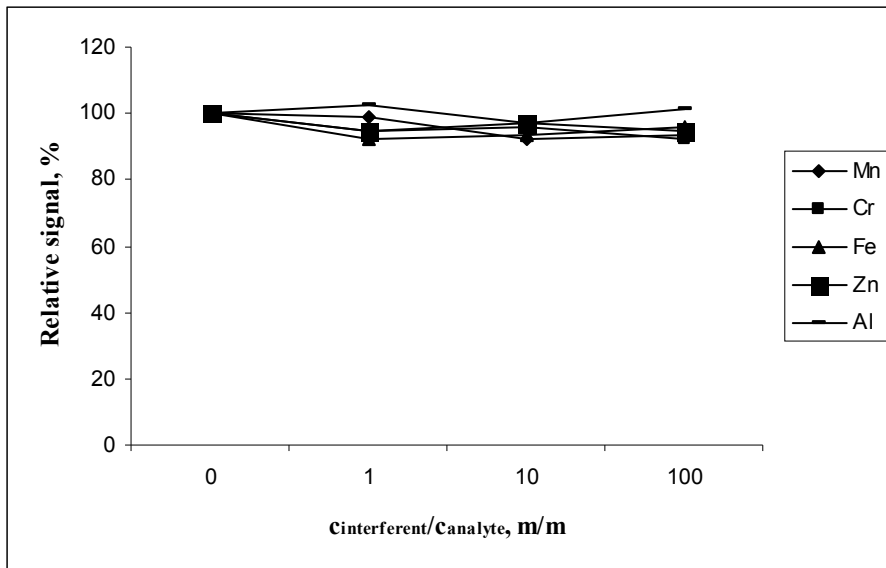


Figure 4.17. Interference effects of Mn, Cr, Fe, Zn and Al on 75.0 ng mL⁻¹ of Bi signal in SQT-AT-FAAS

In Figure 4.18., effect of transition metals (Co, Ni, Cu and Mo) are seen. Decreasing in Bi signal was observed with increasing in Mo concentration. Bi signal was reduced as 7.9% when 100.0 fold of Mo was subjected. The highest decreasing was observed for Co and Ni when their concentrations were 10.0 fold higher than Bi. Although 10.0 and 100.0 folds of Cu did not affect the Bi signal significantly, 75.0 ng mL⁻¹ of Bi signal was decreased in case of 1.0 fold of Cu.

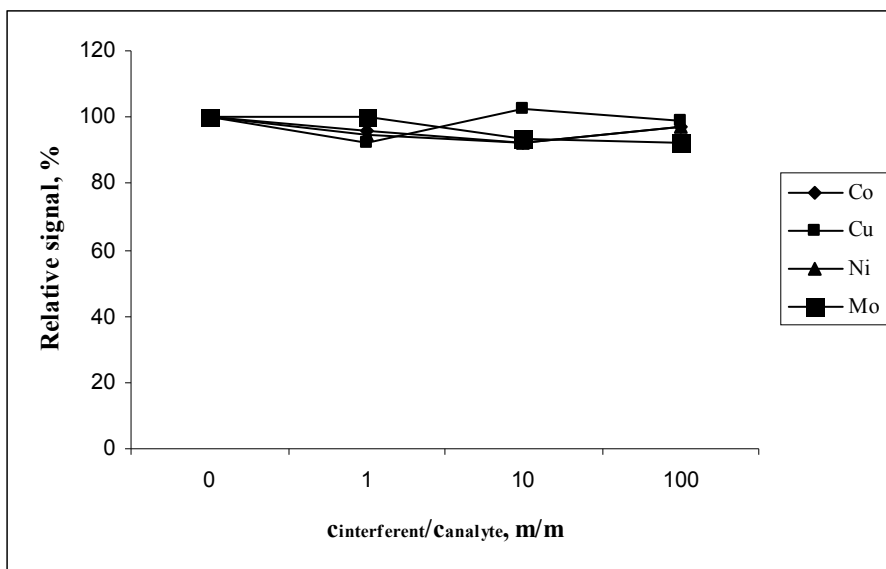


Figure 4.18. Interference effects of Co, Cu, Ni and Mo on 75.0 ng mL⁻¹ of Bi signal in SQT-AT-FAAS

Effect of Sb, Se and Sn was given in Figure 4.19. Sn and Se did not changed Bi signal seriously. 10% decreasing was observed when concentration of Sb was 10.0 fold higher than Bi concentration.

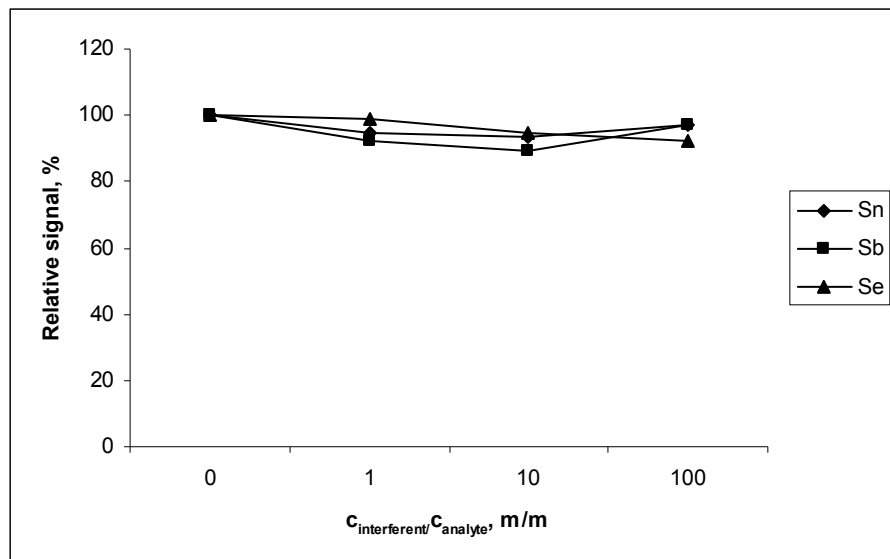


Figure 4.19. Interference effects of Sn, Sb and Se on 75.0 ng mL⁻¹ of Bi signal in SQT-AT-FAAS

As it is seen in the Figure 4.20., Bi signal was decreased when concentration of SO₄²⁻ and NO₂⁻ were 100.0 fold higher than Bi. Re-coating of SQT was required after studies. Approximately 17% decreasing in sensitivity and signal instability was attributed to co effect of Na in solution. Since, ions solutions were prepared from their Na salts. 1 and 10 folds of Cl⁻ did not change. 10% decreasing was observed for 100.0 fold Cl⁻.

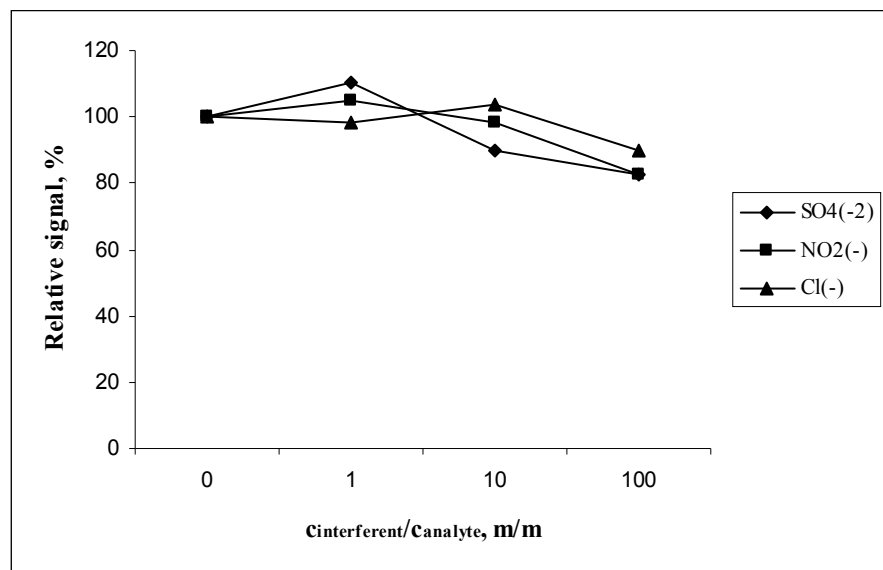


Figure 4.20. Interference effects of SO₄²⁻, NO₂⁻ and Cl⁻ on 75.0 ng mL⁻¹ of Bi signal in SQT-AT-FAAS

4. RESULTS AND DISCUSSION

Effects of interfering ions on 75.0 ng mL⁻¹ of Bi by SQT-AT-FAAS were given in Table 4.9.

Table 4.9. Effect of interfering ions on 75.0 ng mL⁻¹ of Bi by SQT-AT-FAAS

Element	Interferant/ Bi (w/w)		
	1.0	10.0	100.0
Na	99	90	74
Ca	99	95	87
Mg	95	95	86
Mn	99	92	93
Cr	95	96	92
Fe	92	93	96
Zn	95	97	95
Al	103	97	101
Co	96	92	97
Cu	92	103	99
Ni	95	92	97
Mo	100	93	92
Sn	95	93	97
Sb	92	90	97
Se	97	95	92
SO ₄ ²⁻	93	96.	88
NO ₂ ⁻	92	93	91
Cl ⁻	95	92	90

4.4. Optimization of Metal Coated SQT-FAAS Conditions for Determination of Bi

4.4.1. Investigation of Coating Metal for Metal Coated SQT-AAS Determination of Bi

The most important point here is that the melting point of the coating material should be higher than that of the analyte element. Coating material should not be lost significantly from the surface when element volatilizes from the SQT. Effect of Mo, Zr, W and Ta were investigated. Coating procedure was described in previous section.

As seen in the Table 4.10., use of W coated SQT device gave the highest signal with low RSD. Signals of Mo, Zr and Ta were lower than signal obtained from W coated SQT. The lowest analytical signal was obtained from uncoated SQT. Thus, it can be said that coating of SQT surface facilitates the trapping of Bi.

Table 4.10. Effect of coating material on $10.0 \text{ } \mu\text{g mL}^{-1}$ Bi signal for metal coated SQT-FAAS method.

Coating metal	Absorbance
None	0.150
Mo	0.167
Zr	0.176
W	0.194
Ta	0.185

4.4.2. Investigation of Fuel Flow Rate for W Coated SQT-FAAS Determination of Bi

Effect of acetylene flow rate on Bi signal by W coated SQT-FAAS was studied in the range of $0.6\text{--}2.0 \text{ L min}^{-1}$ while air flow rate was constant at 4.0 L min^{-1} (Figure 4.21.). It was found that Bi signal decreased with increasing in acetylene flow rate. Therefore, 0.6 L min^{-1} of acetylene flow was chosen.

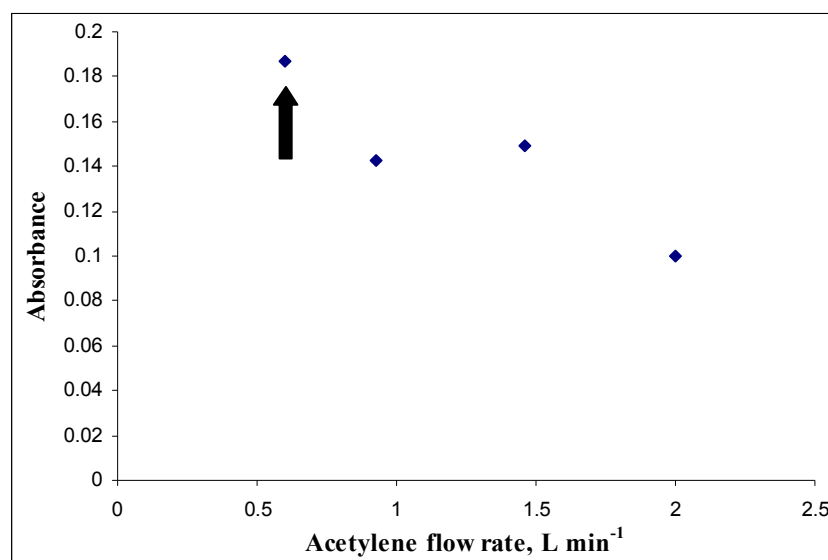


Figure 4.21. Investigation of acetylene flow rate for W coated SQT-FAAS determination of Bi; $10.0 \text{ } \mu\text{g mL}^{-1}$ Bi; flow rate of air: 4.0 L min^{-1} , sample suction rate: 4.5 mL min^{-1} , 2.0 mm height of SQT from burner

4. RESULTS AND DISCUSSION

4.4.3. Investigation of Sample Suction Rate for W Coated SQT-FAAS Determination of Bi

It was known from the previous experience that signal of Bi increased with increasing suction flow of sample as seen in FAAS and SQT-FAAS. It was investigated in the range of $3.4\text{-}5.6\text{ mL min}^{-1}$ (Figure 4.22.). Flow rate of solution was adjusted on entire of solution in nebulizer. 5.6 mL min^{-1} was selected as suction rate in W coated SQT-FAAS method.

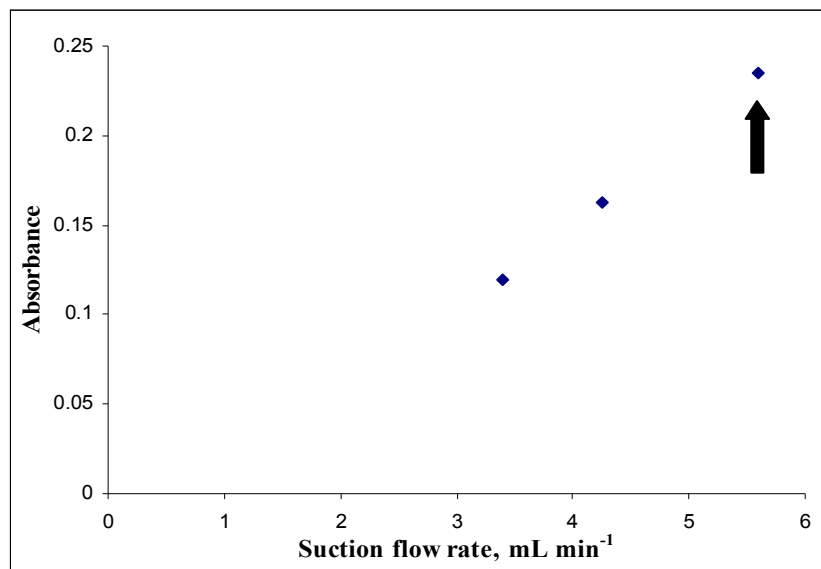


Figure 4.22. Investigation of suction rate of sample for W coated SQT-FAAS determination of Bi; $10.0\text{ }\mu\text{g mL}^{-1}$ Bi; flow rate of air: 4.0 L min^{-1} , flow rate of acetylene: 0.6 L min^{-1} , 2.0 mm height of SQT from burner

4.4.4. Investigation of Height of SQT from Burner Head for W Coated SQT-FAAS Determination of Bi

Effect of height of SQT from burner was examined in the range of 2.0-5.0 mm. Because of physical limitations and compression of fuel and air in the burner, 1.0 mm of height was not tried. Highest signal was recorded when height was the lowest value. Therefore, it was decided to use position the SQT 2.0 mm far from the burner (Figure 4.23.).

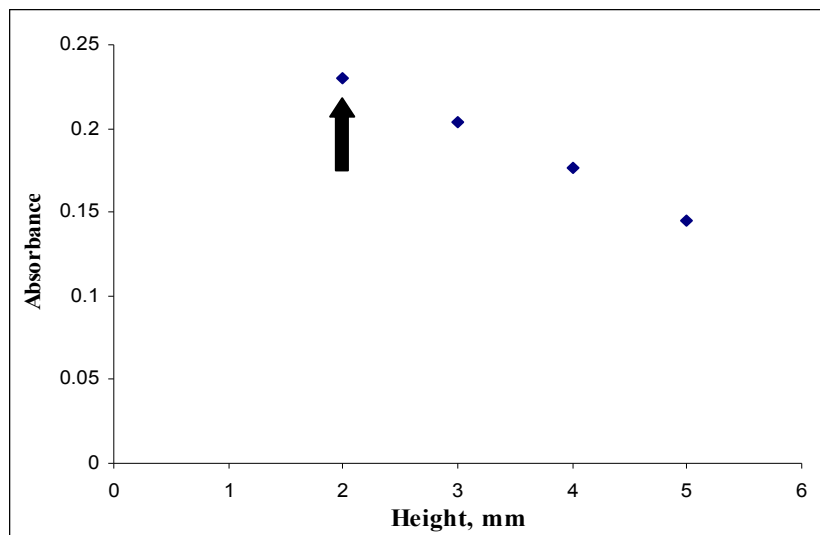


Figure 4.23. Investigation of height of SQT from burner for W coated SQT-FAAS determination of Bi, $10.0 \mu\text{g mL}^{-1}$ Bi; flow rate of air: 4.0 L min^{-1} , flow rate of acetylene: 0.6 L min^{-1} , sample suction rate: 5.6 mL min^{-1}

4.4.5. Calibration Plot for Bi by W Coated SQT-FAAS Method

The optimized conditions of W coated SQT-FAAS method were summarized in Table 4.11.

Table 4.11. Conditions for W coated SQT-FAAS method for Bi

Parameter	W coated SQT-FAAS
Coating metal	W
Flow rate of acetylene	0.6 L min^{-1}
Sample suction rate	5.6 mL min^{-1}
Height of SQT	2.0 mm

Using the optimized parameters, absorbance values of Bi solutions in concentrations between $0.5\text{-}20.0 \mu\text{g mL}^{-1}$ were measured (Figure 4.24). Linear calibration curve was obtained for Bi by using optimized values in W coated SQT-FAAS. The best line equation and correlation coefficient were, $y = 0.0192x + 0.0044$ and 0.9966 respectively, in the concentration range of $0.5\text{-}15.0 \mu\text{g mL}^{-1}$ (Figure 4.25).

4. RESULTS AND DISCUSSION

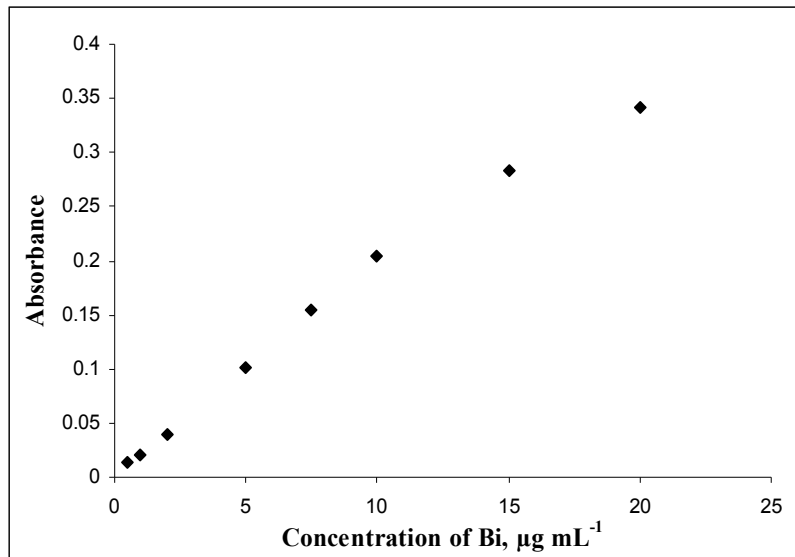


Figure 4.24. Calibration plot for Bi by W coated SQT-FAAS method, 2.0 mm height of SQT from burner, flow rate of air: 4.0 L min^{-1} , flow rate of acetylene: 0.6 L min^{-1} , sample suction rate: 5.6 mL min^{-1}

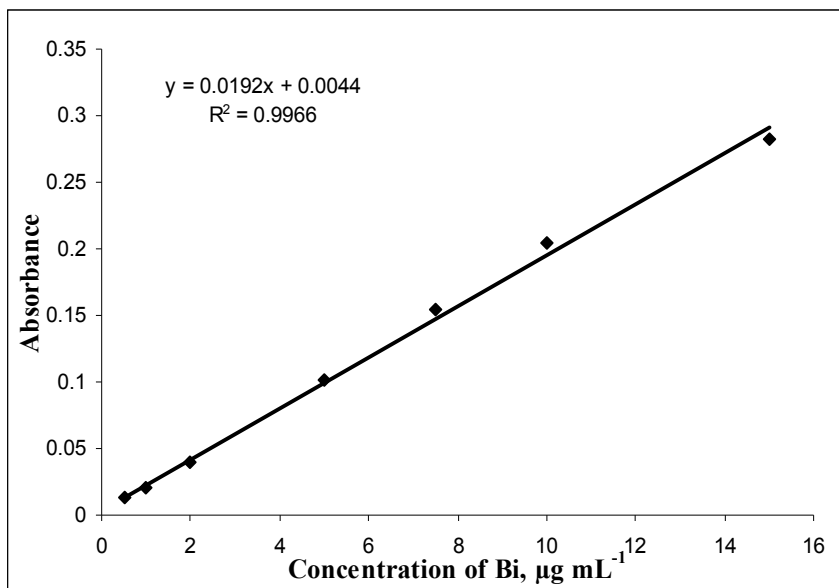


Figure 4.25. Linear calibration plot for Bi in W coated SQT-FAAS method, 2.0 mm height of SQT from burner, flow rate of air: 4.0 L min^{-1} , flow rate of acetylene: 0.6 L min^{-1} , sample suction rate: 5.6 mL min^{-1}

As seen from Table 4.12. LOD and LOQ were calculated as $0.14 \mu\text{g mL}^{-1}$ and $0.46 \mu\text{g mL}^{-1}$, respectively. Characteristic concentration was calculated as $0.22 \mu\text{g mL}^{-1}$. Enhancement factor obtained with respect to FAAS was 3.95. For LOD and LOQ determination 7 measurements of $0.5 \mu\text{g mL}^{-1}$ solution were taken.

Table 4.12. Analytical performance of W coated SQT-FAAS for Bi

Parameter	W coated SQT-FAAS
Limit of Detection (LOD), $\mu\text{g mL}^{-1}$	0.14
Limit of Quantitation (LOQ), $\mu\text{g mL}^{-1}$	0.46
Characteristic Concentration (c_0), $\mu\text{g mL}^{-1}$	0.22
Enhancement (E) (with respect to FAAS)	4.0

4.5. Optimization of Metal Coated SQT-AT-FAAS Conditions for Determination of Bi

4.5.1. Investigation of Coating Material on Metal Coated SQT-AT-FAAS

In section 4.5., it was found that W was the best coating metal to improve the sensitivity of Bi by SQT-FAAS method. Since, W coated SQT was used in atom trapping experiments. Experimental variables such as type and volume of organic solvent, flow rate of fuel and suction rate of sample, height of SQT and trapping time were optimized.

4.5.2. Effect of Organic Solvent for W Coated SQT-AT-FAAS Determination of Bi

A highly flammable organic solvents such as ethyl alcohol, methyl alcohol, acetonitrile, 2-propanole, MEK, M\$IBK and tetrahydrofurane (THF) were used in revolatilization of Bi on surface of W coated SQT. The highest signal was obtained when MIBK was used as organic solvent (Table 4.13.). Ethyl alcohol, methyl alcohol and acetonitrile gave the similar magnitudes of Bi signals. When THF was tried, it was observed that flame was not stable. In this case, flame was over the SQT from upper slit. Another disadvantage of the use of THF was the deformation of quartz windows because, under these conditions the formed flame extended from both ends of SQT towards the sides.

Table 4.13. Effect of organic solvents on 20.0 ng mL^{-1} Bi signal for W coated SQT-AT-FAAS method

Type of organic solvent	Absorbance
Ethyl alcohol	0.056
Methyl alcohol	0.060
Acetonitrile	0.055
Isopropyl alcohol	0.068
Tetrahydrofurane	0.069
Methyl ethyl ketone	0.064
Methyl isobutyl ketone	0.070

4. RESULTS AND DISCUSSION

4.5.3. Investigation of Volume of Organic Solvent for W coated SQT-AT-FAAS Determination of Bi

Effect of volume of MIBK on 20.0 ng mL^{-1} Bi signal was investigated in the range of 20.0-60.0 μL intervals. It could be seen in Figure 4.26. that Bi signal reached to the highest value when 50.0 μL of MIBK was used. Volumes different from this value gave lower signals. The lower signals for volumes lower than 50.0 μL were attributed to insufficient revolatilization, whereas excess solvent could be the reason of instability of flame and decreasing the Bi signal.

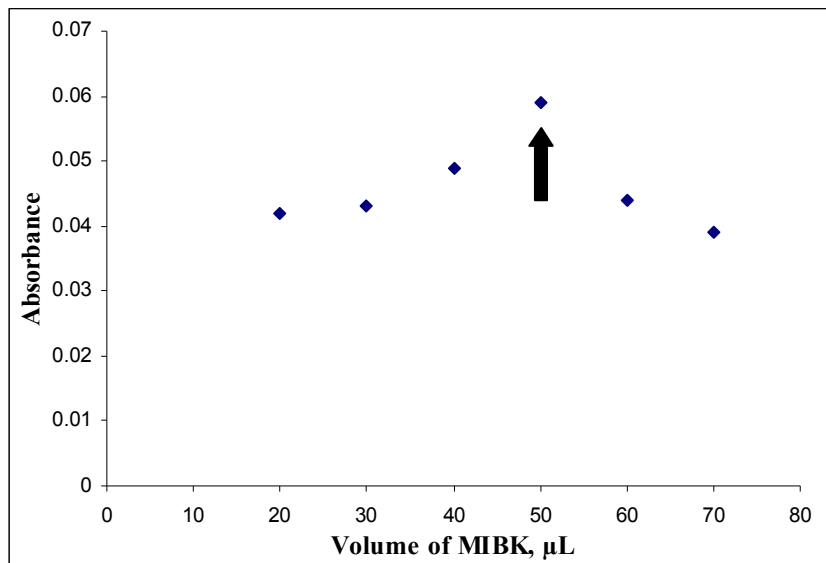
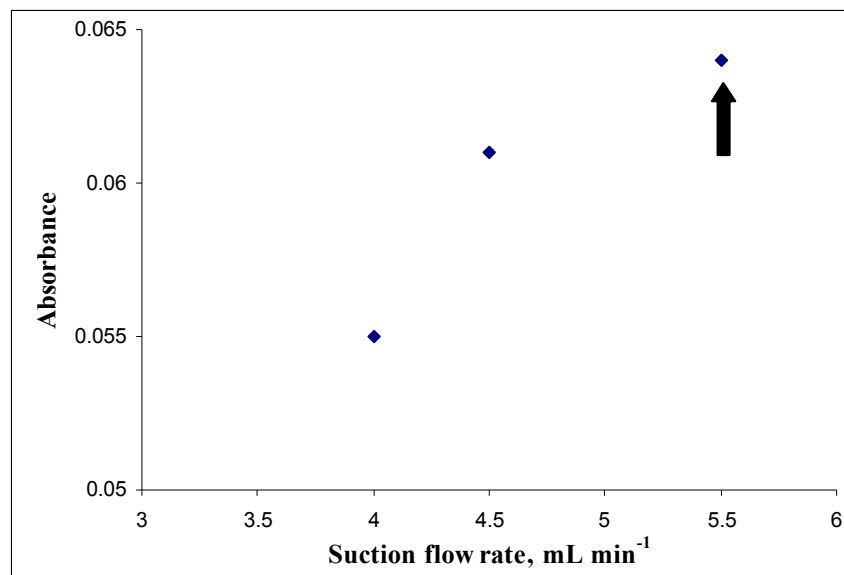


Figure 4.26. Investigation of volume of MIBK for W coated SQT-AT-FAAS determination of Bi; 20.0 ng mL^{-1} Bi; 2.0 mm height of SQT from burner, flow rate of air: 4.0 L min^{-1} , flow rate of acetylene: 0.6 L min^{-1} , sample suction rate: 4.5 mL min^{-1} , 2.0 min of trapping time

4.5.4. Investigation of Sample Suction Rate for W coated SQT-AT-FAAS Determination of Bi

The optimization of sample suction rate was done by using 20.0 ng mL^{-1} Bi solution at a 4.0 L min^{-1} air and 0.6 L min^{-1} acetylene flow rates. Result of the optimization of suction rate of sample was shown in Figure 4.27. It is clear that at high suction rate, better signal was obtained. It is due to the increasing population of analyte atoms per unit time in flame. Higher suction rates, so at lower suction rates signals of Bi are decreasing. Effect of sample suction rate was investigated in the range of $4.0\text{-}5.5 \text{ mL min}^{-1}$. Therefore, 5.5 mL min^{-1} was chosen as sample suction rate for Bi.

**Figure 4.27.**

Investigation of suction rate of sample for W coated SQT-AT-FAAS determination of Bi; 20.0 ng mL^{-1} Bi; 2.0 mm height of SQT from burner, flow rate of air: 4.0 L min^{-1} , flow rate of acetylene: 0.6 L min^{-1} , 2.0 min of trapping time, $50.0 \mu\text{L}$ of MIBK

4.5.5. Investigation of Fuel Flow Rate for W coated SQT-AT-FAAS Determination of Bi

Effect of flow rate of acetylene was investigated in the range of $0.6\text{--}2.5 \text{ L min}^{-1}$ of acetylene (Figure 4.28.). Bi signal was decreased with increasing in flow rate of acetylene. Over flame in SQT and instability of the flame was the result of high flow rate of acetylene. 0.6 L min^{-1} of acetylene was selected as optimum fuel flow. Damaging in SQT was observed when flow rate of acetylene was higher than 1.5 L min^{-1} . Decreasing of signal was attributed to reduced trapping efficiency of W coated SQT. Same procedure as SQT-AT-FAAS studies was applied to clean the W coated SQT and it was recoated.

4. RESULTS AND DISCUSSION

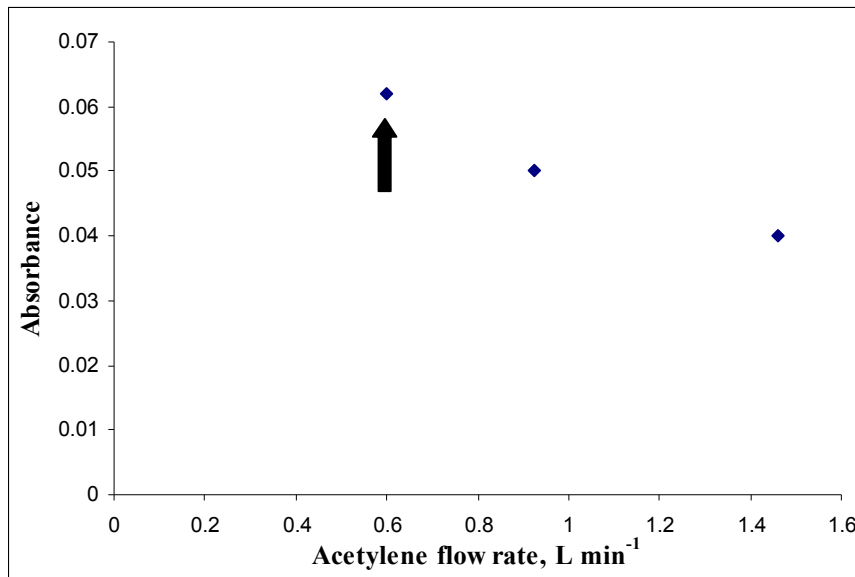


Figure 4.28. Investigation of flow rate of acetylene for W coated SQT-AT-FAAS determination of Bi; 20.0 ng mL⁻¹ Bi; 2.0 mm height of SQT from burner, flow rate of air: 4.0 L min⁻¹, sample suction rate: 5.5 mL min⁻¹, 2.0 min of trapping time, 50.0 µL of MIBK

4.5.6. Investigation of Height of SQT from Burner Head for W coated SQT-AT-FAAS Determination of Bi

From the previous experience, effect of height of W coated SQT from burner was investigated for 2.0-5.0 mm of height (Figure 4.29.). When W coated SQT was closer to burner, introduction and entering of flame into the lower slot was easier. This caused an increase in the Bi signal. 2.0 mm of height was selected for further studies.

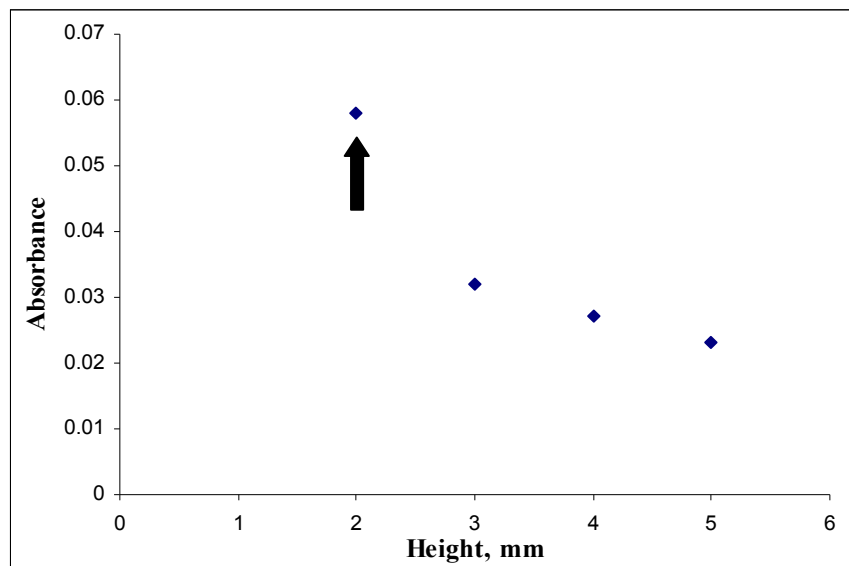


Figure 4.29. Investigation of height of W coated SQT for W coated SQT-AT-FAAS determination of Bi; 20.0 ng mL⁻¹ Bi; flow rate of air: 4.0 L min⁻¹, flow rate of acetylene 0.6 L min⁻¹, sample suction rate: 5.5 mL min⁻¹, 2.0 min of trapping time, 50.0 µL of MIBK

4.5.7. Investigation of Trapping Period for W coated SQT-AT-FAAS Determination of Bi

Trapping time is another important parameter in W coated SQT-AT-FAAS. If analyte atoms are trapped in a longer time interval, sensitivity is improved. However, limitation in sample volume should be considered when selecting the trapping time. Additionally, total analysis time should not be ignored when comparing this method versus others. 20.0 ng mL^{-1} of Bi was trapped on W coated SQT for 1.0-5.0 min and 5.0 min was selected as trapping period (Figure 4.30.).

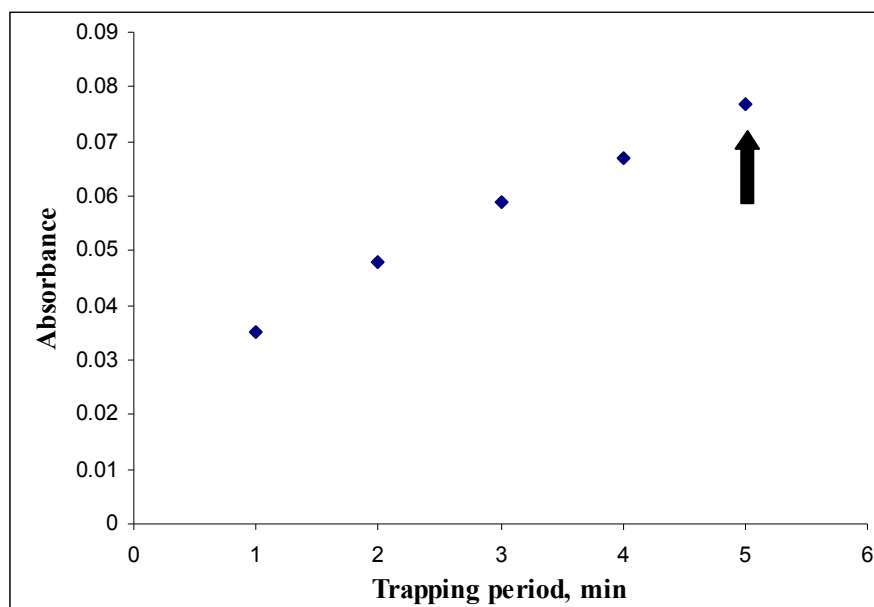


Figure 4.30. Investigation of trapping period for W coated SQT-AT-FAAS determination of Bi; 20.0 ng mL^{-1} Bi; flow rate of air: 4.0 L min^{-1} , flow rate of acetylene 0.6 L min^{-1} , 2.0 mm height of SQT from burner, sample suction rate: 5.5 mL min^{-1} , $50.0 \mu\text{L}$ of MIBK

4.5.8. Calibration Plot for W Coated SQT-AT-AAS Method

The signal for 20.0 ng mL^{-1} Bi solutions by W coated SQT-AT-FAAS is given in Figure 4.31; the optimized conditions given in Table 4.14. were used. The half bandwidth of this signal was found to be 0.41 s.

Table 4.14. Conditions for W coated SQT-AT-FAAS method for Bi

Parameter	W coated SQT-AT-FAAS
Type of organic solvent	MIBK
Volume of organic solvent	$50.0 \mu\text{L}$
Flow rate of acetylene	0.6 L min^{-1}
Sample suction rate	5.5 mL min^{-1}
Height of SQT	2.0 mm
Trapping period	5.0 min

4. RESULTS AND DISCUSSION

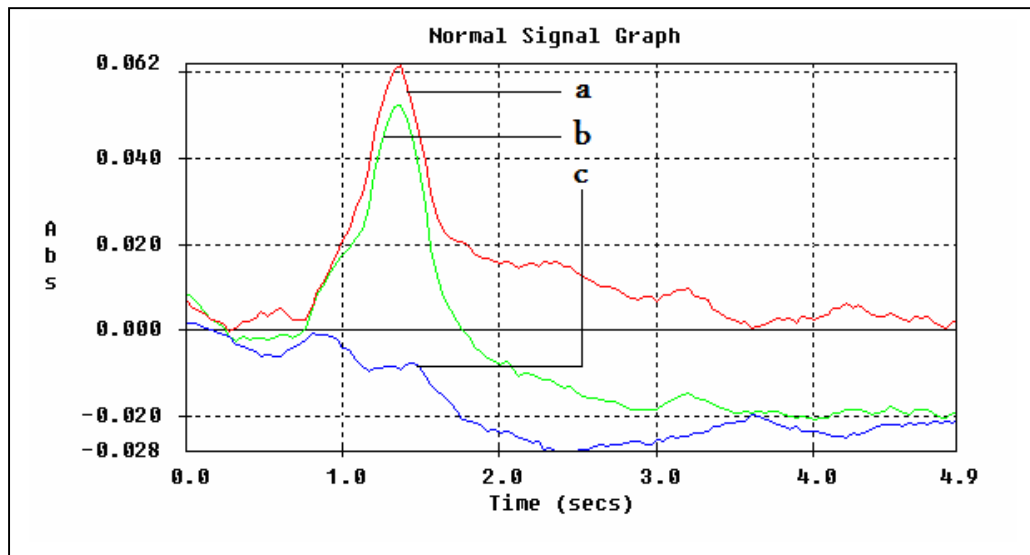


Figure 4.31. Analytical signals for 20.0 ng mL^{-1} Bi, corrected signal (a), total signal (b), D2 background signal (c) by W coated SQT-AT-FAAS using the conditions in Table 4.14.

Using the optimized parameters, absorbance values of Bi solutions in concentrations between $2.5\text{-}100.0 \text{ ng mL}^{-1}$ were measured (Figure 4.32). Calibration plot was linear between $2.5\text{-}25.0 \text{ ng mL}^{-1}$ (Figure 4.33.). The best line equation and correlation coefficient were, $y = 0.0031x + 0.0017$ and 0.9991 respectively.

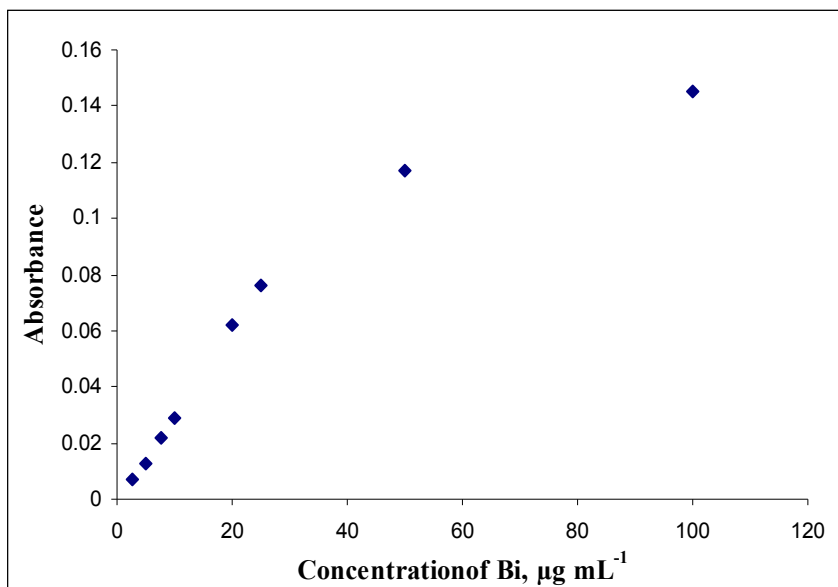


Figure 4.32. Calibration plot for Bi by W coated SQT-AT-FAAS using the conditions in Table 4.14.

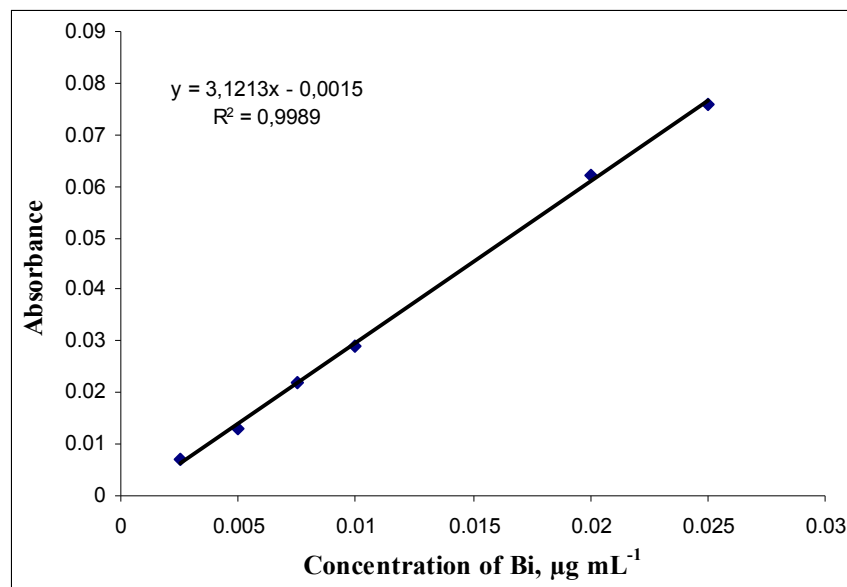


Figure 4.33. Linear calibration plot for Bi by W coated SQT-AT-FAAS using the conditions in Table 4.14.

As seen from Table 4.15. LOD and LOQ were calculated as 0.51 ng mL^{-1} and 1.7 ng mL^{-1} , respectively. Characteristic concentration was calculated as 1.4 ng mL^{-1} . For LOD and LOQ determinations, seven measurements of 2.5 ng mL^{-1} solutions were taken. RSD was calculated as 7.2% for seven replicate measurement of 2.5 ng mL^{-1} Bi. Characteristic mass was calculated as 39 ng. Enhancement factor obtained with respect to FAAS was 613. E_t and E_v values were calculated as 111 min^{-1} and 22 mL^{-1} , respectively.

Table 4.15. Analytical performance of W coated SQT-AT-FAAS for Bi

Parameter	W coated SQT-AT-FAAS
Limit of Detection (LOD), ng mL^{-1}	0.51
Limit of Quantitation (LOQ), ng mL^{-1}	1.7
Characteristic Concentration (c_0), ng mL^{-1}	1.4
Characteristic Mass (m_0), ng	39
Enhancement (E) (with respect to FAAS)	613
Enhancement (E_t)	111
Enhancement (E_v)	22

4. RESULTS AND DISCUSSION

4.5.9. Accuracy Check for W Coated SQT-AT-AAS Method and Application to Real Samples

The SRM, NIST 1643e, trace elements in water, was used for the accuracy check of W coated SQT-AT-FAAS method. The direct calibration was employed and three replicate measurements were done under optimum conditions. The results were in good agreement with the certified value as shown in the Table 4.16. RSD was found as 8.9%. Confidence interval was calculated as $12.66 \pm 2.78 \text{ ng mL}^{-1}$ from student's test.

Table 4.16. Results of the accuracy test for Bi by W coated SQT-AT-FAAS method (n=3)

NIST 1643e Trace elements in water	Certified Bi ng mL ⁻¹	Founded Bi ng mL ⁻¹
	14.09±0.15	12.66±1.12

^a Experimental conditions were given in Table 4.14.

Concentration of Bi in two different tap water samples and two natural spring water samples was determined by W coated SQT-AT-FAAS. Bi concentrations in these samples were lower than detection limit, whereas $12.13 \pm 1.15 \text{ ng mL}^{-1}$ Bi was found in Tigris River water. RSD was found as 9.2% from three replicate measurements.

4.6. Interference Studies for W Coated SQT-AT-AAS Method

Interference studies were performed to determine the effect of other elements and ions to the Bi signal. For this aim, 3 different solutions were prepared in which the concentration of Bi was kept constant, 20.0 ng mL^{-1} , and concentrations of interfering ions were 1.0, 10.0 and 100.0 folds of the analyte concentration, using the mass ratios. By considering the trapping efficiency of the W coated SQT, interference studies were not performed for 1000.0 folds of the analyte concentration.

Results on effects of Na, Ca and Mg on Bi signal were given in Figure 4.34. It was observed that Bi signal was not significantly affected when the interferent concentrations were 10.0 fold higher than that of Bi. However, Bi signal was decreased by 17%, 10% and 2.0 respectively for Na, Ca and Mg when their concentrations were 100.0 fold higher than that of Bi. Trapping efficiency of W coated SQT was decreased by Na and Ca. In this case, SQT was re-coated by aspirating of $100.0 \mu\text{g mL}^{-1}$ of W solution at lean flame.

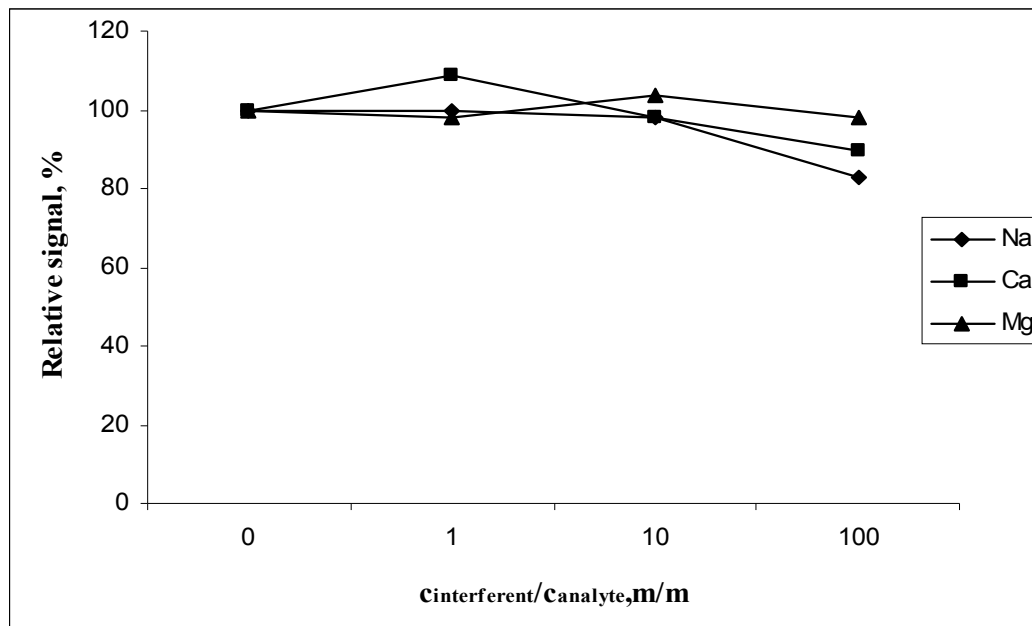


Figure 4.34. Interference effects of Na, Ca and Mg on 20.0 ng mL⁻¹ of Bi signal in W coated SQT-AT-FAAS

Effect of Fe, Mn, Cr, Zn and Al is seen in Figure 4.35., 1.0, 10.0 and 100.0 folds of Fe and Mn did not change Bi signal significantly. However, 100.0 fold of Zn and Al suppressed the Bi signal as 12% and 19%, respectively. 1.0 and 10.0 fold of Cr decreased the Bi signal.

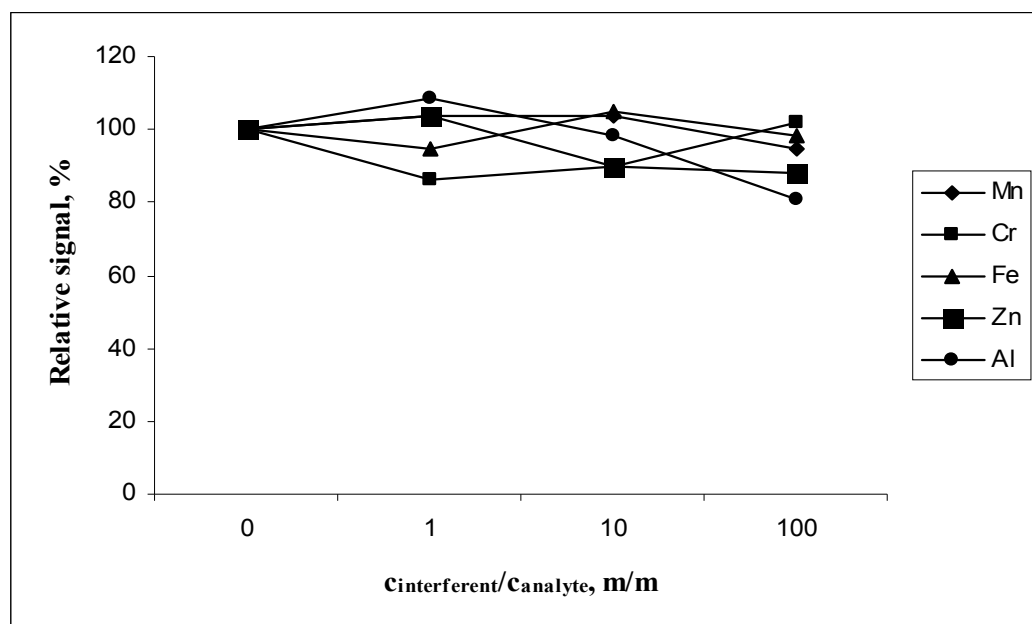


Figure 4.35. Interference effects of Mn, Cr, Fe, Zn and Al on 20.0 ng mL⁻¹ of Bi signal in W coated SQT-AT-FAAS

4. RESULTS AND DISCUSSION

In Figure 4.36., effect of transition metals (Co, Ni, Cu, Mo) are seen. Although 1.0 and 10.0 folds of Co did not affect the Bi signal significantly, 20.0 ng mL⁻¹ of Bi signal was decreased as 10% in case of 100.0 fold Co. The most important effects were caused by 100.0 fold of Cu, Bi signal was suppressed as 14%. Decreasing in Bi signal as 12% was observed when concentration of Ni was 100.0 fold higher than Bi. Bi signal was increased as 6.9% by 100.0 fold of Mo.

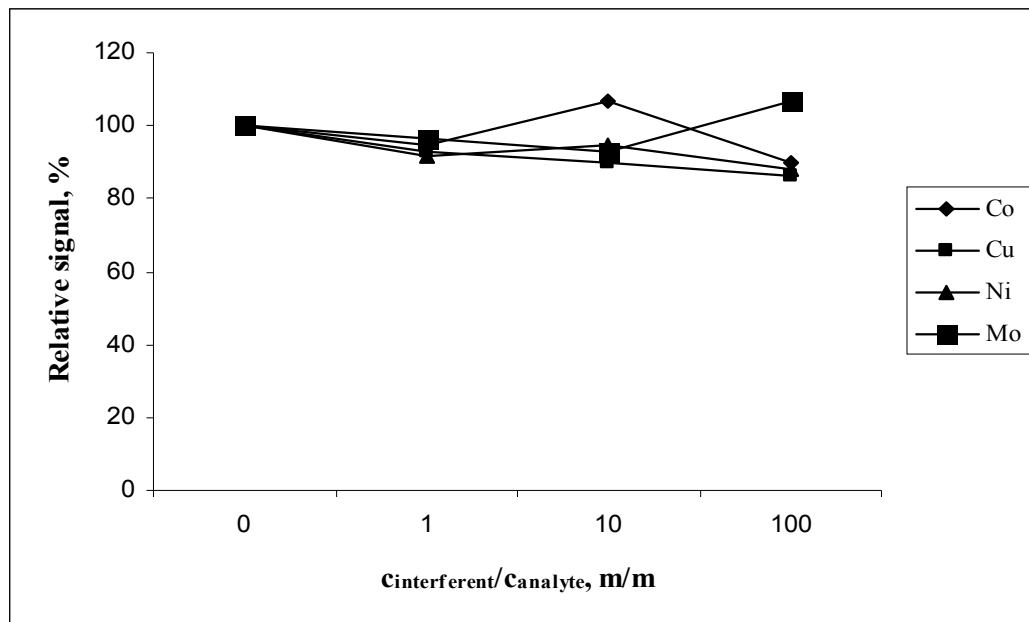


Figure 4.36. Interference effects of Co, Cu, Ni and Mo on 20.0 ng mL⁻¹ of Bi signal in W coated SQT-AT-FAAS

Effect of Sb, Se and Sn was given in Figure 4.37. Sn and Se did not changed Bi signal seriously. 14% decreasing was observed when concentration of Sb was 100.0 fold higher than Bi concentration.

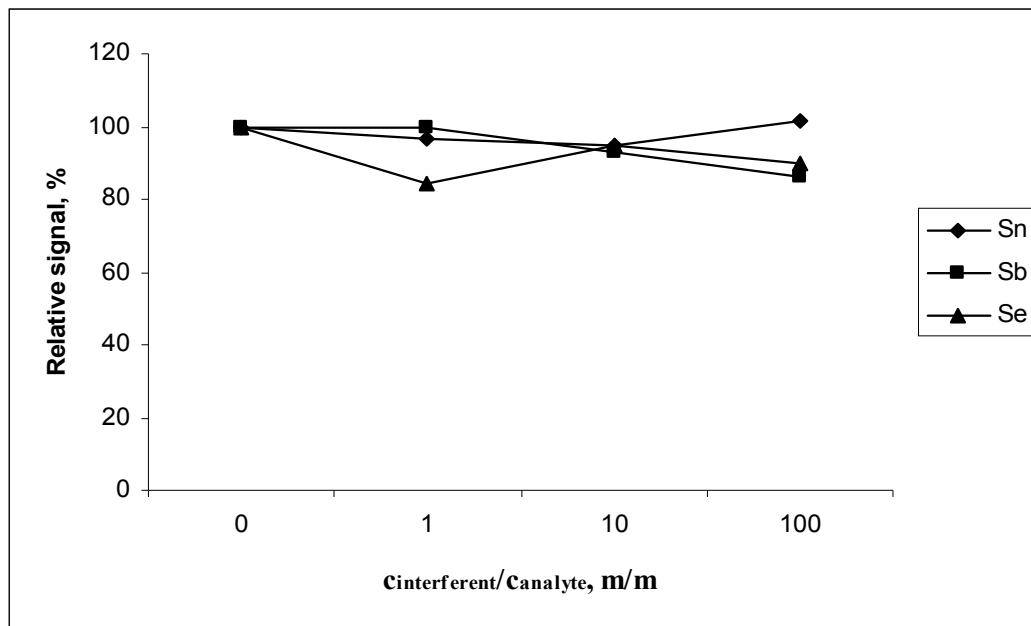


Figure 4.37. Interference effects of Sn, Sb and Se on 20.0 ng mL⁻¹ of Bi signal in W coated SQT-AT-FAAS

As it is seen in the Figure 4.38., Bi signal was decreased when concentration of SO₄²⁻ and NO₂⁻ were 100.0 fold higher than Bi. Re-coating of SQT was required after studies. Approximately 17% decreasing in Bi signal and signal instability was attributed to co effect of Na in solution. Since, ions solutions were prepared from their Na salts. 1.0 and 10.0 folds of Cl⁻ did not change. 10% decreasing was observed for 100.0 fold Cl⁻.

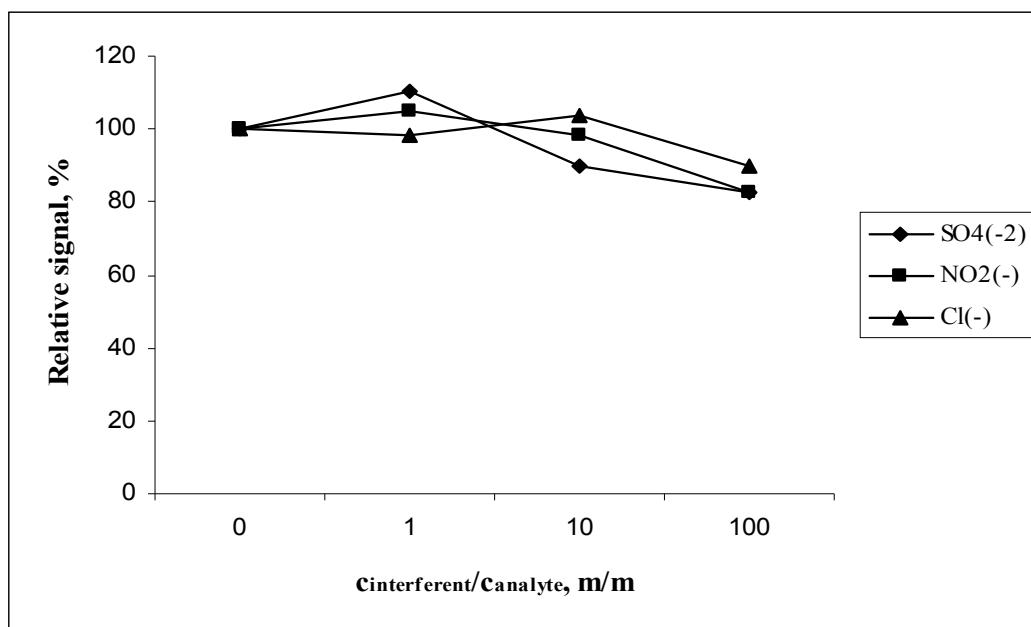


Figure 4.38. Interference effects of SO₄²⁻ and NO₂⁻ and Cl⁻ on 20.0 ng mL⁻¹ of Bi signal in W coated SQT-AT-FAAS

4. RESULTS AND DISCUSSION

Effects of interfering ions on 20.0 ng mL⁻¹ of Bi by W coated SQT-AT-FAAS were given in Table 4.17.

Table 4.17. Effect of interfering ions on 20.0 ng mL⁻¹ of Bi in W coated SQT-AT-FAAS method

Element	Interferant/ Bi (w/w)		
	1.0	10.0	100.0
Na	100	98	83
Ca	109	98	90
Mg	98	103	98
Mn	103	103	95
Cr	86	90	102
Fe	95	105	98
Zn	103	90	88
Al	109	98	81
Co	95	107	90
Cu	93	90	86
Ni	91	95	88
Mo	97	93	107
Sn	97	95	102
Sb	100	93	86
Se	85	95	90
SO ₄ ²⁻	110	90	83
NO ₂ ⁻	105	98	83
Cl ⁻	98	103	90

4.7. Evaluation of System Performance

Analytical features of FAAS, SQT-FAAS, SQT-AT-FAAS, W coated SQT-FAAS and W coated SQT-AT-FAAS methods were summarized in Table 4.18.

Sensitivity of FAAS was improved by using SQT as 2.9 fold with respect to conventional FAAS. It was observed that height of SQT from burner was a critical parameter. Effect of its on Bi signal was investigated in the range of 1.0-5.0 mm. As this value became smaller, a steady increase in signal was observed, corresponding to about 2-fold between 5.0 mm and 1.0 mm. At high values, sample transport into SQT is expected to be lower, causing a lower signal. However, in the case of 1.0 mm height, flame stability was adversely affected and it could be extinguished easily; therefore, optimum height was selected as 2.0 mm. Watling firstly used SQT to improve sensitivity for fourteen elements including Bi; characteristic concentrations were found to be 0.4 and 0.1 µg mL⁻¹, respectively for FAAS and SQT-FAAS (Watling 1977). In another study, Brown et al. calculated the E value as 2.9 for Bi by SQT-FAAS (Brown et al. 1985). It is clear that the enhancement obtained in the present study is comparable to these literature values.

SQT was also used as atom trapping device for further improvement in sensitivity for Bi. 256 fold improvement was obtained by trapping of 36.0 mL solution for 6.0 min. Bi

atoms trapped on SQT surface was revolatilized by aspirating 50.0 μL of MEK. E_t and E_v values were calculated as 43 min^{-1} and 7.1 mL^{-1} , respectively. Accuracy of the method developed was checked by analyzing a standard reference material, NIST 1643e, simulated fresh water. External calibration method was employed and three replicate measurements were performed under optimum conditions. The result of $13.6 \pm 1.1 \mu\text{g L}^{-1}$ ($n=3$) found for Bi which was in good agreement with the reference value of $14.09 \pm 0.15 \mu\text{g L}^{-1}$.

The trapping studies involving hydride generation have inherently higher sensitivity as compared with methods based on nebulization due to the higher sample transport for the former. In the study involving hydride generation and trapping of bismuthine in a graphite cuvette, some of the analytical figures of merit, such as E and c_0 were not available. However, an LOD of 0.13 ng mL^{-1} reported denotes the sensitivity attained (Murphy et al. 1997). Trapping on a heated W-coil followed by AAS (Cankur et al. 2002) or AFS (Liu et al. 2008) also provided low detection limits, 0.0027 ng mL^{-1} and 0.004 ng mL^{-1} , respectively. Use of quartz surface as the atom trap followed by AAS determination of Bi also provided a detection limit of 0.0039 ng mL^{-1} (Kratzer and Dedina 2006), a figure comparable to the W-coil trap systems mentioned (Cankur et al. 2002; Liu et al. 2008). Another method using hydride generation was reported using IAT-AAS having a detection limit of 0.4 ng mL^{-1} (Matusiewicz and Krawczyk 2007b).

Analytical performances of metal coated SQT-FAAS and SQT - *in situ* atom trap- (AT)-FAAS system were evaluated for the determination of Bi. Non-volatile elements such as Mo, Zr, W and Ta were tried as coating materials. It was observed that W coated SQT gave the best sensitivity for the determination of Bi in trap studies. All of the system parameters for W Coated SQT-FAAS and W coated SQT-AT-FAAS were optimized. Sensitivity of FAAS for Bi was improved as 4.0 fold by W Coated SQT-FAAS while 613 fold improvements was achieved by W coated SQT-AT-FAAS with respect to conventional FAAS. MIBK was selected as organic solvent for the re-volatilization of Bi from the trapping surface. LOD values for W coated SQT-FAAS and W coated SQT-AT-FAAS were obtained as 140.0 and 0.51 ng mL^{-1} , respectively. Linear calibration plot was obtained in the range of 2.5-25.0 ng mL^{-1} for W coated SQT-AT-FAAS. SRM, NIST 1643e, trace elements in water, was used to check the accuracy of W coated SQT-AT-FAAS system. Direct calibration method was employed and three replicate measurements were done under optimum conditions. Certified and experimental values were $14.09 \pm 0.15 \text{ ng mL}^{-1}$ and $12.66 \pm 1.12 \text{ ng mL}^{-1}$. As seen from the values, results are in good agreement with the certified value.

Interference studies were performed in order to figure out the effects of some elements and ions such as Na, Ca, Mg, Mn, Cr, Fe, Zn, Al, Co, Cu, Ni, Mo, Sn, Sb, Se, SO_4^{2-} , NO_2^- and Cl^- on the Bi determination by W Coated SQT-AT-FAAS. For this aim, three different solutions for each interferant were prepared where the concentration of Bi was kept constant, 20.0 ng mL^{-1} , and concentrations of interfering ions were 1.0, 10 and 100 folds of the analyte concentration using the mass ratios. By considering the trapping efficiency of the W Coated SQT, interference studies were not performed for 1000.0 folds of the analyte concentration. It is clear in all interference studies that interference tolerance limits will not be exceed in the case of W Coated SQT-AT-FAAS system; this

4. RESULTS AND DISCUSSION

limit was 80% in this study. Hence, it can be stated that developed method can be safely and directly applied to many real samples.

Table 4.18. Analytical features of optimized methods

Analytical parameter	Technique, period, volume				
	FAAS	SQT-FAAS	W coated SQT-FAAS	SQT-AT-FAAS 6.0 min, 36.0 mL	W coated SQT-AT-FAAS 5.5 min, 27.5 mL
LOD, ng mL⁻¹	470	110	140	1.6	0.51
LOQ, ng mL⁻¹	1570	370	460	5.3	1.7
c₀, ng mL⁻¹	870	300	220	3.4	1.4
m₀, ng	-	-	-	122	39
E	-	2.9	4.0	256	613
E_t, min⁻¹	-	-	-	43	111
E_v, mL⁻¹	-	-	-	7.1	22

4.8. Size Optimization for SQT

Influence of inner and outer diameter of SQT on Bi signal was evaluated. Inner diameters were selected as 10.0 and 13.0 mm, while outer diameters were 12.0 and 15.0 mm respectively. By considering the diameter of incident light beam, tube diameter lower than 10.0 mm was not investigated. It was generally observed that there was slightly decreasing in absorbance value of Bi signal while i.d. and o.d. were 13.0 and 15.0 mm, respectively.

Different lengths of lower and upper slots were also tried for possible sensitivity improvement for Bi by SQT-FAAS. Generally, it is known that the lower slit of SQT should be long as slit of flame burner. Thus, flame will directly enter in SQT. In experiments, 100.0 mm length of flame atomizer was used. Optimization was performed only for upper slit. The upper slit should be short than lower one. The reason of this is extent the residence time of atomic vapour in SQT. Thus, absorption of monochromatic radiation will be more versus FAAS without SQT. By considering this situation, three different sizes of upper slit were evaluated. 4.0, 5.0 and 6.0 mm of slit lengths were tried. Higher analytical signal was obtained for SQT that its upper slit length was 5.0 mm while lower slit was 10.0 mm. It could be attributed that flame remains in lath path longer time than other slit length.

Another parameter which influences the sensitivity is wideness of lower slit. In addition to 2.0 mm slit wideness, 4.0 mm was also tried for lower slit. More wide lower slit were tried while upper slit was constant. In case of wide slit, flame from burner can easily enter the insides of SQT. Higher analytical signals for Bi were observed in case of wider lower slit. However, RSD values were higher than thinner slit.

Variation of analytical signal of $10.0 \text{ } \mu\text{g mL}^{-1}$ of Bi depending on different SQT size was presented in Table 4.19.

Table 4.19. Effect of size of SQT on $10.0 \text{ } \mu\text{g mL}^{-1}$ of Bi signal (length of SQT was 14.0 cm in all cases)

Upper slit, cm	Upper slit wideness, mm	Lower slit, cm	Lower slit wideness mm	i.d. mm	o.d. mm	Mean absorbance	RSD, % (N=3)
4.0	2.0	10.0	2.0	10.0	12.0	0.089 ± 0.006	6.7
4.0	2.0	10.0	2.0	13.0	15.0	0.086 ± 0.004	4.7
4.0	2.0	10.0	4.0	10.0	12.0	0.090 ± 0.004	4.4
4.0	2.0	10.0	4.0	13.0	15.0	0.094 ± 0.004	4.3
5.0	2.0	10.0	2.0	10.0	12.0	0.106 ± 0.005	4.7
5.0	2.0	10.0	2.0	13.0	15.0	0.104 ± 0.006	5.8
5.0	2.0	10.0	4.0	10.0	12.0	0.121 ± 0.008	6.6
5.0	2.0	10.0	4.0	13.0	15.0	0.116 ± 0.009	7.7
6.0	2.0	10.0	2.0	10.0	12.0	0.110 ± 0.004	3.6
6.0	2.0	10.0	2.0	13.0	15.0	0.099 ± 0.005	5.1
6.0	2.0	10.0	4.0	10.0	12.0	0.118 ± 0.009	7.6
6.0	2.0	10.0	4.0	13.0	15.0	0.116 ± 0.009	7.8

From the results, it could be said that higher analytical signal for Bi was obtained in case of length of upper slit and lower slits were 5.0 mm and 10.0 mm while wideness of lower slit was 4.0 mm. For this SQT, i.d and o.d. were 10.0 and 12.0 mm. RSD was calculated as 6.6% for three replicate measurement of $10.0 \text{ } \mu\text{g mL}^{-1}$ of Bi.

4. RESULTS AND DISCUSSION

4.9. Optimization of Continuous Flow Hydride Generation Inductively Coupled Plasma - Optical Emission Spectrometry for Determination of Bi

HG-ICP-OES in continuous flow mode with gas-liquid phase separation was employed to determine Bi in trace levels. All of experimental parameters were optimized. Any trapping of hydride was not employed.

4.9.1. Effect of Variables in Hydride Generation Efficiency

The effects of various operating parameters such as concentrations of NaBH_4 , HCl and NaOH , flow rates of NaBH_4 , sample and waste solution, carrier argon flow, radio frequency power, lengths of reaction and stripping coil were examined individually to obtain high S/N for Bi.

It is well known that rate of volatile vapours generation depends on the concentration of NaBH_4 and acidity of solution (Matusiewicz and Ślachciński 2007). Effect of concentration of HCl on 10.0 ng mL^{-1} of Bi was investigated in the range of $0.4\text{-}5.0 \text{ mol L}^{-1}$ of HCl . It was found that the best signal was obtained when concentration of HCl was 5.0 mol L^{-1} (Figure 4.39.).

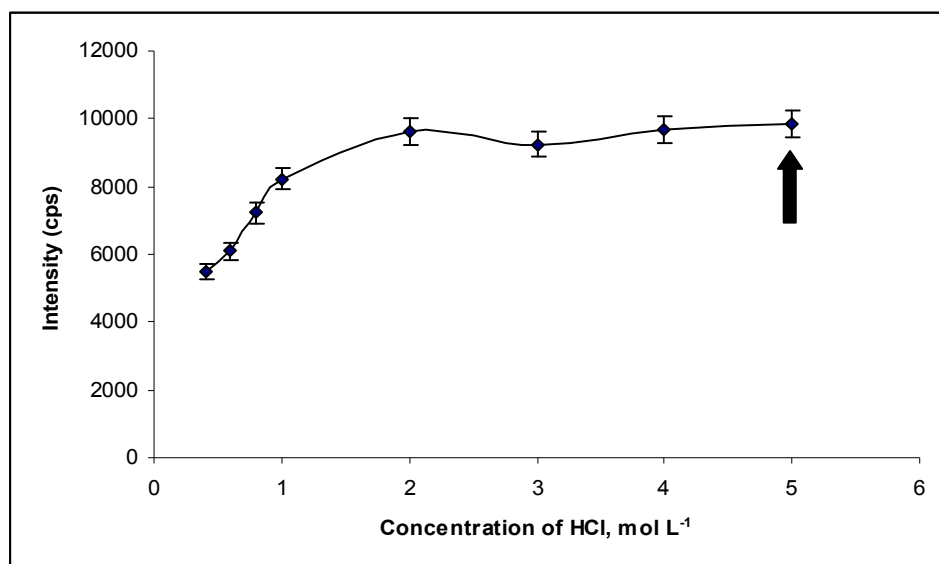


Figure 4.39. Investigation of concentration of HCl ; experimental conditions; 10.0 ng mL^{-1} of Bi, argon flow rate: 17.0 L min^{-1} , carrier argon flow rate 0.6 L min^{-1} , Rf power: 1450 Watt, flow rate of standard solution, NaBH_4 and waste: 1.5 mL min^{-1} , 0.25% NaBH_4 in 1.0% NaOH , reaction coil 11.0 cm, stripping coil 35.0 cm

Then, relationship between the percentage of NaBH_4 as reductant and signal intensity of Bi was investigated in $0.1\text{-}1.0\%$ in 1.0% NaOH . It was found that 1.0% of NaBH_4 gave the relatively best signal (Figure 4.40.).

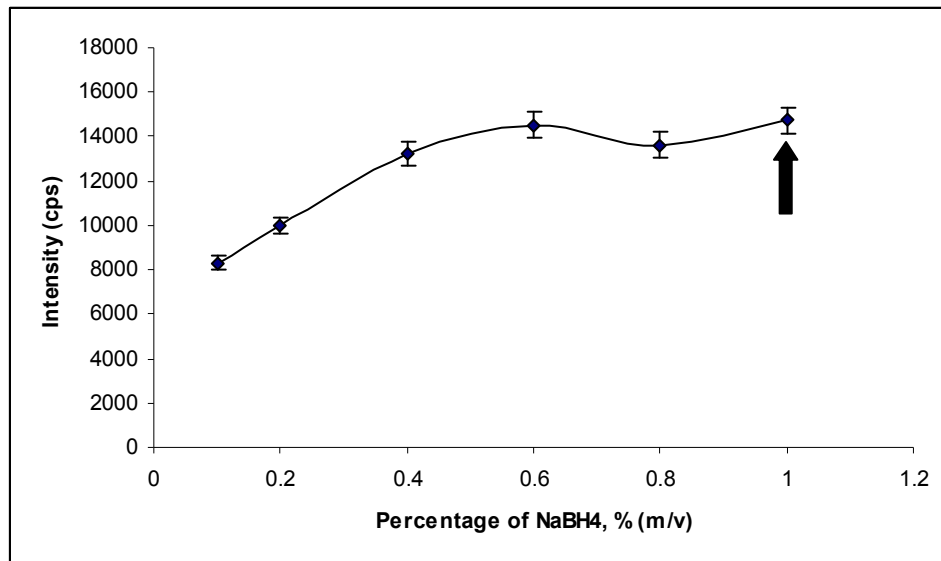


Figure 4.40. Investigation of concentration of NaBH_4 in 1.0 % NaOH ; experimental conditions; 10.0 ng mL^{-1} of Bi in 5.0 mol L^{-1} HCl , argon flow rate: 17.0 L min^{-1} , carrier argon flow 0.6 L min^{-1} , Rf power: 1450 Watt, flow rate of standard solution, NaBH_4 and waste: 1.5 mL min^{-1} , reaction coil 11.0 cm, stripping coil 35.0 cm

Effect of percentage of NaOH to stabilize the NaBH_4 was also investigated. While percentage of NaBH_4 was 1.0%, amount of NaOH was changed between 0.01-4.0 %. It was found that the highest S/N ratio was obtained when the amount of NaOH was the lowest. However, it was observed that plasma was unstable when NaOH was lower than 0.25% due to high hydride formation. Thus, it was decided to use the 1.0% NaBH_4 prepared in 0.25% NaOH .

4.9.2. Optimization of Instrumental Parameters

Carrier gas affects the transport efficiency and extraction of hydrides from the gas/liquid separator in hydride generation system. In this study, high purity argon was used as carrier gas and influence of the carrier gas flow rate on the S/N response of Bi was studied in the range of 0.45-0.70 mL min^{-1} . Relationship between the flow rate of carrier argon flow and intensity of Bi is shown in Figure 4.41. It is clear that signal intensity of Bi decreased with increasing carrier gas flow rate. Maximum signal intensities were obtained at 0.5 mL min^{-1} of flow rate of carrier gas. Hence, 0.5 mL min^{-1} of carrier gas flow rate was selected as optimum one.

4. RESULTS AND DISCUSSION

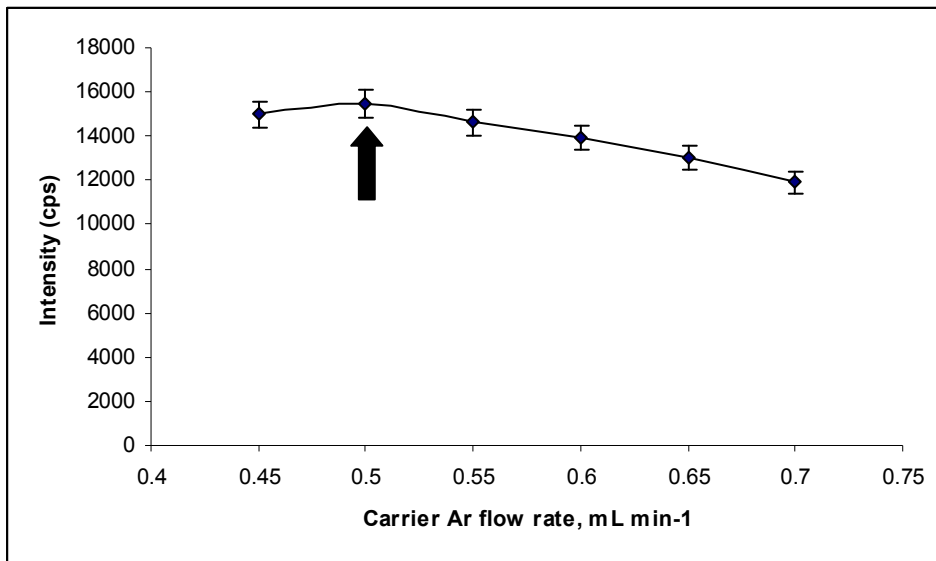


Figure 4.41. Investigation of flow rate of carrier argon; experimental conditions; 10.0 ng mL^{-1} of Bi in 5.0 mol L^{-1} HCl, reductant 1.0% NaBH_4 in 0.25% NaOH , argon flow rate: 17.0 L min^{-1} , Rf power: 1450 Watt, flow rate of standard solution, NaBH_4 and waste: 1.5 mL min^{-1} , reaction coil 11.0 cm, stripping coil 35.0 cm

Stability of ICP was dependent on radio frequency power which applied. Influence of Rf power on Bi signal by CF-HG-ICP-OES was investigated in the range of 1350-1450 Watt (Figure 4.42.). It was found that Bi signal was not significantly changed. However, higher signals were obtained when power was 1375 Watt. Therefore, this point was accepted as optimum.

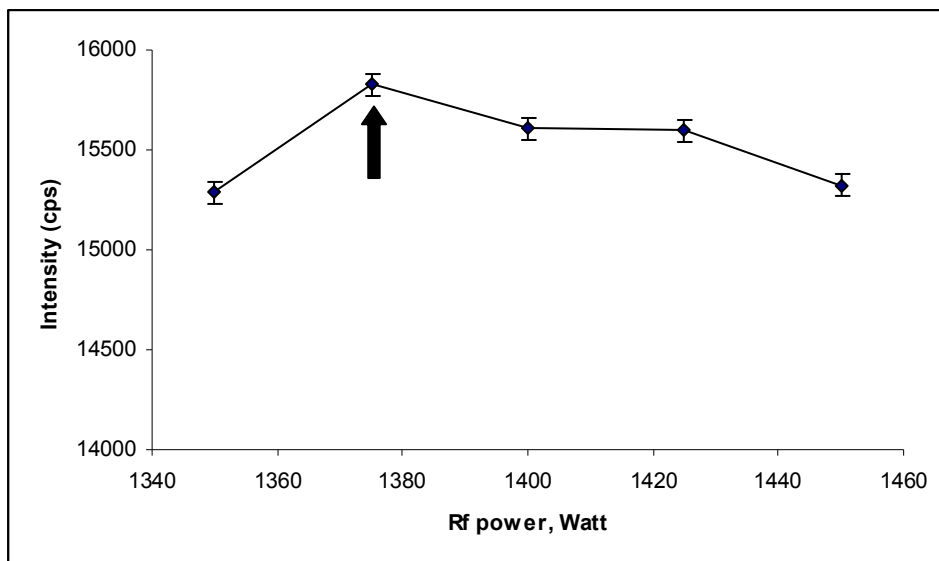


Figure 4.42. Investigation of RF power; experimental conditions; 10.0 ng mL^{-1} of Bi in 5.0 mol L^{-1} HCl, reductant 1.0% NaBH_4 in 0.25% NaOH , argon flow rate: 17.0 L min^{-1} , 0.5 mL min^{-1} of flow rate of carrier, flow rate of standard solution, NaBH_4 and waste: 1.5 mL min^{-1} , reaction coil 11.0 cm, stripping coil 35.0 cm

To optimize the sample and reductant flow rate, optimum flows were investigated in the range of 0.57–2.45 mL min^{-1} (Figure 4.43.). Flow rates were adjusted by using two different peristaltic pumps. Increasing in intensity was observed with increasing flow rate of sample. In this case, 2.45 mL min^{-1} was selected as flow rate of sample.

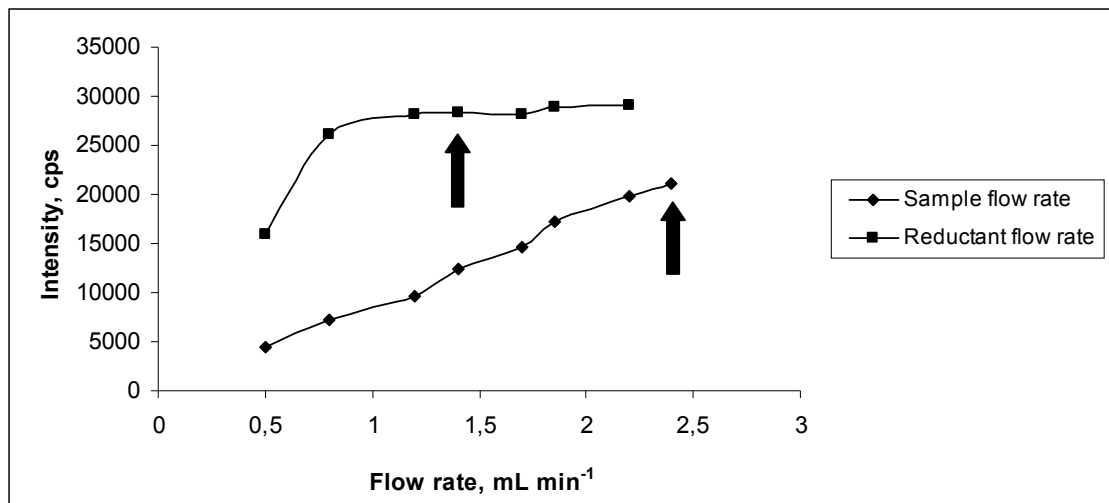


Figure 4.43. Investigation of flow rates of sample solution and reductant; experimental conditions; 10.0 ng mL^{-1} of Bi in 5.0 mol L^{-1} HCl, reductant 1.0% NaBH_4 in 0.25% NaOH , argon flow rate: 17.0 L min^{-1} , Rf power: 1375 Watt, flow rate of waste 1.5 mL min^{-1} , reaction coil 11.0 cm, stripping coil 35.0 cm

It was observed that when flow rate of NaBH_4 was higher than 1.40 mL min^{-1} , the emission intensity was not changed significantly. As a consequence, 1.40 mL min^{-1} was selected as reductant flow rate (Figure 4.47.).

Another optimization parameter in CF-HG-ICP-OES is flow rate of waste. Influence of waste flow rate was investigated in the range of 0.57–2.45 mL min^{-1} . It was found that 1.50 mL min^{-1} was effective to remove the waste of HG process. It should be noted that inner diameter of waste tubing was higher than sample tubing.

Lengths of reaction and stripping coils serve to provide sufficient delay for completion of reaction and transportation of formed hydride. Optimization of this parameter is very important since a too short reaction coil might cause incomplete hydride release and a too long coil increases the risk of interferences in the liquid phase. It was reported that shorter coil length was more effective. One of the reasons is that BiH_3 is generated relatively rapidly and its thermal instability and prolonged residence times will affect the sensitivity (Dedina and Tslev 1995; Marrero et al. 1999; Kula et al. 2009).

In the optimization study, length of reaction coil was varied between 5.0 cm and 20.0 cm while length of stripping coil was changed between 10.0 cm and 50.0 cm. The optimum lengths for reaction coil and stripping coils were found to be 15.0 cm and 25.0 cm, respectively. It was observed that intensity of Bi decreased with the values both lower and higher than the optimum values.

4. RESULTS AND DISCUSSION

4.9.3. Interference Studies on CF-HG-ICP-OES

Determination of Bi by CF-HG-ICP-OES is well known to be susceptible to interferences from various diverse elements (Li and Guo 2005; Das et al. 2006; Benzo et al. 2011). Interfering ions can also compete with the analytes for reaction with reducing agent. Under experimental conditions used here, effect of various other elements on determination of bismuth by CF-HG-ICP-OES system was examined.

Analytical signal of Bi in hydride generation was interfered by other cations such as Cd, Co, Ni and Cu. It was highlighted that decreasing of Bi signal was dependent on concentration of interreferent (Chen et al. 2002; Pohl and Zyrnicki 2002). From this point of view chemical interferences from Cd, Co, Cu, Fe, Ni, As, Hg, Sn and Sb in the determination of Bi by CF-HG-ICP-OES were investigated (Table 4.20.). It was observed that intensity of Bi was suppressed by Cd, Co, Cu, Ni and Sb at their concentrations higher than Bi by 100.0 times. In this case, intensity of Bi was found to be lower about 10%. The highest decreasing was observed when concentration ratio of Cu to Bi was higher than 100.0. It was noted in the literature that Cu interference could be due to the gas phase inter-element interference between the hydride forming elements (Liu et al. 2002). Another parameter which contributes to interference was the length of reaction coil. It was found that when length of reaction coil was increased interferences of Ni and Cu were increased. It was due to reduction of transition metals to metallic state and reaction of theirs with bismuth (Yamamoto et al. 1985). Reduction in Bi signal was dependent on the mass ratio of Cu/Bi (Cankur et al. 2002).

It should be noted that the interferent effect of other elements such as As, Hg, Sb which could form stable hydride on the Bi signal was more serious than other elements. Thus it can be said that applicability of the method also dependent on the concentration ratio of other elements to Bi.

Table 4.20. Effect of interferent concentrations on 10.0 ng mL⁻¹ of Bi by CF-HG-ICP-OES

Ion	$c_{\text{interferent}}/c_{\text{Bi}}^{\text{a}}$ (m/m)	I_R %
Cd	1.0	100
	10.0	93
	100.0	87
Co	1.0	99
	10.0	98
	100.0	90
Cu	1.0	99
	10.0	93
	100.0	77
Fe	1.0	101
	10.0	97
	100.0	97
Ni	1.0	99
	10.0	98
	100.0	91
As	1.0	95
	10.0	94
	100.0	91
Hg	1.0	94
	10.0	87
	100.0	71
Sn	1.0	100
	10.0	99
	100.0	93
Sb	1.0	95
	10.0	91
	100.0	89

^a $c_{\text{interferent}}/c_{\text{Bi}}$: Concentration ratio of interferent ion to Bi

Experimental conditions; 10.0 ng mL⁻¹ of Bi in 5.0 mol L⁻¹ HCl, reductant 1.0% NaBH₄ in 0.25% NaOH, argon flow rate: 17.0 L min⁻¹, Rf power: 1375 Watt, flow rate of sample, reductant and waste were 2.4 mL min⁻¹, 1.4 mL min⁻¹ and 1.5 mL min⁻¹ respectively, reaction coil 15.0 cm, stripping coil 25.0 cm

^b I_R : Relative intensity was defined as the ratio of intensity of 10.0 ng mL⁻¹ of Bi together with interferent ion to intensity of Bi at same concentration without interferent

4. RESULTS AND DISCUSSION

4.9.4. Analytical Figures of Merit

Experimental variables which optimized for Bi by CF-HG-ICP-OES were summarized in Table 4.21.

Table 4.21. Optimized parameters of CF-HG-ICP-OES for Bi

Parameter	CF-HG-ICP-OES
Concentration of HCl	5.0 mol L ⁻¹
Percentage of NaBH ₄	1.0% in 0.25% NaOH
Flow rate of carrier Ar	0.5 mL min ⁻¹
RF power	1375 Watt
Sample flow rate	2.45 mL min ⁻¹
Reducant flow rate	1.4 mL min ⁻¹
Waste flow rate	1.5 mL min ⁻¹
Length of reaction coil	15.0 cm
Length of stripping coil	25.0 cm

By using the optimum parameters linear calibration plot for Bi by CF-HG-ICP-OES was found in the range of 1.0-50.0 ng mL⁻¹ for Bi while it was linear in the range of 25.0-1000.0 ng mL⁻¹ for ICP-OES without HG (Figure 4.44.). Best line equation and correlation coefficient were, $y = 2879.7x - 358.85$ and 0.9995 for Bi by CF-HG-ICP-OES, respectively. LOD, defined as $3s/m$ (where s is standard deviation of the lowest concentration of linear range) was found to be 0.16 ng mL⁻¹, LOQ, defined as $10s/m$ was 0.53 ng mL⁻¹ for Bi. RSD for ten replicate measurements of 10.0 ng mL⁻¹ Bi was calculated as 3.9% for CF-HG-ICP-OES. Analytical characteristics of CF-HG-ICP-OES with respect to conventional ICP-OES were compared in Table 4.22.

Table 4.22. Analytical characteristics of ICP-OES and CF-HG-ICP-OES methods for Bi determination.

Parameter	ICP-OES	CF-HG-ICP-OES
Linear range	25.0-1000.0	1.0-50.0
Calibration plot	$y=235.44x+910.95$	$y=2879.7x-358.85$
LOD	5.55 ng mL ⁻¹	0.16 ng mL ⁻¹
LOQ	18.51 ng mL ⁻¹	0.53 ng mL ⁻¹
RSD	6.6% ²	3.9% ¹
E ³	-	12.2

¹ Calculated from 10 replicate measurement of 10.0 ng mL⁻¹ of Bi

² Calculated from 10 replicate measurement of 25.0 ng mL⁻¹ of Bi

³ Enhancement was calculated from the slope ratio of calibration plots

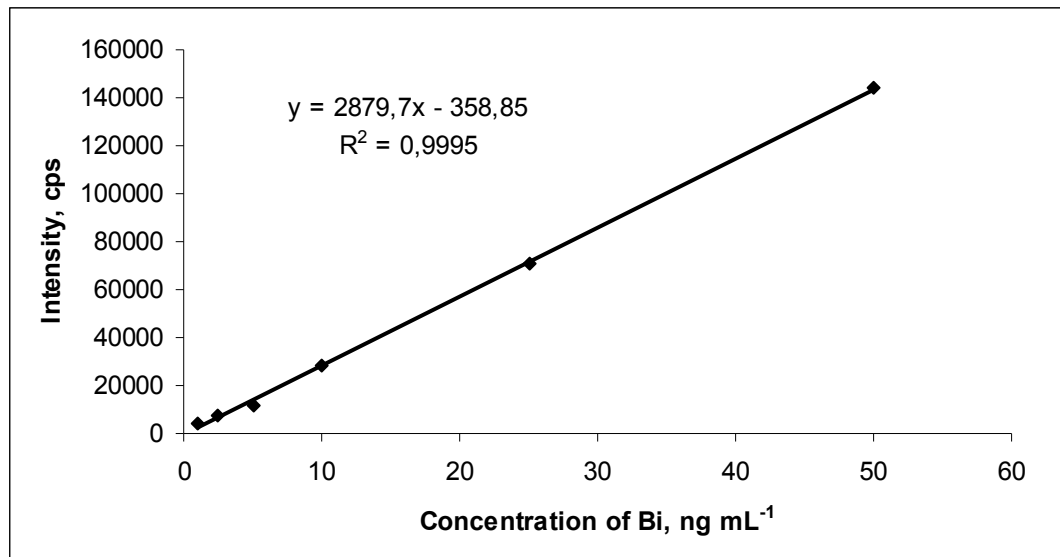


Figure 4.44. Linear calibration graph for Bi by CF-HG-ICP-OES (experimental conditions were given in Table 4.21.)

12.2 times improvement in sensitivity by CF-HG-ICP-OES was reached with respect to conventional ICP-OES. It was calculated from the slope ratio of calibration plot of CF-HG-ICP-OES method to ICP-OES.

From Table 4.23, it can be seen that detection limit of CF-HG-ICP-OES for Bi is better than reported previously by others. Standard reference material, NIST 1643e (trace elements in water), with Bi contents of $14.09 \pm 0.15 \text{ ng mL}^{-1}$ was used to validate the method. Using the optimized method the contents of Bi determined in NIST 1643e was found as $13.88 \pm 0.25 \text{ ng mL}^{-1}$. The close agreement demonstrates the accuracy of the proposed method.

Table 4.23. Comparison of analytical features of optimized method versus literature

Technique	LOD, ng mL ⁻¹	RSD, %	Linear range ng mL ⁻¹	Reference
CF-HG-ICP-OES	0.3-0.7	2.5-4.6	-	Marrero et al. 1999
HG-N ₂ -MIP-AES ^a	110	-	300-30000	Matsumoto et al. 2004
HG-ETV-MIP-OES ^b	3.0	9.2	-	Matusiewicz and Kopras 2003
HG-ICP-OES	2.4	6.0	-	Pohl and Zyrnicki 2002
Ec-HG-AFS ^c	0.15	1.3	-	Zhang et al. 2009
HG-DBD-AFS ^d	0.07	2.0	0.5-300	Xing et al. 2009
CF-HG-ICP-OES	0.16	3.9	1.0-50.0	This study

^a Hydride generation-nitrogen-microwave induced plasma-optical emission spectrometry

^b Hydride generation-electrothermal vaporization-microwave induced plasma-optical emission spectrometry

^c Electrochemical hydride generation atomic fluorescence spectrometry

^d Hydride generation dielectric barrier discharge atomic fluorescence spectrometry

4. RESULTS AND DISCUSSION

4.9.5. Application of CF-HG-ICP-OES for Determination of Bi in Milk

Important parameters which influence the signal intensity of Bi were optimized. Optimized CF-HG-ICP-OES method was applied to milk samples to determine its Bi concentration. Samples were collected from local markets in Diyarbakır-Turkey. Microwave oven was used to digest the samples prior to application of hydride generation procedure. Concentrations of Bi in milk samples determined by CF-HG-ICP-OES were given in Table 4.24. Bi concentrations were lower than LOD for three of samples whereas Bi amounts were found in the range of 8.8-14.5 ng mL⁻¹ for six of samples. One of the samples (M10) was spiked with known amount of Bi before application the microwave procedure. It was found that spiked amount of Bi could be recovered by quantitatively. Recovery value was found as 98.5%. Thus it could be said there was no loss of analyte during digestion procedure.

It should be noted that concentrations of Cd, Cu, Co, Hg, Sb and Se were also low in milk (Bilandzic et al. 2011; Llorent-Martínez et al. 2012). Therefore, interference effects of these were not serious. Thus it can be said that applicability of the method also depended on the concentration ratio of other elements to Bi.

Table 4.24. Determination of Bi in milk samples by CF-HG-ICP-OES

Sample	Bi, ng mL ⁻¹
M1	<LOD
M2	<LOD
M3	<LOD
M4	8.8±0.3
M5	7.8±0.6
M6	9.1±0.4
M7	10.2±0.4
M8	11.6±0.6
M9	11.6±0.4
M10	14.5±0.6
M10 ^a	19.2±0.8

^a Spiked with 5.0 ng mL⁻¹ of Bi

5. CONCLUSION

The main purpose of this thesis was improve the sensitivities of FAAS and ICP-OES for Bi determination.

For FAAS, uncoated and metal coated slotted quartz tube was used during initial stage of study. Different metals were tried as coating material of inner surface of SQT. Afterwards, metal coated and uncoated SQT were used as trapping device for Bi by FAAS. Bi was *in situ* preconcentrated on these surfaces.

For ICP-OES, continuous flow hydride generation as a gas phase sample introduction technique was employed and important experimental parameters were optimized for Bi by CF-HG-ICP-OES.

By optimizing the acetylene flow rate and sample suction rate, analytical characteristics of the FAAS for Bi determination were determined. Then, SQT was placed on burner to improve the sensitivity. In addition to same parameters on FAAS, height of SQT from burner was also optimized. During the studies, it was observed that highest Bi signal could be obtained at the lowest height of SQT as 1.0 mm. However, in the case of 1.0 mm height, flame stability was adversely affected and it could be extinguished easily; therefore, optimum height was selected as 2.0 mm. Sensitivity of conventional FAAS for Bi was improved by using SQT-FAAS. 2.9 fold of enhancement in sensitivity was achieved by using SQT-FAAS.

Uncoated SQT was used as an atom trapping device. In this system, SQT was placed on the burner head and Bi solution was aspirated for a certain time into the flame by using a lean flame. Analyte atoms were collected on the inner surface of SQT. After the *collection cycle*, Bi atoms were released from the surface by aspiration of a low amount of organic solvent, and a transient signal was obtained for Bi. Important system parameters including flame conditions, suction rate of sample, height of the SQT from burner head, type and volume of organic solvent and trapping period were optimized. The highest signal was obtained when MEK was used as organic solvent for revolatilization. Sensitivity of conventional FAAS for Bi was improved by using SQT-AT-FAAS systems. 256 fold of enhancement in sensitivity was achieved by using SQT-AT-FAAS with respect to FAAS, and 88 fold with respect to SQT-FAAS. LOD and LOQ were calculated as 1.6 ng mL^{-1} and 5.3 ng mL^{-1} , respectively, using SQT-AT-FAAS. The technique offers high sensitivity attained using an extremely simple analytical system. A flame AA spectrometer and a simple slotted quartz tube are all needed. Only few minutes are required for the preconcentration process, 6.0 min in this study. The volume consumed was 36.0 mL. The method is suitable for most water analyses where there is no sample size limitation. When the method is compared with the column preconcentration techniques, no chemicals and columns are used; therefore the errors associated with the use of chemicals, column and preconcentrating column material have been eliminated. In addition the method can be applied using a simple procedure, reasonably short amount of time and fairly low sample volume.

4. CONCLUSION

The potential interfering effects of Na, Ca, Mg, Mn, Cr, Fe, Zn, Al, Co, Cu, Ni, Mo, Sn, Sb, Se, SO_4^{2-} , NO_3^- , Cl^- on the SQT-AT-FAAS technique for Bi determination were investigated. Effect of each element was evaluated by individually. Effects of ions on 75.0 ng mL⁻¹ Bi were investigated in case of mass concentration of interferent were 1.0, 10.0 and 100.0 fold with respect to Bi concentration. It was found that Na, Ca and Mg showed serious interferences on Bi determination when their concentrations were 100 fold higher than Bi. In this case, Bi signals were interfered as 26%, 13% and 14%, respectively. 1.0, 10.0 and 100.0 folds of Fe, Mn, Cr and Zn did not change Bi signal significantly. Decreasing was observed for Co and Ni when their concentrations were 10.0 fold higher than Bi. Sn and Se did not change Bi signal seriously. 10% decreasing was observed when concentration of Sb was 10.0 fold higher than Bi concentration. 12% and 9% decreasing were observed in case of SO_4^{2-} and NO_2^- . 10% decreasing was observed for 100.0 fold Cl^- .

Non-volatile metals were tried as coating material for inner surface of SQT. The most important point here is that the melting point of the coating material should be higher than the analyte element. Coating material should not be significantly lost from the surface when element revolatilizes from the SQT. For this purpose Mo, Zr, W and Ta were selected as coating metal. Use of W coated SQT device gave the highest signal. Signals of Mo, Zr and Ta were lower than signal obtained from W coated SQT. The lowest analytical signal was obtained from uncoated SQT. Thus, it could be said that coating of SQT surface facilitate the trapping of Bi on its. Linear calibration plot was obtained for Bi in the range of 0.5-15.0 $\mu\text{g mL}^{-1}$ by using optimized values in W coated SQT-FAAS. Enhancement factor was calculated as 4.0 with respect to conventional FAAS. RSD was calculated as 7.0% for seven replicate measurement of 0.5 $\mu\text{g mL}^{-1}$.

W coated SQT was also used in atom trapping experiments. Experimental variables such as type and volume of organic solvent, flow rate of fuel and suction rate of sample, height of SQT and trapping time were optimized for W coated SQT-AT-FAAS. Highly flammable organic solvents such as ethyl alcohol, methyl alcohol, acetonitrile, isopropyl alcohol, THF, MEK and MIBK were examined for revolatilization of Bi on W coated SQT surface. The highest signal was obtained when MIBK was used as organic solvent. Ethyl alcohol, methyl alcohol and acetonitrile gave the near Bi signal. When THF was tried, it was observed that flame was not stable. In this case, flame was over the SQT from upper slit. Another disadvantage of the use of THF was that deformation of quartz windows of FAAS because of over flame in side walls of SQT like horn. Optimum sample suction rate was investigated by using 20.0 ng mL⁻¹ Bi solution. At high suction rate, better signal was obtained. It was due to the increasing population of analyte atoms per unit time in flame higher suction rates, so at lower suction rates signals of Bi were decreasing. Therefore, 5.5 mL min⁻¹ was chosen as optimum sample suction rate for Bi. Bi signal decreased with increasing in flow rate of acetylene. Over flame in SQT and instability of the flame was the result of high flow rate of acetylene. Thus, effect of flow rate of acetylene was investigated in the range of 0.6-2.5 L min⁻¹ of acetylene. 0.6 L min⁻¹ of acetylene was selected as optimum fuel flow. Damaging in SQT was observed when flow rate of acetylene was higher than 1.5 L min⁻¹. Decreasing of signal was attributed to loss of trapping efficiency of W coated SQT. Same procedure as SQT-AT-FAAS studies was applied to clean the W coated SQT and it was recoated. Trapping time is another important parameter in W coated SQT-AT-FAAS. If analyte atoms are

trapped in longer time interval, sensitivity is improved. However, limitation in sample volume should be considered when selecting the trapping time. Additionally, total analysis time should not be ignored when comparing this method versus others. 20.0 ng mL⁻¹ of Bi was trapped on W coated SQT for 1.0-5.0 min and 5.0 min was selected as optimum for trapping of Bi. Using the optimized parameters of W coated SQT-AT-FAAS, absorbance values of Bi solutions in concentrations between 2.5-100.0 ng mL⁻¹ were measured. 613 fold of enhancement in sensitivity was achieved by using Wcoated SQT-AT-FAAS with respect to FAAS, and 153 fold with respect to W coated SQT-FAAS. LOD and LOQ were calculated as 0.51 ng mL⁻¹ and 1.7 ng mL⁻¹. The half bandwidth of this signal was found to be 0.41 s.

Bi signal was decreased by 17%, 10% and 2.0%, respectively for Na, Ca and Mg when their concentrations were 100.0 fold higher than Bi. In this case, SQT was re-coated by aspirating of 100.0 µg mL⁻¹ of W solution at lean flame. 100.0 fold of Zn, Al, Ni, Sb suppressed the Bi signal as 12, 19, 12, 14%, respectively. 1.0 and 10.0 fold of Cr decreased the Bi signal. Bi signal was increased as 6.9% by 100.0 fold of Mo. Bi signal was decreased when concentration of SO₄²⁻ and NO₂⁻ were 100.0 fold higher than Bi. Re-coating of SQT was required after studies. 17%, 17% and 10% decreasing in sensitivity and signal instability were attributed to co effect of Na in solution. Since, ions solutions were prepared from their Na salts. 1.0 and 10.0 folds of Cl⁻ did not change. 10% decreasing was observed for 100.0 fold Cl⁻.

The method is suitable for most water analyses where there is no sample size limitation. When the method is compared with the column preconcentration techniques, no chemicals and columns are used; therefore the errors associated with the use of chemicals, column and preconcentrating column material have been eliminated. In addition the method can be applied using a simple procedure, reasonably short amount of time and fairly low sample volume.

Experimental variables in CF-HG-ICP-OES were optimized for determination of Bi. It was found that not only conditions such as concentrations of acid and reductant but also flow rates of their, lenghts of reaction and stripping coils, radio frequency power of ICP source, influences the determination of Bi in CF-HG-ICP-OES. Thus concentrations of NaBH₄, HCl and NaOH, flow rates of NaBH₄, sample solution, waste and carrier argon, radio frequency power, lengths of reaction and stripping coils were optimized to obtain lower detection limits. Under optimum conditions, detection limit was calculated as 0.16 ng mL⁻¹, and calibration plot was linear between the 1.0-50.0 ng mL⁻¹. 12.2 times of improvement in detection limit by CF-HG-ICP-OES was reached versus ICP-OES. RSD for ten replicate measurements of 10.0 ng mL⁻¹ Bi was calculated as 3.9%. Effect of possible interferic ions on Bi signal was evaluated. Accuracy of method was verified by using a standard reference material, SRM 1643e. Results found for Bi were in satisfactory agreement with certified values. Concentration of bismuth in milk samples was determined as application of method. Bi amounts in samples were found in the range of 8.8-19.2 ng mL⁻¹, while Bi concentrations were lower than detection limit in three samples. One of the samples (M10) was spiked with known amount of Bi. It was found that spiked amount of Bi could be determined quantitatively, %98.5 of recovery. Thus it can be said that there was not lost of analyte.

4. CONCLUSION

The following two articles were published from this work.

1. Kılınç, E., Bakırdere, S., Aydın, F., Ataman, O.Y. Sensitive determination of bismuth by flame atomic absorption spectrometry using atom trapping in a slotted quartz tube and revolatilization with organic solvent pulse. *Spectrochim. Acta B* (2012), doi:10.1016/j.sab.2012.06.004
2. Kılınç, E., Aydın, F. Optimization of continuous flow hydride generation inductively coupled plasma optical emission spectrometry for sensitivity improvement of bismuth. *Anal. Lett.* (2012), doi:10.1080/00032719.2012.696224

The following article from this work will submitted to journal for publishing.

Kılınç, E., Bakırdere, S., Aydın, F., Ataman, O.Y. *In situ* atom trapping of Bi on W coated slotted quartz tube atomic absorption spectrometry and interference studies

6. REFERENCES

Aastroem, O. 1982. Flow injection analysis for the determination of bismuth by atomic absorption spectrometry with hydride generation. *Anal. Chem.*, 54: 190-193.

Abbaspour, A., Baramekeh, L. 2005. Simultaneous determination of antimony and bismuth by beta-correction spectrophotometry and an artificial neural network algorithm. *Talanta*, 65: 692-699.

Abrankó, L., Stefánka, Z., Fodor, P. 2003. Possibilities and limits of the simultaneous determination of As, Bi, Ge, Sb, Se, and Sn by flow injection–hydride generation–inductively coupled plasma–time-of-flight mass spectrometry (FI–HG–ICP–TOFMS). *Anal. Chim. Acta*, 493: 13-21.

Afkhami, A., Madrakian, T., Siampour, H. 2006. Cloud point extraction spectrophotometric determination of trace quantities of bismuth in urine. *J. Braz. Chem. Soc.*, 17: 797-802.

Alkemade, C.Th.J., Milatz, J.M.W. 1955. Double-beam method of spectral selection with flames. *Appl. Sci. Res. B*, 4: 288-299.

Alp, O., Ertaş, N. 2008. In situ trapping of antimony hydride on iridium-coated tungsten coil and interference studies. *J. Anal. At. Spectrom.*, 23: 976-980.

Arslan, Y., Kendüzler, E., Ataman, O.Y. 2011. Indium determination using slotted quartz tube-atom trap-flame atomic absorption spectrometry and interference studies. *Talanta*, 85: 1786-1791.

Ataman, O.Y. 2007. Economical alternatives for high sensitivity in atomic spectrometry laboratory. *Pak. J. Anal. Environ. Chem.*, 8: 64-68.

Ataman, O.Y. 2008. Vapour generation and atom traps: Atomic absorption spectrometry at the ng/L level. *Spectrochim. Acta B*, 63: 825-834.

Ari, B. 2009. Development of sensitive analytical methods for thallium determination by atomic absorption spectrometry. M.S. thesis. Middle East Technical University Graduate School of Natural and Applied Sciences, Ankara-Turkey.

Arhab-Zavar, M.H., Hashemi, M. 2000. Evaluation of electrochemical hydride generation for spectrophotometric determination of As(III) by silver diethyldithiocarbamate. *Talanta*, 52: 1007-1014.

Arhab-Zavar, M.H., Chamsaz, M., Yousefi, A., Ashraf, N. 2009. Electrochemical hydride generation of thallium. *Talanta*, 79: 302-307.

Bakirdere, S., Aydin, F., Bakirdere, E.G., Titretir, S., Akdeniz, İ., Aydin, I., Yıldırım, E., Arslan, Y. 2011. From mg/kg to pg/kg levels: A story of trace element determination: a review. *App. Spectrosc. Rev.*, 46: 38-66.

Basicmines 2010, <http://www.basicmines.com/bismuth/index.html>

6. REFERENCES

Bedard, M., Kerbyson, J.D. 1975. Determination of trace bismuth in copper by hydride evolution atomic absorption spectrophotometry. *Anal. Chem.*, 47: 1441-1444.

Benzo, Z., Matos-Reyes, M.N., Cervera, M.L., Guardia, M. 2011. Simultaneous determination of hydride and non-hydride forming elements by inductively coupled plasma optical emission spectrometry. *J. Braz. Chem. Soc.*, 22: 1782-1787.

Bilandzic, N., Dokic, M., Sedak, M., Solomun, B., Varenina, I., Knezevic, Z., Benic, M. 2011. Trace element levels in raw milk from northern and southern regions of Croatia. *Food Chem.* 127: 63-66.

Blasdale, W.C., Parle, W.C. 1936. Determination of bismuth as phosphate. *Analytical Edition*, 15: 352-353.

Bolea, E., Laborda, F., Belarra, M.A., Castillo, J.R. 2001. Interferences in electrochemical hydride generation of hydrogen selenide. *Spectrochim. Acta B*, 56: 2347-2360.

Boertz, J., Hartmann, L.M., Sulkowski, M., Hippler, J., Mosel, F., Diaz-bone, R.A., Michalke, K., Rettenmeier, A.W., Hirner, A.V. 2009. Determination of trimethylbismuth in the human body after ingestion of colloidal bismuth subcitrate. *Drug Metab. Dispos.*, 37: 352-358.

Bonsak, C.P., Dovidowski, L. Perkin Elmer Life and Analytical Science, Field application report

Boss, C.B., Fredeen, K.J. 2004. Concepts, Instrumentation and Techniques in Inductively Coupled Plasma Optical Emission Spectrometry. Perkin Elmer Inc. USA

Brindle, I.D. 2007. Vapor-generation analytical chemistry: from Marsh to multimode sample-introduction system. *Anal. Bioanal. Chem.*, 388: 735-741.

Brown, A.A., Milner, B.A., Taylor, A. 1985. Use of slotted quartz tube to enhance the sensitivity of conventional flame atomic absorption spectrometry. *Analyst*, 110: 505-505.

Brown, A.A., Roberts, D.J., Kahokola, K.V. 1987. Methods for improving the sensitivity in flame atomic absorption spectrometry. *J. Anal. At. Spectrom.*, 2: 201-204.

Burguera, J.L., Burguera, M., Rivas, C., Rondon, C., Carrero, P., Gallignani, M. 1999. Determination of bismuth in biological samples using on-line flow-injection microwave-assisted mineralization and precipitation:dissolution for electrothermal atomic absorption spectrometry. *Talanta*, 48: 885-893.

Cadore, S., dos Anjos, A.P., Bacan, N. 1998. Determination of bismuth in urine and prescription medicines using atomic absorption with an on-line hydride generation system. *Analyst*, 123: 1717-1719.

Campbell, A.D. 1992. A critical survey of hydride generation techniques in atomic spectroscopy. *Pure. Appl. Chem.*, 64(2): 227-244.

Campos, R.C., Grinberg, P., Takase, I., Luna, A.S. 2002. Minimization of Cu and Ni interferences in the determination of Sb by hydride generation atomic absorption spectrometry : the use of picolinic acid as masking agent and the influence of L-cysteine. *Spectrochimica Acta B*, 57:463-472.

Candolena, J.P., Bolshov, M.A., Rudniev, S.N., Hong, S., Boutron, C.F. 1994. Determination of bismuth down to sub pg/g level in Greenland snow by laser excited atomic fluorescence spectrometry. *J. de Physique III*, 4: 661-664.

Campbell, A.D. 1992. A critical survey on hydride generation techniques in atomic spectroscopy. *Pure Appl. Chem.*, 64: 227-244.

Cankur, O., Ertaş, N., Ataman, O.Y. 2002. Determination of bismuth using on-line preconcentration by trapping on resistively heated Wcoil and hydride generation atomic absorption spectrometry. *J Anal At Spectrom.*, 17: 603-609.

Cankur, O., Ataman, O.Y. 2007. Chemical vapor generation of Cd and on-line preconcentration on a resistively heated W-coil prior to determination by atomic absorption spectrometry using an unheated quartz absorption cell. *J Anal At Spectrom.*, 22: 791-799.

Cava-Montesinos, P., Cervera, M.L., Pastor, A., Gurdia, M. 2003. Determination of ultratrace bismuth in milk samples by atomic fluorescence spectrometry, *J AOAC Int.*, 86(4): 815-822.

Chan, C.C Y., Baig, M.W.A., Lichti, P.A. 1990. Determination of bismuth in geological materials by flow injection hydride generation atomic absorption spectrometry. *Anal. Lett.*, 23: 2259-2272.

Chang, J.P. 2004. Determination of Bi impurity in lead stock standard solutions by hydride-generation inductively coupled plasma mass spectrometry. *Bull. Korean Chem. Soc.*, 25: 233-236.

Chen, S.Y., Zhang, Z.F., Yu, H.M. 2002. Determination of trace bismuth by flow injection-hydride generation collection-atomic absorption spectrometry. *Anal. Bional. Chem.*, 374:126-130.

Cheng, K.L., Bray, R.H., Melsted, S.W. 1955. Spectrophotometric determination of bismuth with sodium diethyldithiocarbamate. *Anal. Chem.*, 27(1): 24-26.

Chineseop 2012 <http://www.chineseop.com/beer/Why-is-Bismuth-added-to-red-wine-.html>

Codony, F., Domenico, P., Mas, J. 2003. Assessment of bismuth thiols and conventional disinfectants on drinking water biofilms. *J. Appl. Microbiol.*, 95: 288-293.

Davidowski, L. 1993. Perkin Elmer ICP Application Study Number 67

Das, A.K., Chakraborty, R., Cervera, M.L., Guardia, M. 2006. Analytical techniques for the determination of bismuth in solid environmental samples. *TRAC-Trend. Anal. Chem.*, 25 (6): 599-608.

Dedina, J., Tsalev, D.L. 1995. Hydride generation atomic absorption spectrometry, Wiley&Sons Inc., Chichester.

Dedina, J. 2007. Atomization of volatile compounds for atomic absorption and atomic fluorescence spectrometry: On the way towards the ideal atomizer. *Spectrochim. Acta B*, 62: 846-872.

6. REFERENCES

Demirtaş, İ. 2009. Lead determination by flame atomic absorption spectrometry using a slotted quartz tube atom trap and metal coatings. M.S. thesis. Middle East Technical University Graduate School of Natural and Applied Sciences, Ankara-Turkey.

Deng, T., Chen, Y., Belzile, N. 2001. Antimony speciation at ultra trace levels using hydride generation fluorescence spectrometry and 8-hydroxyquinoline as an efficient masking agent. *Anal. Chim. Acta*, 432: 293-302.

Docekal, B., Gucer, S., Selecka, A. 2004. Trapping of hydride forming elements within miniature electrothermal devices: part 1. Investigation of collection of arsenic and selenium hydrides on a molybdenum foil strip. *Spectrochim. Acta B*, 59: 487-495.

Docekal, B. 2004. Trapping of hydride forming elements within miniature electrothermal devices: part 2. Investigation of collection of arsenic and selenium hydrides on a surface and in a cavity of a graphite rod. *Spectrochim. Acta B*, 59: 497-503.

Doncker, K.D., Dumarey, R., Dams, R., Hoste, J. 1985. The use of 1,10 -phenanthroline in minimizing the nickel interference in determinations of bismuth and antimony by hydride generation/atomic absorption spectrometry. *Anal. Chim. Acta*, 169: 339-341.

D'Ulivo, A., Dědina, J., Mester, Z., Sturgeon, R.E., Wang, Q., Welz, B. 2011. Mechanisms of chemical generation of volatile hydrides for trace element determination (IUPAC Technical Report). *Pure Appl. Chem.*, 83: 1283-1340.

Ellis, L.A., Roberts, D.J. 1996. Further development of the 'bent' tube water cooled atom trap for arsenic, antimony, copper and manganese. *J. Anal. At. Spectrom.*, 11: 259-263.

Ertaş, N., Korkmaz, D.K., Kumser, S., Ataman, O.Y. 2002. Novel traps and atomization techniques for flame AAS. *J. Anal. At. Spectrom.*, 17: 1415-1420.

Ertaş, N., Arslan, Z., Tyson, J.F. 2008. Determination of lead by hydride generation atom trapping flame atomic absorption spectrometry. *J. Anal. At. Spectrom.*, 23: 223-228.

Evans, E.H., Day, J.A., Palmer, C.D., Smith, C.M.M.. 2009. Atomic spectrometry update. advances in atomic spectrometry and related techniques. *J. Anal. At. Spectrom.*, 24:711-733.

Eskilsson, H., Jagner, D. 1982. Potentiometric stripping analysis for bismuth(III) in seawater, *Anal. Chim. Acta*, 138: 27-33.

Ewing, GW. 1960. Instrumental methods of chemical analysis, 4th edition, McGraw-Hill Book Company, page 150. USA.

FDA 2006
<http://www.fda.gov/Safety/MedWatch/SafetyInformation/SafetyAlertsforHumanMedicalProducts/ucm150503.htm>

Feldmann, J., Krupp, E.M., Glindemann, D., Hirner, A.V., Cullen, W.R. 1999. Methylated Bismuth in environment. *Appl. Organomet. Chem.*, 13: 739-748.

Flores, E.M.M.<http://www.sciencedirect.com/science/article/pii/S0584854702001787> - COR1, Silva, F.E.B., Santos, E.P., Paula, F.R., Barin, J.S., Zanella, R., Dressler, V.L.,

Bittencourt, C.F. 2002. Determination of total arsenic by batch hydride generation atomic absorption spectrometry in injectable drugs containing high levels of Sb(V) as *N*-methylglucamine antimonate. *Spectrochim. Acta B*, 57: 2095-2102.

Fraser, S.M., Ure, A.M., Mitchell, M.C., West, T.S. 1986. Determination of cadmium in calcium chloride extracts of soils by atom-trapping atomic absorption spectrometry. *J. Anal. At. Spectrom.*, 1: 19-21.

Freschi, G.P.G., Freschi, C.D., Neto, J.A.G. 2008. Evaluation of different rhodium modifiers and coatings on the simultaneous determination of As, Bi, Pb, Sb, Se and of Co, Cr, Cu, Fe, Mn in milk by electrothermal atomic absorption spectrometry. *Microchim. Acta*, 161: 129-135.

Gholami, M., Farjoud, M.J., Sepehri, M., Nazari, A., Gholami, M., Behkami, S., Ataman, O.Y. 2011. Sensitivity enhancement for slotted quartz tube flame atomic absorptin spectrometry using a gas screen. *Anal. Lett.*, 44: 2513-2520.

Gordeeva, V.P., Statkus, M.A., Tsybin, G.I., Zolotov, Y. 2003. X-ray fluorescence determination of As, Bi, Co, Cu, Fe, Ni, Pb, Se, V and Zn in natural water and soil extracts after preconcentration of their pyrrolidinedithiocarbamates on cellulose filters. *Talanta*, 61: 315-329.

Guo, X., Guo, X. 2001. Determination of ultra-trace amounts of selenium by continuous flow hydride generation AFS and AAS with collection on gold wire. *J. Anal. At. Spectrom.*, 16: 1414-1418.

Guyon, J.C., Cline, L.J. 1965. Spectrophotometric determination of bismuth. *Anal. Chem.*, 27(8): 1221-1254.

Han-wen, S., Li-li, Y., De-ciang, Z. 1996. Direct determination of lead in alcoholic drinks and waters by flame atomic absorption spectrometry using an atom-trapping technique. *J. Anal. At. Spectrom.*, 11: 265-269.

Holak, W. 1969. Gas-sampling technique for arsenic determination by atomic absorption spectrophotometry, *Anal. Chem.*, 412: 1712-1713.

Infante, H.G., Sanchez, M.L.F., Sanz-Medel, A. 1996. Ultratrace determination of cadmium by atomic absorption spectrometry using hydride generation with in situ preconcentration in a palladium-coated graphite atomizer. *J. Anal. At. Spectrom.*, 11: 571-575.

Itoh, S., Kneco, S., Ohta, K., Mizuno, T. 1999. Determination of bismuth in environmental samples with Mg±W cell-electrothermal atomic absorption spectrometry. *Anal. Chim. Acta*, 379: 169-173.

IUPAC 2008 http://old.iupac.org/publications/analytical_compendium/Cha10sec346.pdf

Jia, X., Han, Y., Li, X., Duan, T., Chen, H. 2010. Dispersive liquid-liquid microextraction combined with flow injection inductively coupled plasma mass spectrometry for simultaneous determination of cadmium, lead and bismuth in water samples. *Microchim. Acta*, 171: 49-56.

Jiang, X., Gan, W., Han, S., Zi, H., He, Y. 2009. Design and application of a novel integrated electrochemical hydride generation cell for the determination of arsenic in seaweeds by atomic fluorescence spectrometry. *Talanta*, 79: 314-318.

6. REFERENCES

Jiang, X., Gan, W., Wan, L., Deng, Y., Yang, Q., He, Y. 2010. Electrochemical hydride generation atomic fluorescence spectrometry for detection of tin in canned foods using polyaniline-modified lead cathode. *J. Hazard. Mater.*, 184:331-336.

Kaya, G., Yaman, M. 2008. Online preconcentration for the determination of lead, cadmium and copper by slotted tube atom trap (STAT) - flame atomic absorption spectrometry. *Talanta*, 75: 1127-1133.

Khaloo, S.S., Ensafi, A.A., Khayamian, T. 2007. Determination of bismuth and copper using adsorptive stripping voltammetry couple with continuous wavelet transform. *Talanta*, 71: 324-332.

Klassen, A., Kim, M.L., Tudino, M.B., Bacan, N., Arruda, M.A.Z. 2008. A metallic furnace atomizer in hydride generation atomic absorption spectrometry: Determination of bismuth and selenium. *Spectrochim. Acta B*, 63: 850-855.

Korkmaz, D., Kumser, S., Ertaş, N., Mahmut, M., Ataman, O.Y. 2002. Investigations on nature of re-volatilization from atom trap surfaces in flame AAS. *J. Anal. At. Spectrom.*, 17: 1610-1614.

Korkmaz, D., Mahmut, M., Helles, R., Ertaş, N., Ataman, O.Y. 2003. Interference studies in slotted silica tube trap technique. *J. Anal. At. Spectrom.*, 18: 99-104.

Korkmaz, D., Dedina, J., Ataman, O.Y. 2004. Stibine preconcentration in a quartz trap with subsequent atomization in the quartz multiatomizer for atomic absorption spectrometry. *J. Anal. At. Spectrom.*, 19: 255-259.

Korkmaz, D., Demir, C., Aydin F., Ataman, O.Y. 2005. Cold vapor generation and on-line trapping of cadmium species on quartz surface prior to detection by atomic absorption spectrometry. *J. Anal. At. Spectrom.*, 20: 46-52.

Kratzer, J., Dedina, J. 2005. In-situ trapping of stibine in externally heated quartz tube atomizers for atomic absorption spectrometry. *Spectrochim. Acta B*, 60: 859-864.

Kratzer, J., Dědina, J. 2006. In situ trapping of bismuthine in externally heated quartz tube atomizers for atomic absorption spectrometry. *J. Anal. At. Spectrom.*, 21: 208-210.

Kratzer, J., Dedina, J. 2007. Arsine and selenium hydride trapping in a novel quartz device for atomic absorption spectrometry. *Anal. Bioanal. Chem.*, 388: 793-800.

Kratzer, J., Dedina, J. 2008. Stibine and bismuthine trapping in quartz tube atomizers for atomic absorption spectrometry - Method optimization and analytical applications. *Spectrochim. Acta B*, 63: 843-849.

Kratzer, J., Vobecy, M., Dedina, J. 2009. Stibine and bismuthine trapping in quartz tube atomizers for atomic absorption spectrometry. Part 2: a radiotracer study. *J. Anal At Spectrom.*, 24: 1222-1228.

Krejci, P., Docekal, B., Hrusovska, Z. 2006. Trapping of hydride forming elements within miniature electrothermal devices. Part 3. Investigation of collection of antimony and bismuth on a molybdenum foil strip following hydride generation. *Spectrochim. Acta B*, 61: 444-449.

Kula, İ., Arslan, Y., Bakirdere, S., Ataman, O.Y. 2008. A novel analytical system involving hydride generation and gold-coated W-coil trapping atomic absorption spectrometry for selenium determination at ng l^{-1} level. *Spectrochim. Acta B*, 63: 856-860.

Kula, İ., Arslan, Y., Bakirdere, S., Titretir, S., Kendüzler, E., Ataman, O.Y. 2009. Determination and interference studies of bismuth by tungsten trap hydride generation atomic absorption spectrometry. *Talanta*, 80: 127-132.

Kumar, A.R., Riyazuddin, P. 2010. Chemical interferences in hydride-generation atomic spectroscopy. *TRAC-Trend. Anal. Chem.*, 29: 166-176.

Kumser, S. 1995. Atom trapping atomic absorption spectrometry using organic solvent atomization. M.S. thesis. Middle East Technical University Graduate School of Natural and Applied Sciences, Ankara-Turkey.

Laborda, F., Bolea, E., Castillo, J.R. 2007. Electrochemical hydride generation as a sample-introduction technique in atomic spectrometry: Fundamentals, interferences, and applications. *Anal. Bioanal. Chem.*, 388: 743-751.

Lajunen, L.H.J. Spectrochemical analysis by atomic absorption and emission, Cambridge: Royal Soc. of Chemistry, 1992. Page 131-132. (<http://books.google.com.tr/books?id=yWvE1XHo7ZMC&dq=delves+microsampling+technique&q=delves#v=snippet&q=delves&f=false>)

Lau, C., Held, A., Stephens, R. 1976. Sensitivity enhancements to flame AAS by use of a flame atom trap. *Can. J. Spectrocs.*, 21:100-104.

Lau, C.M., Ure, A.M., West, T.S. 1988. Atom trapping atomic absorption spectrometric determination of some trace elements in soils, natural waters, seawater, and bovine liver. *Bull. Chem. Soc.*, 61: 79-85.

Laug, E.P. 1949. Determination of bismuth in biological material. *Anal. Chem.*, 21:188-189.

Lee, Y., Lee, D.S., Yoon, B.M., Hwang, H. 1991. Semi-automatic hydride generation and atomic absorption determination of bismuth with *in situ* concentration in a graphite furnace. *Bull. Korean Chem. Soc.*, 12: 290-295.

Li, Z., Guo, Y. 2005. Simultaneous determination of trace arsenic, antimony, bismuth and selenium in biological samples by hydride generation-four-channel atomic fluorescence spectrometry. *Talanta*, 65: 1318-1325.

Liao, M., Deng, T. 2006. Arsenic species analysis in porewaters and sediments using hydride generation atomic fluorescence spectrometry. *J. Environ. Sci.*, 18(5): 995-999.

Liu, H., Chen, S., Chang, P., Tsai, S.J. 2002. Determination of bismuth, selenium and tellurium in nickel-based alloys and pure copper by flow-injection hydride generation atomic absorption spectrometry—with ascorbic acid-prereduction and cupferron chelation-extraction. *Anal. Chim. Acta*, 459: 161-168.

Liu, R., Wu, P., Xu, K., Lv, Y., Hou, X. 2008. Highly sensitive and interference-free determination of bismuth in environmental samples by electrothermal vaporization atomic fluorescence spectrometry after hydride trapping on iridium-coated tungsten coil. *Spectrochim. Acta B*, 63: 704-709.

6. REFERENCES

Llorent-Martínez, E.J., Córdovam, M.L.F., Ruiz-Medina, A., Ortega-Ba, P. 2012. Analysis of 20 trace and minor elements in soy and dairy yogurts by ICP-MS. *Microchem. J.* 102: 23-27.

Lott, P.F., Vitek, R.K. 1960. Gravimetric determination of bismuth with dimethylgloxime. *Anal. Chem.*, 32(3): 391-393.

L'vov, B. 2005. Fifty years of atomic absorption spectrometry. *J. Anal. Chem.*, 60 (4): 382-392.

Madrakian, T., Afkhami, A., Esmaeili, A. 2003. Spectrophotometric determination of bismuth in water samples after preconcentration of its thiourea-bromide ternary complex on activated carbon. *Talanta*, 60: 831-838.

Manning, T.J., Grow, W.R. 1997. Inductively coupled plasma optical emission spectrometry, *The Chemical Educator*. 2(1): 1430-1471.

Marrero, J., Arisnabaretta, S.P., Smichowski, P. 1999. The effect of six reaction media on the determination of bismuth at trace levels in environmental samples by hydride generation and inductively coupled plasma-atomic emission spectrometry, *J. Anal. At. Spectrom.*, 14: 1875-1881.

Matos-Reyes, M.N., Cervera, M.L., Campos, R.C., Guardia, M. 2010. Total content of As, Sb, Se, Te and Bi in Spanish vegetables, cereals and pulses and estimation of the contribution of these foods to the Mediterranean daily intake of trace elements, *Food Chem.*, 122: 188-194.

Matsumoto, A., Shiozaki, T., Nakahara, T. 2004. Simultaneous determination of bismuth and tellurium in steels by high power nitrogen microwave induced plasma atomic emission spectrometry coupled with the hydride generation technique. *Anal. Bioanal. Chem.*, 379: 90-95.

Matusiewicz, H. 1997. Atom trapping and in situ preconcentration techniques for flame atomic absorption spectrometry. *Spectrochim. Acta B*, 52: 1711-1736.

Matusiewicz, H., Kopras, M. 1997. Methods for Improving the Sensitivity in Atom Trapping Flame Atomic Absorption Spectrometry: Analytical Scheme for the Direct Determination of Trace Elements in Beer. *J. Anal. At. Spectrom.*, 12: 1287-1291.

Matusiewicz, H., Kopras, M., Sturgeon, R.E. 1997. Determination of Cadmium in Environmental Samples by Hydride Generation with In Situ Concentration and Atomic Absorption Detection. *Analyst*, 122: 331-336.

Matusiewicz, H., Kopras, M. 2003. Simultaneous determination of hydride forming elements (As, Bi, Ge, Sb, Se) and Hg in biological and environmental reference materials by electrothermal vaporization-microwave induced plasma-optical emission spectrometry with their in situ trapping in a graphite furnace. *J. Anal. At. Spectrom.*, 18: 1415-1425.

Matusiewicz, H., Krawczyk, M. 2006. Determination of cadmium and lead in reference materials by volatile species generation with in situ trapping flame atomic absorption spectrometry. *Microchem. J.*, 83: 17-23.

Matusiewicz, H., Ślachciński, M. 2007. Simultaneous determination of hydride forming (As, Bi, Ge, Sb, Se, Sn) and Hg and non-hydride forming (Ca, Fe, Mg, Mn, Zn) elements in sonicate

slurries of analytical samples by microwave induced plasma optical emission spectrometry with dual-mode sample introduction system. *Microchem. J.*, 86: 102-111.

Matusiewicz, H., Krawczyk, M. 2007a. Determination of tellurium by hydride generation with *in situ* trapping flame atomic absorption spectrometry. *Spectrochim. Acta B.*, 62: 309-316.

Matusiewicz, H., Krawczyk, M. 2007b. Determination of trace amounts of bismuth by *in-Situ* trapping hydride generation flame atomic absorption spectrometry. *Chem. Anal-Warsaw*, 52: 565-578.

Matusiewicz, H., Ślachciński, M. 2010. Method development for simultaneous multi-element determination of hydride forming elements (As, Bi, Ge, Sb, Se, Sn) and Hg by microwave induced plasma-optical emission spectrometry using integrated continuous-microflow ultrasonic nebulizer-hydride generator sample introduction system. *Microchem. J.*, 95: 213-221.

Menemenlioğlu, İ., Korkmaz, D., Ataman, O.Y. 2007. Determination of antimony by using a quartz atom trap and electrochemical hydride generation atomic absorption spectrometry. *Spectrochim. Acta B.*, 62: 40-47.

Mester, Z., Sturgeon, R. 2003. Comprehensive Analytical Chemistry: Volume XLI Sample preparation for trace element analysis, Elsevier B.V., page 117-127. Amsterdam-Netherland

Moffett, J. Sensitivity Enhancement for flame atomic absorption spectrometry using an atom concentrator tube, the ACT 80. Application note. Agilent Technologies, <http://www.chem.agilent.com/Library/applications/aa091.pdf>

Moor, C., Lam, J.W.H., Sturgeon, R.E. 2000. A novel introduction system for hydride generation-inductively coupled plasma mass spectrometry: determination of selenium in biological materials. *J. Anal. At. Spectrom.*, 15: 143-149.

Moscoso-Perez, C., Moreda-Pineiro, J., Lopez-Mahia, P., Muniategui-Lorenzo, S., Fernandez-Fernandez, E., Prada-Rodriguez, D. 2003. Bismuth determination in environmental samples by hydride generation/electrothermal atomic absorption spectrometry. *Talanta*, 61: 633-642.

Moyano, S., Gasquez, J.A., Olsina, R., Marchevsky, E., Martinez, L.D. 1999. Pre-concentration system for bismuth determination in urine using FI-ICP-AES with ultrasonic nebulization. *J. Anal. At. Spectrom.*, 14: 259-262.

Murphy, J., Jones, P., Schlemmer, G., Shuttler, I.L., Hill, S.J. 1997. Investigations into the simultaneous determination of bismuth and selenium by 'in atomizer trapping' electrothermal atomic absorption spectrometry. *Anal. Commun.*, 34: 359-362.

Nakahara, T., Nakanishi, K., Wasa, T. 1987. Determination of trace concentrations of bismuth by inductively coupled plasma-atomic emission spectrometry with hydride generation. *Spectrochim. Acta B*, 42: 119-128.

Narasaki, H., Ikeda, M. 1990. Determination of total tin in river water by hydride generation atomic absorption spectrometry. *Fresenius J. Anal. Chem.*, 336: 5-7.

NAS-NS, National Academy of Sciences - National Research Council, Radiochemistry of Bismuth, 1977

6. REFERENCES

Niazi, A., Afshar, S.K. 2011. Design novel optical sensor for determination of bismuth base on immobilization of 4-(4-nitrophenyl)-1-naphthol on a triacetylcellulose membrane, *J. Iran Chem. Res.*, 4: 105-111.

Park, C.J. 2004. Determination of Bi impurity in lead stock standard solutions by hydride-generation inductively coupled plasma mass spectrometry. *Bull. Korean Chem. Soc.*, 25: 233-236.

Pohl, P., Zyrnicki, W. 2001. On the transport of some metals into inductively coupled plasma during hydride generation process. *Anal. Chim. Acta*, 429: 135-143.

Pohl, P. 2004. Hydride generation-recent advances in atomic emission spectrometry. *TRAC-Trend. Anal. Chem.*, 23: 87-101.

Pournaghi-Azar, M.H., Hossein, M., Bahar, S. 2001. Selective determination of trace-bismuth by extraction-differential pulse polarography in non-aqueous media. *Iran. J. Chem. Chem. Eng.*, 20: 59-65.

Pyen, G.S., Browner, R.F. 1988. System for simultaneous determination of As, Sb, and Se by hydride generation and inductively coupled plasma optical emission spectrometry. *Appl. Spectrosc.*, 42: 262-266.

Rahman, L., Corns, W.T., Bryce, D.W., Stockwell, P.B. 2000. Determination of mercury, selenium, bismuth, arsenic and antimony in human hair by microwave digestion atomic fluorescence spectrometry. *Talanta*, 52: 833-843.

Reyes, M.N.M., Cervera, M.L., de la Guardia, M. 2009. Determination of total Sb, Se, Te, and Bi and evaluation of their inorganic species in garlic by hydride-generation-atomic-fluorescence spectrometry. *Anal. Bioanal. Chem.*, 394: 1557-1562.

Roberts, D. J., Kahokola, K. V. 1989. Improving Sensitivity and Precision by Automated Dual Silica Tube Atom Trapping. *J. Anal. At. Spectrom.*, 4: 185-189.

Pahan, S., Saçmacý, S., Pahin, U., Ülgen, A., Kartal, S. 2010. An on-line preconcentration/separation system for the determination of bismuth in environmental samples by FAAS. *Talanta*, 80: 2127-2131.

Silverman, L., Shideler, M. 1954. Determination of bismuth in pure bismuth-lead eutectic alloy: improved phosphate method. *Anal. Chem.*, 26(5): 911-914.

Shemirani, F., Baghdadi, M., Ramezani, M., Jamali, M.R. 2005. Determination of ultra trace amounts of bismuth in biological and water samples by electrothermal atomic absorption spectrometry (ET-AAS) after cloud point extraction. *Anal. Chim. Acta*, 534: 163-169.

Skoog, D.A., Holler, E.J., Niemann, T.A. 1998. Principles of Instrumental Analysis. 5th Edition. Thomsan Learning, US

Sturgeon, R.E., Liu, J., Boyko, V.J., Luong, V.T. 1996. Determination of copper in environmental matrices following vapor generation, *Anal. Chem.* 68: 1883-1887.

Sun, H. 2011. Biological chemistry of arsenic, antimony and bismuth, Wiley

Sun, M., Wu, Q. 2011. Determination of trace bismuth in human serum by cloud point extraction coupled flow injection inductively coupled plasma optical emission spectrometry, *J. Hazard. Mater.*, 192(3): 935-939.

Şahan, S., Saçmacı, Ş., Şahin, U., Ülgen, A., Kartal, Ş. 2010. An on-line preconcentration/separation system for the determination of bismuth in environmental samples by FAAS. *Talanta*, 80: 2127-2131.

Taher, M. A., Rezaeipour, E., Afzali, D. 2004. Anodic stripping voltammetric determination of bismuth after solid-phase extraction using amberlite XAD- resin modified with 2-(5-bromo-2-pyridylazo)-5-diethylaminophenol. *Talanta*, 63: 797-801.

Titretir, S., Kendüzler, E., Arslan, Y., Kula, İ., Bakirdere, S., Ataman, O.Y. 2008. Determination of antimony by using tungsten trap atomic absorption spectrometry. *Spectrochim. Acta B*, 875-879.

Tsalev, D.L. 1999. Hyphenated vapor generation atomic absorption spectrometric techniques. *J. Anal. At. Spectrom.*, 14: 147-162.

Turner, A.D., Roberts, D.J., Cor, Y.L. 1995. Improving the design of a water-cooled atom trap to increase sensitivity and precision. *J. Anal. At. Spectrom.*, 10: 721-725.

Turner, A.D., Roberts, D.J. 1996. Metal determinations with a novel slotted-tube water-cooled atom trap. *J. Anal. At. Spectrom.*, 11: 231-234.

USGS (U.S. Geological Survey) 2010, <http://minerals.usgs.gov/minerals/pubs/commodity/bismuth/mcs-2010-bismu.pdf>

Walsh, A. 1955. The application of atomic absorption spectra to chemical analysis. *Spectrochim. Acta*, 7: 108-117.

Watanabe, N., Inoue, S., Ito, H. 1999. Improvement of a batch hydride generation-atomic absorption spectrometry. *J. Environ. Chem.*, 9: 75-81.

Watling, R.J. 1977. The use of slotted quartz tube for the analysis of trace metals in fresh water. *Water SA*, 3 (4): 218-220.

Welz, B. 1999. Atomic absorption spectrometry-pregnant again after 45 years. *Spectrochim. Acta B*, 54: 2081-2094.

West, P.W., Coll, H. 1955. Spectrophotometric determination of bismuth with ethylenediaminetetraacetic acid. *Anal. Chem.*, 37(13): 1778-1779.

West, T.S. 1988. In situ preconcentration in flame atomic spectroscopy. *Anal. Proc.*, 25: 240-244.

Wikipedia 2012a, http://en.wikipedia.org/wiki/Bismuth#cite_note-usgs2010-10

Wikipedia 2012b, <http://en.wikipedia.org/wiki/Bismacine>

Wu, H., Du, B., Fang, C. 2007. Flow Injection On-line preconcentration coupled with hydride generation atomic fluorescence spectrometry for ultra-trace amounts of bismuth determination in biological and environmental water samples. *Anal. Lett.*, 40:2772-2782.

6. REFERENCES

Xing, Z., Wang, J., Zhang, S., Zhang, X. 2009. Determination of bismuth in solid samples by hydride generation atomic fluorescence spectrometry with a dielectric barrier discharge atomizer. *Talanta*, 80: 139-142.

Xiu-ping, Y., Zhe-ming, N. 1991. Determination of lead by hydride generation atomic absorption spectrometry with in situ concentration in a zirconium coated graphite tube. *J. Anal. At. Spectrom.*, 6: 483-486.

Xu, S., Sun, L., Fang, Z. 1992. Application of the slotted quartz tube in flow injection-flame atomic-absorption spectrometry. *Talanta*, 39 (6): 581-587.

Ye,R.D., Khoo, S.B. 1997. Continuous flow and flow injection stripping voltammetric determination of silver(I), mercury(II), and bismuth(III) at a bulk modified graphite tube electrode, *Electroanal.*, 9: 481-489.

Yaman, M., Akdeniz, I. 2004. Sensitivity enhancement in flame atomic absorption spectrometry for determination of copper in human thyroid tissues. *Anal. Sci.*, 20: 1363-1366.

Yaman, M. 2005. The improvement of sensitivity in lead and cadmium determinations using flame atomic absorption spectrometry. *Anal. Bioanal. Chem.*, 339: 1-8.

Yamamoto, M., Yasuda, M., Yamamoto, Y. 1985. Hydride-generation atomic absorption spectrometry coupled with flow injection analysis. *Anal. Chem.*, 57: 1382-1385.

Zhang, W., Yang, X., Chu, X. 2009. Electrochemical hydride generation for the determination of hydride forming elements by atomic fluorescence spectrometry. *Microchem. J.*, 93: 180-187.

Zhang, N., Fu, N., Fnag, Z., Feng, Y., Ke, L. 2011. Simultaneous multi-channel hydride generation atomic fluorescence spectrometry determination of arsenic, bismuth, tellurium and selenium in tea leaves. *Food. Chem.*, 124: 1185-1188.

CURRICULUM VITAE

Personel Informations

Name - Surname : Ersin KILINÇ
Birth : Elazığ - 1983
Address : Dicle University, Faculty of Science, Department of Chemistry, TR-21280 Diyarbakır
Contact : 0 412 2488550 – 3054
E-mail : ekilinc@dicle.edu.tr

Education and Academic Informations

BS : 2005 Firat University, Faculty of Art ad Science, Dep. Chem.
MS : 2008 Dicle University, Grad. Sch. of Nat. and Appl. Sci., Dep. of Chem.
‘Determination of flurbiprofen in tablets by chromatographic techniques and investigation of its degradation kinetic’